

Proposal Cover Sheet

NASA Research Announcement 02-OES-06
Proposal No. _____ (Leave Blank for NASA Use)

Title: Atmospheric Transport of Trace Gases and Aerosols: Evaluating Models and Observations

Principal Investigator: Mark R. Schoeberl

Department: Earth Sciences Directorate

Institution: NASA/GSFC

Street/PO Box: Code 916

City: Greenbelt,

State: Md. 20771

Zip: 20771

Country: United States

E-mail: Mark.R.Schoeberl@nasa.gov

Telephone: 301-614-6002

Fax: 301-614-6301

Co- Investigators

| Name | Institution | Contact Address | Phone | email |
|------------------|--------------------|--|--------------|--------------------------------|
| A. Douglass | GSFC | Code 916 GSFC Greenbelt, Md. 20771 | 301-614-6028 | Anne.R.Douglass@nasa.gov |
| R. Stolarski | GSFC | Code 916 GSFC Greenbelt, Md. 20771 | 301-614-5982 | Richard.S.Stolarski@nasa.gov |
| P. Newman | GSFC | Code 916 GSFC Greenbelt, Md. 20771 | 301-614-5985 | Paul.A.Newman@nasa.gov |
| A. Thompson | GSFC | Code 916 GSFC Greenbelt, Md. 20771 | 301-614-5731 | Anne.M.Thompson@nasa.gov |
| S Pawson | GSFC | Code 910.3 GSFC Greenbelt, Md. 20771 | 301-614-6159 | spawson@dao.gsfc.nasa.gov |
| M. Chin | Georgia Inst. Tech | Code 916 GSFC Greenbelt, Md. 20771 | 301-614-6007 | chin@carioca.gsfc.nasa.gov |
| J. Rosenfield | GEST/UMBC | Code 916 GSFC Greenbelt, Md. 20771 | 301-614-5986 | rose@eterpe.gsfc.nasa.gov |
| L. R. Lait | SSAI | Code 916 GSFC Greenbelt, Md. 20771 | 301-614-5990 | lait@ertel.gsfc.nasa.gov |
| L. Sparling | U. Md Balt. Co. | Code 916 GSFC Greenbelt, Md. 20771 | 301-614-6009 | sparling@carioca.gsfc.nasa.gov |
| S. Hollandsworth | SSAI | Code 916 GSFC Greenbelt, Md. 20771 | 301-614-5984 | smh@carioca.gsfc.nasa.gov |
| G. Morris | Rice Univ. | Dept. of Physics & Astr. Rice University Houston, Tx 77251 | 713-348-5727 | em.gm@carioca.gsfc.nasa.gov |
| O. Torres | JCET | Code 916 Greenbelt, Md. 20771 | 301 614-5551 | torres@carioca.gsfc.nasa.gov |
| P. Colarco | GEST | Code 916 Greenbelt, Md. 20771 | 301 614-6055 | colarco@carioca.gsfc.nasa.gov |
| M. Olsen | GEST/UMBC | Code 916 Greenbelt, Md. 20771 | 301-614-5984 | olsen@carioca.gsfc.nasa.gov |

Non Full Cost Budget:

1st Year: \$697,600 2nd Year: \$719,500 3rd Year: \$742,100 Total: \$2,159,200

Full Cost Budget:

1st Year: \$1,040,000 2nd Year: \$1,073,500 3rd Year: \$1,113,600 Total: \$3,227,400

(OVWST Only)

Certification of Compliance with Applicable Executive Orders and U.S. Code

By submitting the proposal identified in this *Cover Sheet/Proposal Summary* in response to this Research Announcement, the Authorizing Official of the proposing institution (or the individual proposer if there is no proposing institution) as identified below:

- certifies that the statements made in this proposal are true and complete to the best of his/her knowledge;
- agrees to accept the obligations to comply with NASA award terms and conditions if an award is made as a result of this proposal; and
- confirms compliance with all provisions, rules, and stipulations set forth in the two Certifications contained in this NRA [namely, (i) *Certification of Compliance with the NASA Regulations Pursuant to Nondiscrimination in Federally Assisted Programs*, and (ii) *Certifications, Disclosures, And Assurances Regarding Lobbying and Debarment & Suspension*].

Willful provision of false information in this proposal and/or its supporting documents, or in reports required under an ensuing award, is a criminal offense (U.S. Code, Title 18, Section 1001).

Title of Authorizing Institutional Official: Franco Einaudi, Director of Earth Sciences

Signature: _____ Date: _____

Name of Proposing Institution: NASA/Goddard Space Flight Center

Telephone: 301-614-5634 E-mail: Franco.Einaudi-1@nasa.gov Facsimile: 301-614-5620

Program Element

EOS Interdisciplinary Science Program (EOS/IDS)

Table of Contents

| | |
|--|----|
| <u>Abstract</u> | 2 |
| <u>1.0 Introduction</u> | 3 |
| <u>1.1 IDS History and Strategic Approach</u> | 3 |
| <u>1.2 Previous IDS Activity</u> | 4 |
| <u>2.0 Proposed Research</u> | 13 |
| <u>2.1 (Q1) Is the ozone layer recovering?</u> | 13 |
| <u>2.2 (Q2) Do we understand the process that control mid-latitude STE</u> | 17 |
| <u>2.3 (Q3) How does the long range transport of pollutants affect local air quality and chemical processes?</u> | 25 |
| <u>2.4 (Q4) How do chemical changes in the atmosphere affect climate?</u> | 33 |
| <u>2.5 Statistical Analysis of Data Sets and Aura Validation</u> | 37 |
| <u>2.6 Other Relevant Activities</u> | 40 |
| <u>3.0 Timeline and Expected Results</u> | 40 |
| <u>4.0 Management Plan</u> | 41 |
| <u>5.0 Personnel</u> | 42 |
| <u>6.0 Facilities and Equipment</u> | 42 |
| <u>6.1 Upgrading the Trajectory models</u> | 43 |
| <u>6.2 Improved Data Set Management</u> | 43 |
| <u>7.0 Current Support</u> | 43 |
| <u>Appendix A Publications funded or partially funded by the IDS over the last proposal period.</u> | 44 |
| <u>Appendix B Related IDS and ACMAP Proposals</u> | 47 |
| <u>Appendix C: Participation in the Global Modeling Initiative (GMI)</u> | 49 |
| <u>Appendix D Model Descriptions</u> | 50 |
| <u>D.1 The FVGCM</u> | 50 |
| <u>D.2 Troposphere - Stratospheric Chemical Transport Model (CTM)</u> | 50 |
| <u>D.3 The GOCART microphysics and aerosol model</u> | 51 |
| <u>D.4 Radiative Transfer Model</u> | 53 |
| <u>D.5 The trajectory model group</u> | 53 |
| <u>D.6 The Interactive 2D Model</u> | 53 |
| <u>Appendix E Equipment Costs and Upgrades under this Proposal</u> | 54 |
| <u>References</u> | 55 |
| <u>Tables</u> | 69 |

Atmospheric Transport of Trace Gases and Aerosols: Evaluating Models and Observations

Mark R. Schoeberl, PI
Laboratory for Atmospheres, Code 910, NASA/GSFC
Greenbelt, Md. 20771

Co-Investigators

A. Douglass, R. Stolarski, P. Newman, A. Thompson
Atmospheric Chemistry and Dynamics Branch
Code 916, NASA/GSFC
Greenbelt, Md. 20771

S. Pawson
Data Assimilation Office, 910.3 NASA/GSFC
Greenbelt, Md. 20771

M. Chin
School of Earth and Atmospheric Sciences, Georgia Institute of Technology, Atlanta, Ga.
30332

J. Rosenfield, M. Olsen, P. Colarco
GEST, Univ. of Maryland, Baltimore Co.
Baltimore, Md.
21250

L. Sparling
Department of Physics, Univ. of Maryland, Baltimore County, MD 21250

L. R. Lait and S. Hollandsworth-Frith
SSAI Corp.
Lanham, Md. 20706

G. Morris
Rice Univ., Houston, Texas 77251

O. Torres
JCET, Univ. of Maryland, Baltimore Co.
Baltimore, Md.
21250

Statement of relevance: This proposal is relevant to the EOS IDS program because it uses a variety of different data sets (chemical, meteorological, radiative, microphysical) from multiple platforms, because the modeling studies include cross disciplinary activities, and because the results of the studies will impact multiple disciplines.

Abstract

This proposal builds on our previous IDS effort on stratospheric transport and chemistry. In this proposal we focus on four questions relevant to atmospheric chemical and climate change: **(Q1) Is the ozone layer recovering? (Q2) Do we understand the processes that control mid-latitude Strat.-Trop. exchange (STE)? (Q3) How does the long range transport of pollutants affect local air quality and chemical processes? (Q4) How do chemical changes in the atmosphere affect climate?** This IDS effort proposes to use a variety of data analysis tools and multi-dimensional models to diagnose processes and trends. Our previous efforts have focused on sub-orbital missions and non-EOS satellite data (e.g. UARS, POAM). In this proposal period we begin the exploitation of Terra and Aqua (MOPITT and MODIS aerosol), SAGE III and Envisat data. We also intend to capitalize on aerosol height data from IceSat (launch 2003), from Aura (launch 2004), from EOS validation campaigns, and from ground and balloon based data sets.

For **(Q1)** we propose to continue our study of polar ozone loss using trajectory techniques described by Schoeberl et al [2002b] and PV/ ϕ coordinate transformation described by Lait et al. [2002] for SOLVE II. We propose to use our new refinement of the MATCH technique for estimating polar ozone loss and we intend to extend its application to SAGE III and POAM data sets. We also propose to use our standard methods of analyzing ozone loss to continue the record initially developed using TOMS data using data from the Ozone Monitoring Instrument (OMI) on Aura. Under **(Q2)** we propose to continue to develop diagnostic estimates of the extra tropical strat-trop exchange (STE) of ozone and mass. One issue we plan to resolve is whether there is a net adiabatic flux of air into the stratospheric middle world as our calculations show, or whether there is a net adiabatic outflow as estimated by Dethof et al. [2000]. This issue is critical for the recycling of short-lived halocarbons. The sign of the mass flow appears to highly variable between models for reasons that are not understood. Our new STE ozone mass flux algorithm [Olsen et. Al., 2002] will be applied to the next generation of chemical transport GCM's and assimilation models as a diagnostic. Under **(Q3)** we propose to study boreal smoke plumes and their impact on air quality. Understanding these events and using space data to diagnose plume transport, evolution and impact on air quality will be a new focused effort. This activity will exploit aerosol data from MODIS, TOMS, and OMI (after 2004), MOPITT CO data and IceSat aerosol altitude (lidar) data. Preliminary study of the East Coast Smoke event (July 5-8, 2002) under this IDS previews our proposed effort. We will first focus on boreal fires and then extend our study to tropical biomass burning. The goal of this later effort is to understand the interrelationship between biomass burning and tropical ozone anomalies. We will also characterize transport properties of tropospheric aerosol using the GOCART and trajectory models. Under **(Q4)** we propose to use our interactive 2D model to understand the chemical response of the stratosphere to changes in trace gases such as water vapor and to further investigate volcanic effects. We will also be analyzing the new 50-year Finite Volume General Circulation Model (FVGCM) climate run. Analysis of tracer transport and the age-spectrum of this model have been shown to provide good insight into the transport characteristics of the model dynamics and thus the suitability of the model for dynamical feedbacks in climate. Finally this proposal effort is strongly linked to Aura Project. We have been especially involved in developing the Aura Validation Plan and we propose to continue investigating the proper statistical use of data for satellite validation.

1.0 Introduction

1.1 IDS History and Strategic Approach

We propose to continue the previous Interdisciplinary Science (PIDS) investigation originally titled “A Proposal to Investigate the Chemical and Dynamical Changes in the Stratosphere Up to and During the EOS Observing Period.” The original proposal was funded in 1989 and reviewed in 1994 and 1999. Because the first EOS platforms did not launch until 1999, the PIDS took advantage of aircraft mission data (AASE II, STRAT, SPADE, POLARIS, TOTE/VOTE, SONEX, ASHOE/MAESA, PEM-Topics, SOLVE) as well as Upper Atmospheric Research Satellite (UARS) observations, Stratospheric Aerosol and Gas Experiment (SAGE) II and Total Ozone Mapping Spectrometer (TOMS) observations. These data were used to develop both data analysis and modeling tools in preparation for EOS observations. Now, with the appearance of limited MODIS (aerosol) and MOPITT (CO) data from Terra we have begun some analyses of aerosol and CO transport. By the end of this investigation the Aura platform will have been launched (Jan., 2004), and we intend to take full advantage of the constituent data sets provided by the four Aura instruments (MLS, HIRDLS, TES, OMI). We also intend to exploit the aerosol altitude information provided by IceSat (2003) and aerosol size distribution from Aqua MODIS. If CALIPSO launches in this period, the lidar aerosol height information will be used from that instrument as well. In 2002-3 we will participate in SAGE III validation (SOLVE II). In 2005, because of our strong connection to the Aura mission, we plan to participate in the TC3 mission targeting tropical upper troposphere as well as other Aura validation missions covering stratosphere and upper tropospheric processes.

During the most recent proposal period we have addressed the issue of the magnitude and amount of mid-latitude stratosphere-troposphere mass and ozone exchange (STE). We have also completed a detailed analysis of the ability of the current assimilation models to accurately reproduce stratospheric transport. We have increased the capability of our modeling tools and applied them to new phenomenology – especially tropospheric processes and stratospheric ozone loss. We have used our 2D modeling capability to look the impact of increasing CO₂ and periodic volcanic aerosols on the stratospheric ozone layer recovery. Appendix A summarizes the publications that our group has participated in or generated during the last proposal period.

This proposal will focus more broadly on understanding the transport processes within the stratosphere and troposphere. Observations made by TOMS, MODIS, MOPITT and the four Aura instruments will provide unprecedented information on the flow characteristics of the stratosphere and troposphere. We will be using our tools to answer four basic questions:

(Q1) Is the ozone layer recovering?

(Q2) Do we understand the processes that control mid-latitude STE?

(Q3) How does the long-range transport of pollutants affect local air quality and chemical processes?

(Q4) How do chemical changes in the atmosphere affect climate?

To answer these questions we must understand the transport of mass, chemical constituents and aerosols in the stratosphere and troposphere. In answering (Q1) we continue our analysis of the aircraft mission, balloon and satellite ozone observations. We will use new techniques developed over the last year by this IDS for estimating ozone loss. In (Q2) we have developed a new technique to estimate the extra-tropical STE of ozone and mass. We plan to apply these techniques to new data assimilation system

(DAS) products as well as GCM data sets that have become available in the last year. In (Q3) we have begun research into the long-range transport of pollutants using satellite and ground based observations. In (Q4) we have developed a suite of tools to diagnose transport characteristics of meteorological fields from a GCM and a data assimilation system (DAS). We will continue work with chemical transport models driven by winds from the FVGCM and FVDAS (finite volume DAS). We will continue to interact with the Data Assimilation Office (DAO) in evaluating their products. We will also use our interactive 2d chemical model to investigate the climatic impact of trace gas changes on the stratospheric circulation. The four science questions in this proposal are linked by the use of our dynamical transport models and analysis of constituent observations being produced by satellite and in situ sensors.

Our IDS proposal effort is also connected to the Aura Project as the PI for this proposal is the Aura Project Scientist and one of the CoI's (Douglass) is a Deputy Project Scientist responsible for validation. The breadth and depth of this IDS investigation allow us to lead development of the Aura validation plan and provide direction to the Aura Project on instrument data product issues.

This IDS proposal is also being coordinated with other relevant investigations. Some of the collaborative proposals are listed in Appendix B. Each of the collaborative proposals and this proposal stand alone, but the scientific progress of all of the proposals in this confederation is enhanced by the collaboration.

1.2 Previous IDS Activity

Over the last proposal period we have focused on stratospheric processes and chemical change as well as stratosphere-troposphere exchange. As the Goddard DAO has continued to improve their product, we have been using the Goddard CTM and trajectory model to characterize the transport properties of the meteorological data sets.

1.2.1 New Tool Development

One important development by the PIDS has been the construction of a fast kinematic trajectory model and a simplified isentropic trajectory model (for use in field deployments). The kinematic trajectory model was built to take advantage of assimilation data sets that do not include diabatic heating rates that required for multi-week integration of our diabatic trajectory model. The kinematic model is also more useful for tropospheric investigations where the computation of diabatic heating rates may not include latent heat release and the radiative effects of clouds. The kinematic model was also developed to examine volcanic aerosol distributions following eruptions that took place prior to the availability of UKMO data (the launch of UARS in 1991). This model is available within the Goddard Science System and via the trajectory web page.

The simplified diabatic trajectory model was developed to operate on laptop computers for use during field missions. The simplified model operates on a single isentropic level using winds, temperatures and potential vorticity pre-interpolated to that level. The model is designed for developing flight plans and was successfully used during the SOLVE mission along with a new simplified flight planner developed by the PI.

1.2.2 Polar Ozone Loss

Members of the PIDS participated in the SOLVE (1999-2000) mission. The PI was Co-Mission Scientist for the DC-8 and a Co-I's (Newman) was Co-Mission scientist for the

ER-2. The SOLVE mission is discussed in Newman et al. [2002]. In addition, members of our IDS team have continued analyzing TOMS column ozone observations (see Figure 2.1.1.1 below) for Antarctic and Arctic trends.

During the SOLVE mission a new method to estimate ozone loss was developed. This method takes advantage of all measurements made during SOLVE by satellite, ozonesonde and aircraft by starting a trajectory whenever a measurement is made. These trajectories are carried forward diabatically until the end of the measurement period (December – mid-March). Comparison of recent and early mission observations for local parcels gives ozone loss. This analysis method is reported in Schoeberl et al. [2002b]. The authors also showed in this work that biases in the analysis made by POAM can develop because POAM preferentially samples the edge of the vortex. The POAM loss rate estimates were thus higher in January than loss rates over the entire vortex. We also made PV/ σ coordinate transformation estimates of ozone loss during SOLVE [Lait et al., 2002] which agreed well with the trajectory method [Newman et al., 2002].

1.2.3 STE

Our PIDS proposed to study the processes of mid-latitude STE. Ozone STE significantly impacts climate and upper-tropospheric/lower-stratospheric constituent budgets. However, the magnitude, variability, and trends in the exchange of chemical species such as ozone remain uncertain. Mass exchange estimates are typically made using bulk methods that do not provide spatial distribution [e.g., Appenzeller et al., 1996]. This limits the ability to use mixing ratio information with total mass exchange methods to derive an accurate estimate of constituent exchange. Olsen and Stanford [2001] show that tropospheric diabatic heating and cross-jet isentropic transport, the primary mechanisms of mid-latitude downward exchange, are sub-synoptic scale local processes. Thus, constituent exchange estimates based on total air mass schemes are not adequate for chemical species such as ozone that have significant horizontal variability near the tropopause.

Within our PIDS, we have developed a new method to quantify the mid-latitude ozone transport to the troposphere using total ozone observations and analyzed potential vorticity (PV) [Olsen et al., 2002a]. We use the observation that PV is lost in irreversible mass transport to the troposphere. Advantages of this method include the use of global observed or modeled ozone, and the location as well as the magnitude of the ozone flux is calculated. Results for each hemisphere in the year 2000 are shown in Figure 1.2.3.1. A distinct seasonal variability is seen and shorter time scale variability is greater during the winter/spring months when the total ozone flux is enhanced. The locations of ozone flux for a single day are shown in Figure 1.2.3.2.

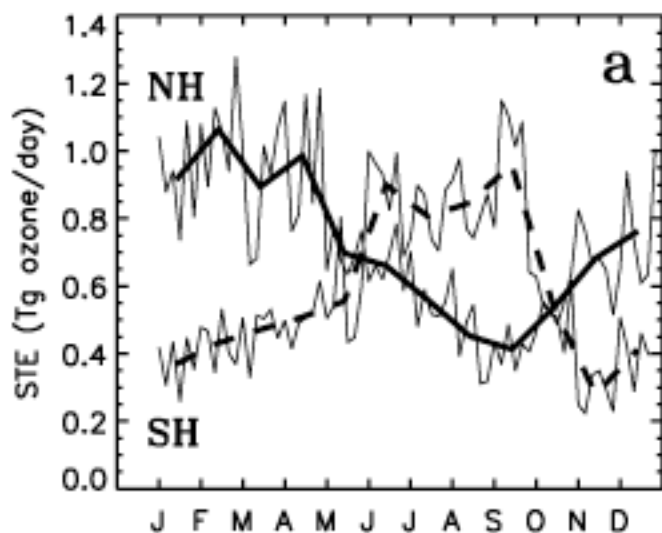


Figure 1.2.3.1 Year 2000 downward cross-tropopause ozone mass flux in units of Tg day^{-1} . Bold lines are the monthly averages based upon 6 days per month for the NH (solid) and SH (dashed) mid-latitudes. Thin lines are the flux for the 6 days of each month.

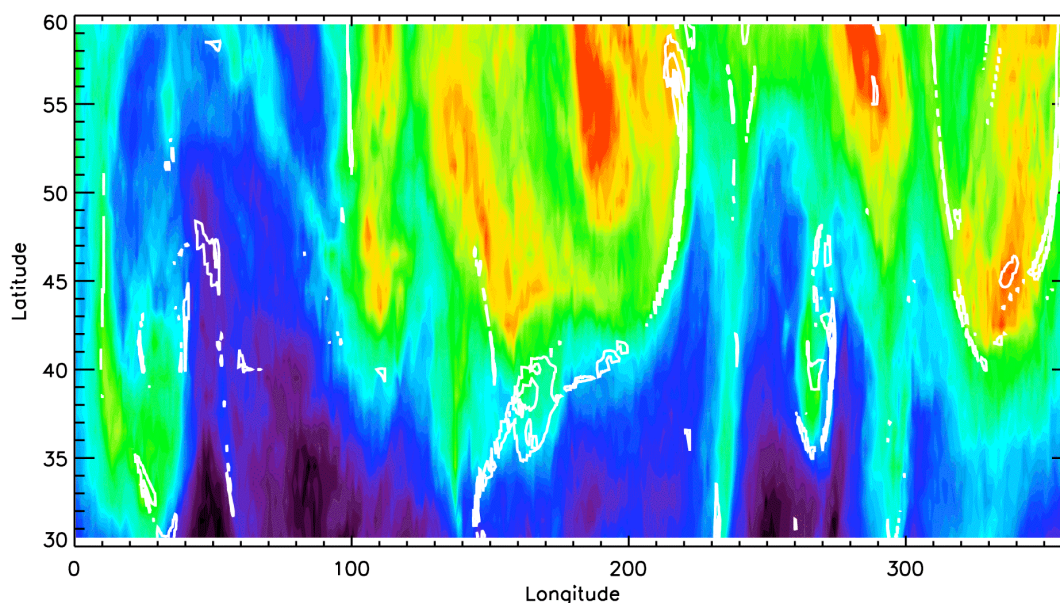


Figure 1.2.3.2. EP/TOMS total column ozone (color shading) and downward cross-tropopause ozone flux (white contours) for April 20, 2000. Total column ozone ranges from 270 DU to 458 DU with warmer colors indicating greater values. Ozone flux contour interval is 5 DU beginning at 10 DU.

Significant flux is associated with cross-jet transport and tropopause folding (near large ozone gradients) and diabatic heating (near ozone maxima). This technique has recently been applied to the Southern Hemisphere midlatitudes. In Olsen et al. [2002b], we show that the ozone flux into the northern hemisphere midlatitudes is higher than in the southern hemisphere not because of increased mass flux but because of increased ozone

amounts in the lower stratospheric Northern Hemisphere lower stratosphere. Below we discuss further proposed work along this line.

1.2.4 Analysis of assimilation models and chemical simulations

Our PIDS had a strong link to the DAO and the analysis of their meteorological products. Two important papers have been produced by this IDS relating to the transport characteristics of the FVDAS compared to the UKMO DAS and the FVGCM. In the first publication, Schoeberl et al. [2002a] a series of back trajectory analyses showed that the tropics are excessively ventilated in the assimilation analysis. This ventilation produces flattened constituent and age-of-air gradients [Douglass et al. 2002]. Schoeberl et al. (op. cit.) goes on to show that for non-isentropic transport, the vertical dispersion associated with the DAS motion fields offsets the bias created by the excessive tropical ventilation, producing reasonable tropical mean ages. These results show that the long-term constituent transport by the DAS fields (including the UKMO) will produce trace gas biases. Figure 1.2.4.1 shows the tropical age spectra computed using trajectories. Figure 1.2.4.2 shows a comparison of constituent gradients observed by aircraft and computed by the DAS driven chemical transport model (CTM).

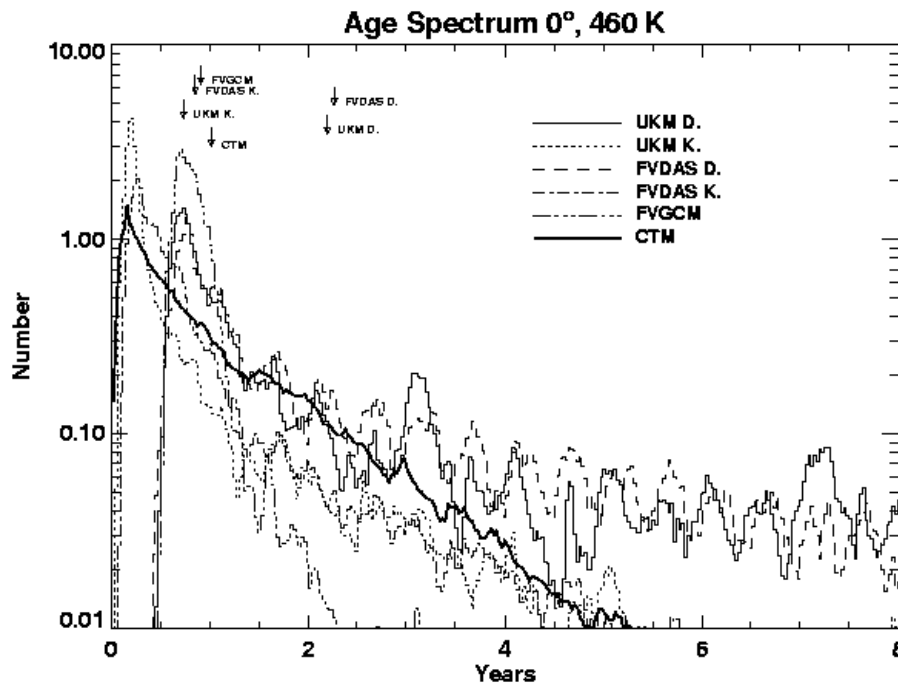


Figure 1.2.4.1 The age spectra computed using the trajectory models for UKMO, FVDAS and FVGCM. Both diabatic (D) and kinematic (K) trajectories were run. The age spectrum using UKMO data and the chemical transport model is also shown. Note the lack of age offset in the kinematic results, and the stretched out spectra in the diabatic cases. These biases lead to a year difference in the mean ages.

In contrast to the DAS, the FVGCM shows good tropical isolation compared with observations (Fig. 1.2.3.2). Both Douglass et al. and Schoeberl et al. suggest that this significant problem with tropical meteorological fields arises from the failure of the GCM to simulate tropical phenomenon such as the QBO and the MJO. As a result, assimilation

of tropical data can produce bogus circulations that disrupt the tropical transport barriers. The extra ventilation of the tropics explains the flat mixing ratios across the tropics seen in almost every chemical model and also explains the too-young air at mid-latitudes. It is clear that this extra-ventilation will hamper the use of these models for chemical/climate predictions. The good news is that the FVGCM appears to do a reasonable job of maintaining tropical isolation and thus should be suitable for long term integrations in a climate-chemistry coupling mode.

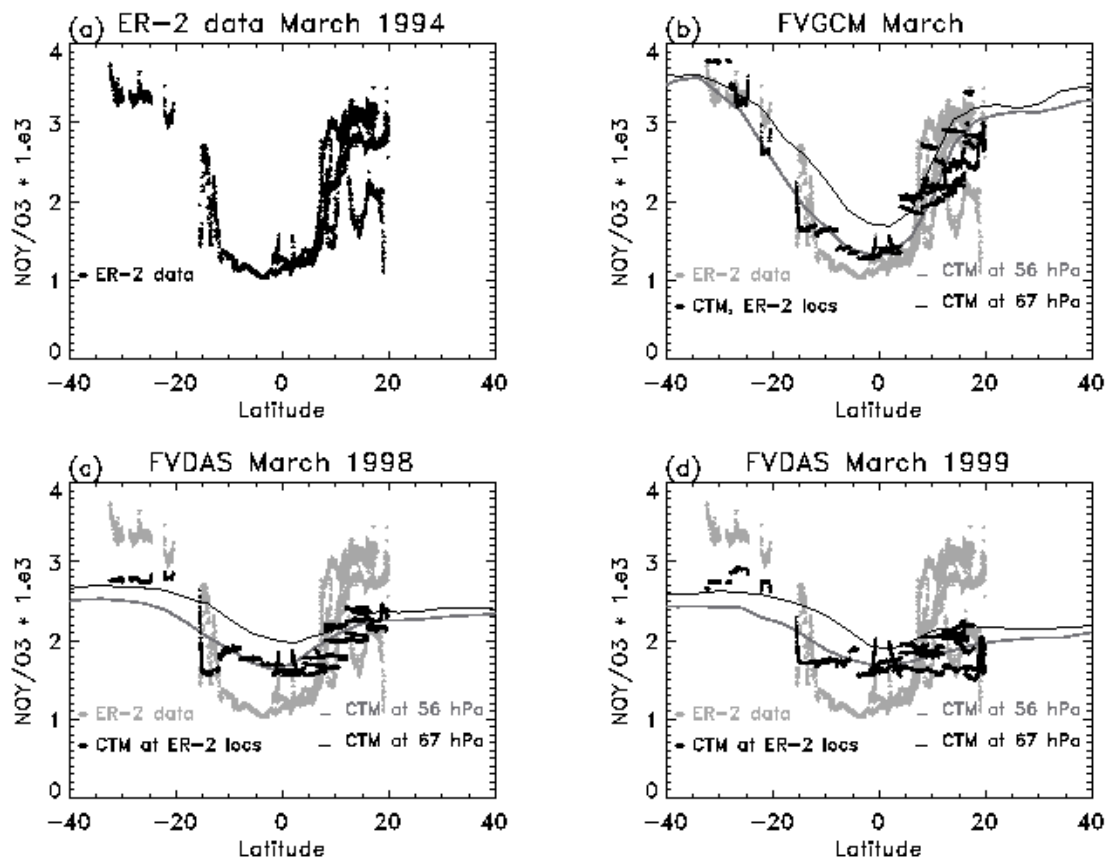


Figure 1.2.4.2 Comparison of ER2 observations of NO_y/O_3 with CTM calculations using the FVDAS and the FVGCM. The upper left figure shows the observations, the upper right shows a CTM calculation using the FVGCM while the two lower figures show the same calculation using the FVDAS.

1.2.5 Climate change in the stratosphere

1.2.5.1 The impact of increasing CO_2 on ozone recovery

The GSFC interactive 2D model developed under this IDS (Appendix D) has been used to study the impact of increasing CO_2 from 1980 to 2050 on the recovery of ozone to its pre-1980 amounts as the chlorine loading of the stratosphere decreases. Natural and anthropogenic source gas changes were specified according to WMO scenarios. The changes in temperature and circulation arising from increasing CO_2 affect column ozone recovery in a manner which varies greatly with latitude and time of year, as shown in Figure 1.2.5.1.1. While the gas phase ozone chemical loss rates in the middle and upper

stratosphere are slowed down due to the decreasing temperatures, high latitude ozone loss increases in the springtime lower stratosphere due to increased heterogeneous chemical loss. High latitude ozone recovery is speeded up in fall and winter due to increased downwelling. Annual mean column ozone is predicted to recover faster at all latitudes, and globally averaged ozone is predicted to recovery approximately ten years faster as a result of increasing CO₂ [Rosenfield et al., 2002].

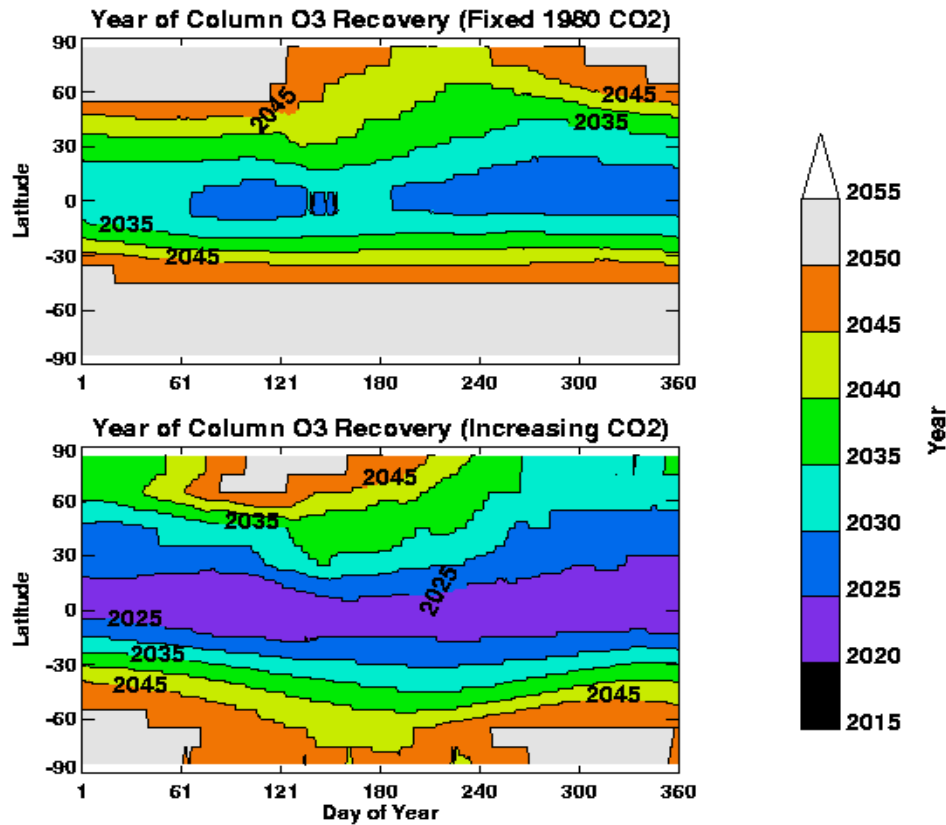


Figure 1.2.5.1.1 The interactive 2D model estimate of year ozone returns to climatological values with and without CO₂ increases. Note that the recovery accelerates if CO₂ increases because acceleration of the stratospheric circulation brings more ozone down to the lower altitudes at higher latitudes. This result was published in Rosenfield et al. [2002].

1.2.6 Volcanic impacts

Using the interactive 2D model, the effects of future volcanic eruptions on the recovery of the ozone layer were studied. Simulations to the year 2050 were completed. In these simulations volcanic eruptions having the characteristics of the Mount Pinatubo volcano took place in the model at ten-year intervals starting in the year 2010. These eruptions resulted in transient reductions of globally averaged column ozone of 2-3% relative to background aerosol conditions. These transient losses revert to the nonvolcanic situation within about five years after the eruption, suggesting that the long-term recovery of stratospheric ozone would not be strongly affected by infrequent volcanic eruptions the magnitude of Mount Pinatubo. A sensitivity test was carried out in which a 10% per year increase of the background aerosol loading was imposed. This was found to have a large

effect, leading to a slowing of the ozone recovery by more than ten years. These results have been submitted for publication.

We have also studied volcanic emissions using the kinematic trajectory model. We performed simulations of eruptions into the Arctic vortex as part of a collaboration with the aerosol group at NASA/Ames. The simulations showed how the vortex could contain the volcanic material. Observations of the Hekla eruption during SOLVE showed that the stratospheric plume could be contained within the vortex for weeks. A massive eruption would create enough aerosol surface area to produce an Antarctic-like ozone hole in the Arctic Tabazadeh et al. [2002]. In our previous IDS we intended to use the Pinatubo eruption data combined with a reanalysis of the meteorological observations during the Pinatubo period to study stratospheric transport. The meteorological observations were to be supplied by a Pathfinder Data Set proposal (Pawson, PI). Unfortunately, that data set is just now becoming available. In addition, as described above, we have found that the FVDAS provides inadequate tropical stratospheric isolation [Schoeberl et al., 2002a] thus limiting the utility of the data for transport simulations. However, with the FVGCM simulations we should be able to provide reasonable assessment of the impact of volcanic processes on the stratospheric/tropospheric region as outlined below.

1.2.7 Estimation of tropospheric ozone amounts

Under the current IDS proposal, we have investigated various methods of deriving lower stratospheric global time-dependent ozone fields from available data sets. We use SAGE II, UARS/HALOE, POAM II/III and balloonsonde profile measurements to characterize lower stratospheric ozone. These instruments provide the high vertical resolution necessary to capture small-scale dynamical variations, but at a limited spatial and temporal sampling. PV/ σ mapping is used to estimate daily global ozone fields on isentropic surfaces from these data. This technique, formally developed by Schoeberl and Lait (1993), takes advantage of the well-known correlation between PV and ozone, which are both quasi-conserved tracers in the lower stratosphere in adiabatic flow. Using NCEP Reanalysis global meteorological fields, we established linear regression relationships between available ozone and PV for each month from 1985-2001. The data are fit separately in successive PV-bins in a piecewise linear fashion. The fit parameters are then used with daily PV fields to estimate daily ozone fields. No extrapolation is allowed, so locations with PV values outside the range of values associated with actual measurements are not reconstructed.

While this technique is commonly employed to map ozone data from various sources and its premise is generally accepted, a thorough analysis of the validity of reconstructed fields as a function of latitude and altitude has not been presented previously. We tested the internal consistency of the mapping technique by comparing reconstructed data to the original data and investigate the differences as a function of latitude, altitude, and season. In this study we considered only northern hemisphere latitudes. In most regions, average differences are within 5%. However, the reconstructed data are biased high below 525K and equatorward of 40° N in all seasons. The fundamental cause of the bias is a consistent variation of ozone with latitude in certain PV bins. To reduce this bias, we fit the ozone in each PV range to PV as before, but then test for a latitude-dependent residual. The latitude bias is reduced to less than 10% in winter months, but is not eliminated completely. We then use the reconstructed data in an effort to derive global tropospheric ozone fields. By subtracting the stratospheric ozone column from a coincident total column ozone measurement, an estimate of the tropospheric column ozone can be obtained [Fishman and Larsen, 1987]. We use profile data from the Solar Backscatter Ultraviolet (SBUV and SBUV/2) series of instruments as our primary stratospheric data

source, but the vertical resolution of the SBUV data in the lower stratosphere is insufficient to resolve the tropopause. We therefore use the PV-mapped ozone fields to fill in the lower portion of each profile, from 64 hPa to the 380K surface. For the altitude region from the tropopause to 380K, we have developed a balloonsonde climatology based on latitude, month, and the pressure depth of the tropopause to 380K layer. Daily variations in tropopause height are reflected in the variations of the layer depth. With this additional parameter, we can reproduce ~50% more of the observed variability than would a simple monthly latitude-based climatology.

Figure 1.2.7.1 shows comparisons between estimated ozone column amounts in each altitude region and integrated ozonesonde data from 1985-1999. The data are from 13 sonde stations between 37 and 80 degrees north latitude. The top panel tests the representativeness of the upper stratospheric portion of the profile by comparing the TOMS minus SBUV-column-above-64 hPa residual to the sonde integrated ozone from the ground to 64mb. The second panel shows the direct comparison of sonde and PV-mapped data for 64hPa - 380K, the third shows the comparison between the sonde raw data and estimates from the sonde climatology between the tropopause and 380K, and the final panel shows the final residual tropospheric ozone compared to corresponding sonde values. The estimated values in each region of the stratosphere compare reasonably well with the sonde data, but when combining data and inherent uncertainties from each region, the uncertainty in the residual tropospheric ozone is nearly twice as great as the actual variability in the data. These results suggest that this methodology alone cannot be used to accurately represent variations in tropospheric ozone on a daily basis. However, we anticipate a reduction in the uncertainty of the tropospheric ozone residual estimates with data from the Aura satellite. The uncertainties in the current analysis result from calibration differences among a large array of instruments and dynamical variability between measurements taken at different locations and times. The total and profile ozone from Aura will originate from the same platform, reducing the time and spatial variations in the location of the measurements, and thus the noise in the comparisons should be reduced. The technique could be applied to HIRDLS and OMI data, for example.

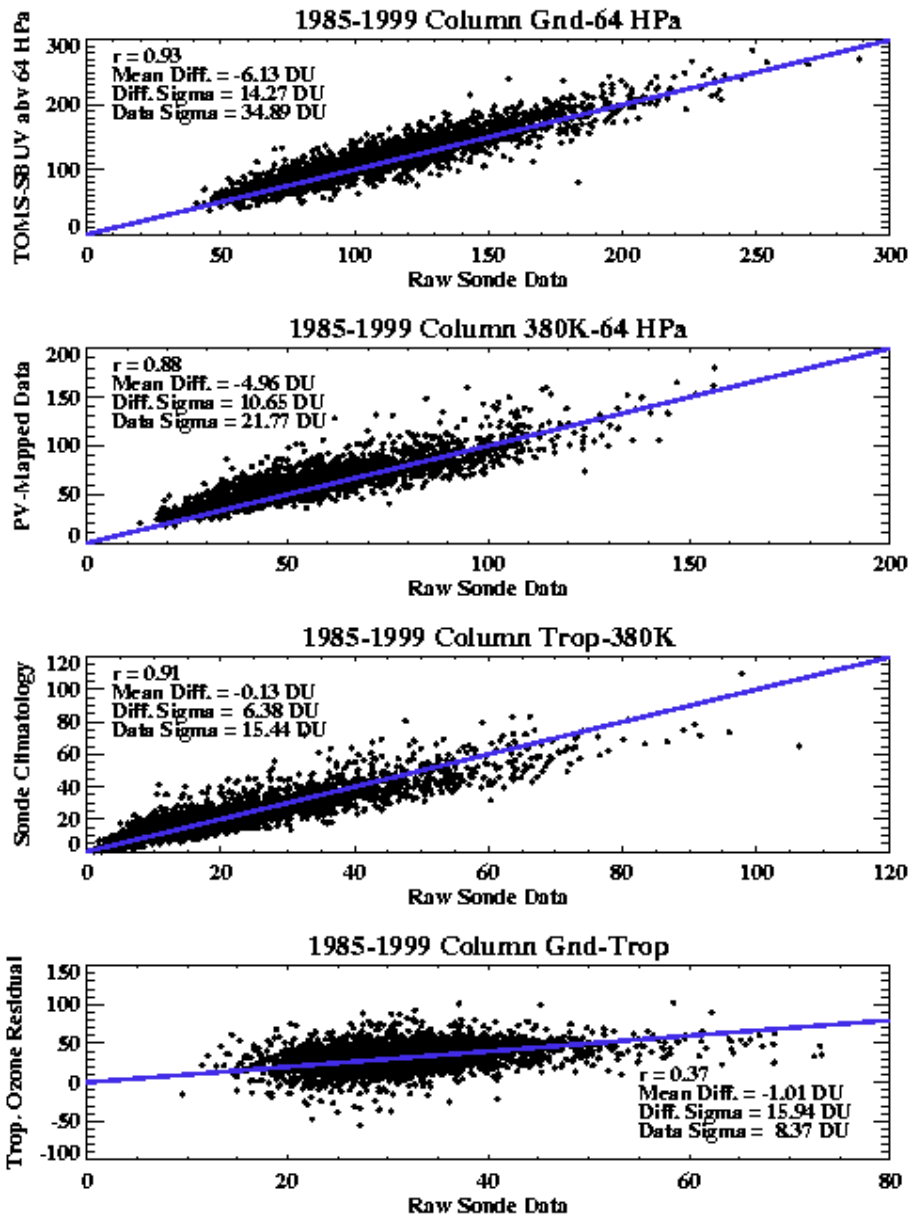


Figure 1.2.7.1 Scatter plot of daily data from integrated ozonesonde data and estimated ozone column amounts in each altitude region from 1985-1999. Data are from 13 sonde stations between 37 and 80 degrees north latitude. Sonde data are plotted along the x-axis, and estimated values are along the y-axis. The top panel shows the TOMS minus SBUV-above-64 HPa residual column amount from the ground to 64mb. The second panel shows PV-mapped data from 64hPa - 380K. The third panel shows sonde climatology reconstructions between the tropopause and 380K, and the final panel shows the final residual tropospheric ozone compared to corresponding sonde values.

2.0 Proposed Research

Historically, the stratosphere and troposphere have been viewed as more or less distinct domains, with the transport of trace constituents between the two domains being the residual effect of complex dynamical processes within each domain. In the PIDS we moved our research efforts to the upper troposphere and lower stratosphere (UTLS). In this proposal, we continue our research efforts in the stratosphere and upper troposphere but we extend our tools lower into the troposphere. This IDS proposal intends to exploit the EOS observations that have just begun to appear (e.g MOPITT data and MODIS aerosol data) and those that will soon appear (e.g. Aura data) as well as new FVDAS and FVGCM fields that have become available to us. The proposed activity below is organized around the four questions stated in the introduction.

2.1 (Q1) Is the ozone layer recovering?

2.1.1 Polar ozone loss

We propose to continue our research into the polar ozone loss using both in situ and remote measurements.

2.1.1.1 Satellite Measurements of the Ozone Hole

The Antarctic ozone hole has shown considerable growth since the early 1980's. We currently use TOMS total ozone observations to estimate the severity of the Antarctic ozone hole by calculating the areal coverage of total column ozone having values less than 220 Dobson Units (DU). Figure 2.1.1.1 displays this areal estimate from 1979 to the present (updated from Randel and Newman, 1998). The areal extent of the ozone hole showed steady increase through the 1980's and early 1990's with a slow increase over the last 5 years. Schoeberl et al. [1996] simulated the size of the ozone using a trajectory model through 1994. In this study, it was shown that the size is strongly controlled by the levels of chlorine and bromine in the stratosphere. Given the current decreases of Cly and Bry resulting the Montreal Protocol, we estimate that the ozone hole should be currently decreasing in size approximately 1% per year. However, the size simulation did not represent the interannual variability.

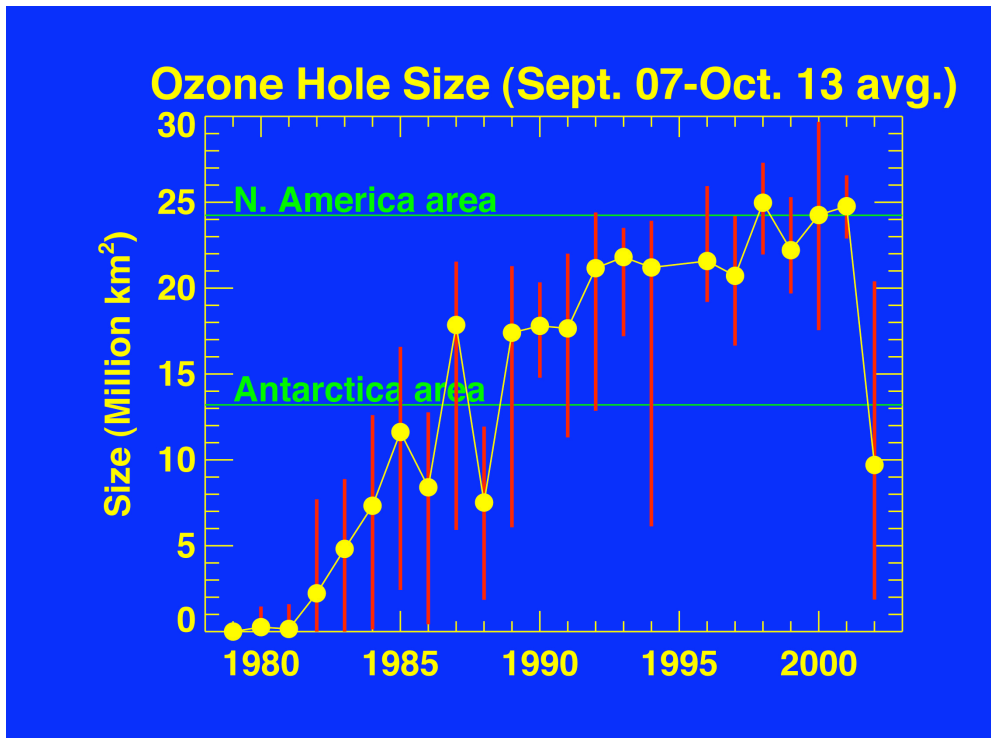


Figure 2.1.1.1.1 displays this areal estimate from 1979 to the present (updated from Randel and Newman, 1998).

The areal estimate for 2002 was exceptionally small as a result of a series of stratospheric warmings that took place over the course of the southern winter, and which culminated in a major stratospheric warming on September 22, 2002. The size was half as large as the previous winters, and was the smallest ozone hole since 1988. Meteorological analyses reveal that the edge of the ozone hole was exceptionally warm during early September, thereby inhibiting the formation of polar stratospheric clouds. The results of the 2002 hole provide new guidance for understanding the interannual variability of the Antarctic ozone hole.

The area of the ozone hole, combined with standard meteorological observations, is extremely important to determining whether ozone is recovering to normal levels (e.g., see WMO 1998). In this IDS, we propose to use OMI (Aura, see Table 2) observations to extend our time series of observations. First, we will compare the EP-TOMS observations during the September 2004 period to the estimates from the OMI instrument. We will use 3-D CTM simulations of future ozone levels to estimate ozone hole size. The CTM (Appendix D) is currently able to simulate the ozone hole as observed although there is an overall bias in the ozone amounts. Our analysis techniques will be refined over the next proposal period and extended to include Aura's MLS and HIRDLS when they become available. In the interim we propose to use the continuous observation trajectory technique [Schoeberl et al., 2002b] for SOLVE II data and POAM data (for other winters) to assess the ozone loss within the vortex region.

Ozone loss can also be estimated using non-trajectory methods. Since the late 1980s, our group has mapped trace gas constituents into potential vorticity - potential temperature (θ) coordinates to arrive at large-scale three-dimensional constituent fields. One of the strengths of this approach is that it permits combining measurements from many

instruments in many locations to create a coherent large-scale picture of a trace gas distribution. Recently, Lary [2002] has used the technique to examine the requirement for coincident data in validation. We propose to continue to improve quasi-conservative coordinate mapping techniques to examine polar ozone processes (see Lait, et al., 2002). Among the enhancements we envision are:

- Improving the statistical characterization of the reconstructed field in PV/ ϕ coordinates, replacing the ad hoc computations currently used with a more formally justifiable procedure. This characterization would include the effects of persistent PV anomalies found in some analysis products.
- Improving the adjustments for diabatic effects. We have had some success with replacing a measurement's actual theta value with one that has been adjusted using diabatic trajectory calculations. We wish to explore the possibility of doing continuous adjustments directly in PV/ ϕ space using the heating rate fields.
- Better characterizing the degree to which the technique may be applicable in the "middle world" region of the upper troposphere/lower stratosphere. Reconstruction of total ozone fields for comparison with TOMS data indicate that good agreement is sensitive to the tropopause height (see Section 1.2.7). Improving our ability to handle lower altitudes could improve the feasibility of using PV/ ϕ mapping to determine total stratospheric column ozone, which could then be used to better determine tropospheric ozone amounts. We may be best able to solve this problem using ozone assimilation as is being tested in the data assimilation office.

2.1.1.2 MATCH Analysis

We have developed new tools that make it possible to address issues related to sampling, trajectories, and data quality that allows us to gain an understanding of the uncertainties that affect MATCH results. We have developed a new versions of the MATCH technique (Rex et al., 1998a, Rex et al., 1998b, Rex et al., 1999, Rex et al, 2002a; Rex et al., 2002b) using data from the SOLVE campaign for the period January 1 – March 31, 2000. The MATCH technique involves a network of coordinated balloon launches across Canada and Northern Europe. Balloons are launched from one station and record profiles of ozone. A dynamical model applied in a forecast mode to predict the trajectory of the sampled air mass at multiple levels. When the model indicates that the sampled air mass will pass nearby another sonde station, a second balloon is launched to coincide with the predicted arrival of the previously sampled air mass. A new ozone profile is then recorded and then matched with the older air parcel. From the trajectory information ozone loss and ozone loss per sunlit hour can be obtained.

We have modified the MATCH analysis to increase the number of parcels and sondes used. We make no assumption about zero time photochemistry, and we include diabatic effects. In Figures 2.1.2.1 we simply reproduce the results of Rex et al. [2002a] using a nearly identical approach to verify that using their assumptions we can reproduce their results.

In Figure 2.1.2.2, we apply trajectory matching conditions and a MATCH scheme that better accounts for uncertainties in the technique. This includes adding more parcels to the integration and using a careful analysis of the interception air mass and further filtered the sondes for bogus observations. Both versions produce results with loss rates of 2 – 7 ppbv/hr for SOLVE, consistent with those reported by Rex et al. [2002a] but the uncertainties associated with are data we find are typically much larger than those found by Rex et al. [2002a,b]. Rex et al. [2002b] argue that the January Arctic loss calculated using ozonesondes data and the MATCH technique agrees with the loss suggested by observations from POAM and MLS, but it is clear from their Figure 4 that this conclusion is contingent on the uncertainty of the calculation.

We propose to apply our revision of MATCH to both SOLVE II observations and to POAM measurements using the basic idea of MATCH and also providing careful characterization of the errors. It will be useful to compare the results of the continuous injection technique [Schoeberl et al. 2002b] with our new MATCH analysis. We have been in communication with Markus Rex on the different calculations and have exchanged ozonesonde match information. We have also noted that ozonesondes that have unusual instrument temperatures (box temperatures) can produce reasonable looking profiles that are offset giving bad matches. We have also obtained ECMWF data for the SOLVE winter period and will be rerunning our codes using the ECMWF meteorological analysis (the data set used by Rex) to make sure differences are not a result of the different meteorological fields. We propose to include POAM, ILAS II and SAGE III data sets. These data sets provide 12-15 profiles each day and have excellent precision although the profiles do not have the vertical resolution of the sondes. One complication of using the POAM, ILAS II and SAGE III is that temperature measurements must be interpolated to the profile locations from DAS data.

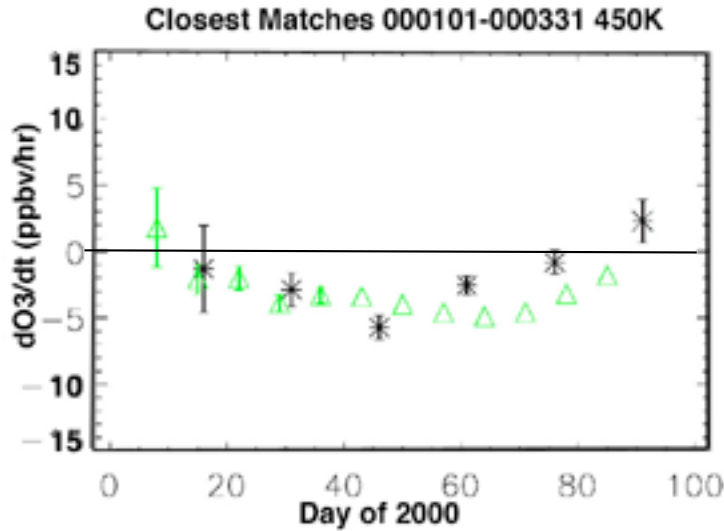


Figure 2.1.2.1 Our reproduction of the results of Rex et al. [2002a] with one sigma error bars for the SOLVE campaign of January 1 – March 31, 2000. Stars are our results; triangles are from Rex et al.

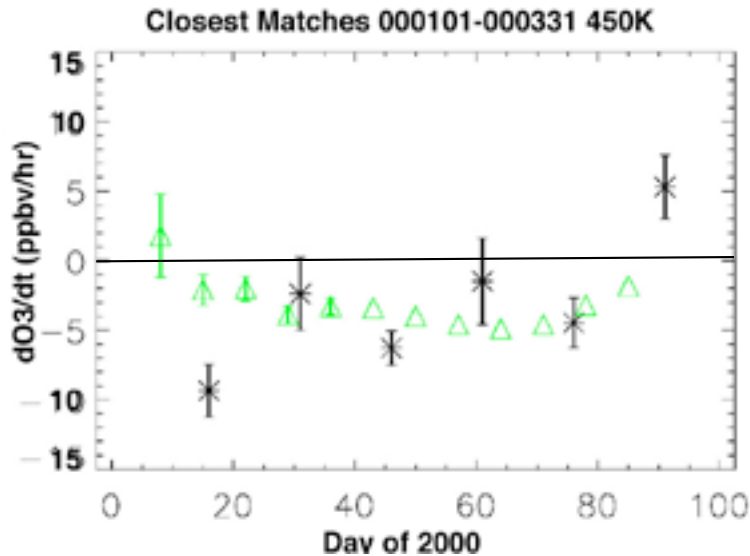


Figure 2.1.2.2 New version of MATCH with one sigma error bars for the SOLVE campaign of January 1 – March 31, 2000 (stars) with MATCH results from Rex et al. [2000a] (triangles).

2.2 (Q2) Do we understand the process that control mid-latitude STE

The tropopause is a complex internal boundary within the atmosphere related to both radiative and dynamical mechanisms [Thuburn and Craig, 1997]. The classic review of stratosphere-troposphere exchange (STE) was given by Holton et al. [1995] (H95). H95 argued that the conceptual model of a wave-driven pump (McIntyre, 1992) inducing upward motion at the tropical tropopause with downward motion at middle and high latitudes provides an effective paradigm for STE. In fact, this global dynamic framework, most clearly appropriate for the stratospheric overworld (region above 380K), is often more effective than explicit consideration of the variety of dynamical events that occur in the vicinity of the tropopause [e.g. WMO, 1986, Danielsen et al., 1970; Shapiro, 1980; Lamarque and Hess, 1994; Langford et al., 1996; Beekmann et al., 1997; Bamber et al., 1984; Vaughan and Price, 1989; Price, 1990; Price and Vaughan, 1993; Ancellet et al., 1994]. Improved observations and modeling capabilities since the H95 review have led to important refinements of the schematic view of STE.

In our IDS we have focused on the midlatitude tropopause rather than the tropics (the cooperative IDS under Dessler (Appendix B) focuses on the tropical tropopause.) Modeling studies at mid-latitudes show that the middleworld stratosphere (the region of the stratosphere between the tropopause and the 380K isentrope) exchanges mass with the troposphere on much shorter time scales than the stratosphere above 380K [e.g., Schoeberl et al., 1998, Gettelman, et al., 1999, Dethof, et al., 2000]. Transport diagnostics derived from meteorological analyses, including 3-D tracer calculations, suggests that mixing associated with Rossby waves keeps the middle latitude upper troposphere and lower stratosphere more stirred than historically believed [Haynes et al., 2001]. This means that while consideration of how much mass flows across the 380 K surface might indicate how much stratospheric air is available for transport into the troposphere, the amount of mass flux across the tropopause itself is probably significantly larger because of local mixing of air into the middleworld stratosphere (region between 380K and the tropopause) from the troposphere.

The importance of the UT/LS in chemistry and climate problems is well stated in a number of international assessment documents (e.g. Houghton et al., 1995, Kawa et al., 1999, Penner et al., 1999). Because the concentrations of many trace gases vary greatly across the tropopause, changes in the UT/LS impact not only the radiative attributes of the atmosphere, but also the chemical environment. Within the context of chemical problems one of the largest uncertainties is how much ozone and odd nitrogen is supplied to the troposphere from the stratosphere as well as the fate of short-lived halocarbons.

2.2.1 Mass Transport from the Stratosphere to the Troposphere

A good conceptual model of the stratospheric circulation is that of a poleward pump driven by breaking planetary waves in winter. As this pump moves material poleward, by mass continuity, air must rise in the tropics and sink at polar latitudes. This concept has been clearly documented in satellite and in situ trace gas observations (Mote et al., 1996, Russell et al., 1993, Schoeberl et al., 1995, Shepherd, 2002, and others). By definition, the exchange of air between the middle and upper stratosphere and lower atmosphere is controlled by the rate at which the air crosses the 380K surface. Diabatic descent occurs throughout the seasons at the boundary between the middleworld stratosphere and the overworld stratosphere (Appenzeller et al., 1996, Schoeberl et al., 1998), and ascent occurs in the tropics. Because of the diabatic descent, it is very unlikely for gases that have entered the middleworld stratosphere to move directly into the stratosphere above. Thus air can only enter the stratosphere through the tropical tropopause [Plumb et al., 1999, Plumb, 2002].

Trace gases enter the stratospheric middleworld from both the troposphere (e.g. Hoskins, 1991; Rood et al., 1992, Seo and Bowman, 2001) and from the stratospheric above 380K, the latter being rich in ozone and other stratospheric trace gases. Since the lifetime of air within the middleworld is short, about 2-3 months on average [Schoeberl et al., 1998a, 1998b], there is a strong link between the amount of ozone in the troposphere (exchanged via the middleworld) and the large scale circulation of the stratosphere which controls the flux of ozone across the 380K surface. Unfortunately estimates of the amount of mass exchanged across the extra-tropical 380K surface are uncertain to 30% or higher [Appenzeller et al., 1996; Yang and Tung, 1996]. Even though there are dynamical constraints on this flux, there are complexities in exploiting these constraints [Plumb, 2002]. A significant amount of uncertainty also comes from the imbalance in the globally integrated heating rates and mass fluxes [Shine, 1989, Olaguer et al., 1992].

Dethof et al. [2000] has attempted to evaluate the UTLS exchange rate of mass using contour advection techniques. Intrusions from the upper troposphere into the middle world and vice versa are tracked using contour advection, and the mass of this transfer is evaluated. They found that there was net adiabatic flux from the upper troposphere into the stratosphere even though the two processes had nearly the same magnitude. The approach of estimating the stratospheric component of tropospheric mass flux by examining the large scale circulation would appear to be far more fruitful than estimating transfer from contour advection, because it is not clear whether spectacular intrusions are responsible for most of the flux of mass from the stratosphere or whether the more frequent smaller intrusions transfer the bulk of the mass into the troposphere (H95). In our recent research we have attempted to extend the Appenzeller et al., [1996] technique to ozone transport, but because of the highly variable ozone amounts in the middle world as revealed by sondes, we found that the calculation was too sensitive to the assumed ozone profile in the middleworld (i.e. Logan [1999] ozone climatology).

Postel and Hitchman [1999] have identified additional preferred regions of mass transfer between the tropical upper troposphere and the middleworld stratosphere. These regions occur near summer monsoons where the isentropes extend from the middleworld stratosphere

into the tropical troposphere and the flow is north-south. Monsoon transfer may dominate the exchange between the middleworld stratosphere and the troposphere in the summer hemisphere. Interest in the summer Asian monsoon region has increased since HALOE data appears to show that the injection of water vapor into the lower stratosphere through that region [Rosenlof, 2001]

2.2.1 Proposed STE Research

Knowing the net flux of mass and tracers into (and out of) the troposphere from (and to) the stratosphere is a key issue for both stratospheric and tropospheric chemistry. This issue impacts our understanding of the chemical processes of both regions – both the budget of tropospheric ozone and the budget of stratospheric trace gases that control stratospheric ozone.

a. Mass transport and age

The stratospheric middleworld is a highly variable region. During winter, the mid-latitude 380K surface rises and the tropopause descends. The volume of the stratospheric middleworld increases. Air within this region becomes more stratospheric in character when as the mass transfer from the overworld across the 380 K surface increases due to diabatic descent. By the end of winter, trace gas measurements show that 60-80% of stratospheric middleworld air may have come from the overworld [Ray et al., 1999]. The depth of the stratospheric middleworld also varies under the influence of the tropospheric weather systems. Figure 2.2.1.1 shows the mass within the stratospheric middleworld using FVDAS data on Jan 2, 2000 assigning 2 PVU for the midlatitude tropopause. The high degree of longitudinal variability reflects the upward and downward displacement of the tropopause.

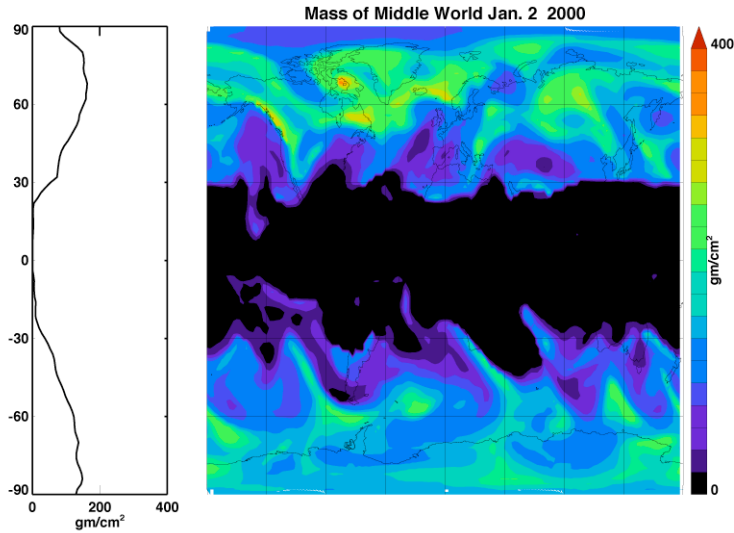


Figure 2.2.1.1 The mass column of the middle world (zonal mean value is shown to the left) on Jan 2, 2000 using the FVDAS observations. Mass column in gm/cm^2 is a rough equivalent of depth.

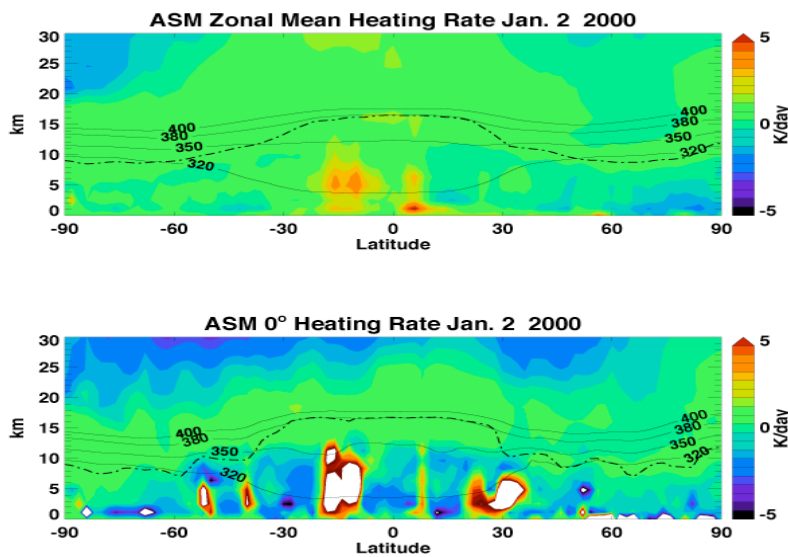


Figure 2.2.1.2 The FVDAS diabatic (radiative plus diabatic plus turbulent) heating rate (colors) in K/day as well as selected isentropic surfaces. The tropopause is dashed. Upper figure is the zonal mean, the lower figure shows the cross section at 0° longitude. White areas show regions of latent heat release.

Mass exchange can be partitioned into flow across potential temperature isentropes (adiabatic) and flow across isentropes (diabatic). Figure 2.2.1.2 shows that although isentropes and the tropopause cross more obviously between about 20° and 40° latitude such crossings occur at higher latitudes as well. One of the complicating factors of adiabatic exchange is its reversibility. For example, both Dethof et al. [2000] and Seo and Bowman [2001] found that nearly as much air moved adiabatically into the stratosphere as moved into the troposphere.

Diabatic as well as adiabatic flow can exchange material across the tropopause boundary at all latitudes (as might be expected. This means that the approach used by Dethof et al. [2000] which emphasized the exchange in the 20-40° region may have incorrectly estimated the adiabatic exchange between the middle world and the troposphere at higher latitudes [Wernli and Bourqui, 2002]. The approach of Appenzeller et al. [1996] can be generalized to include the diabatic cross tropopause fluxes of mass. We can describe the middle world mass balance as follows:

$$\frac{dM}{dt} = F_{380K} - (F_t^d + F_t^a)$$

where M is the mass of the middle world and F are the fluxes across the boundaries. F_t is the tropopause flux (superscript means adiabatic or diabatic). By definition the 380K flux at the top of the middle world is a diabatic flux – adiabatic fluxes would be parallel to the isentropic surface.

Using a standard diabatic radiative transfer model, we can compute F_t^d and F_{380K} as well as dM/dt from an estimate of the tropopause height. This allows us to solve for F_t^a . Using UKMO data and our computed diabatic heating rates we balance the mass flux so that the net is zero. Figure 2.2.1.3 illustrates the expected annual cycle in the middleworld volume change; dM/dt is negative in the spring as the middleworld collapses and positive in the fall when it grows. The 380K fluxes show little seasonal change as noted by Appenzeller et al. [1986]. The net flux computed from the difference between the 380K flux and the rate of change in the middleworld mass agrees with the estimates of Appenzeller et al. The diabatic tropopause flux (smoothed using a 30 day box car filter) is negative with smaller fluxes in the summer and larger fluxes in the winter as might be expected simply from the annual cycle of baroclinic activity. Subtracting the diabatic flux from the net flux the adiabatic flux is positive. This means that there is a net adiabatic flux of tropopause air into the stratospheric middle world balancing the downward diabatic tropopause flux. The direction of the adiabatic flux is opposite to that deduced by Dethof et al. [2000].

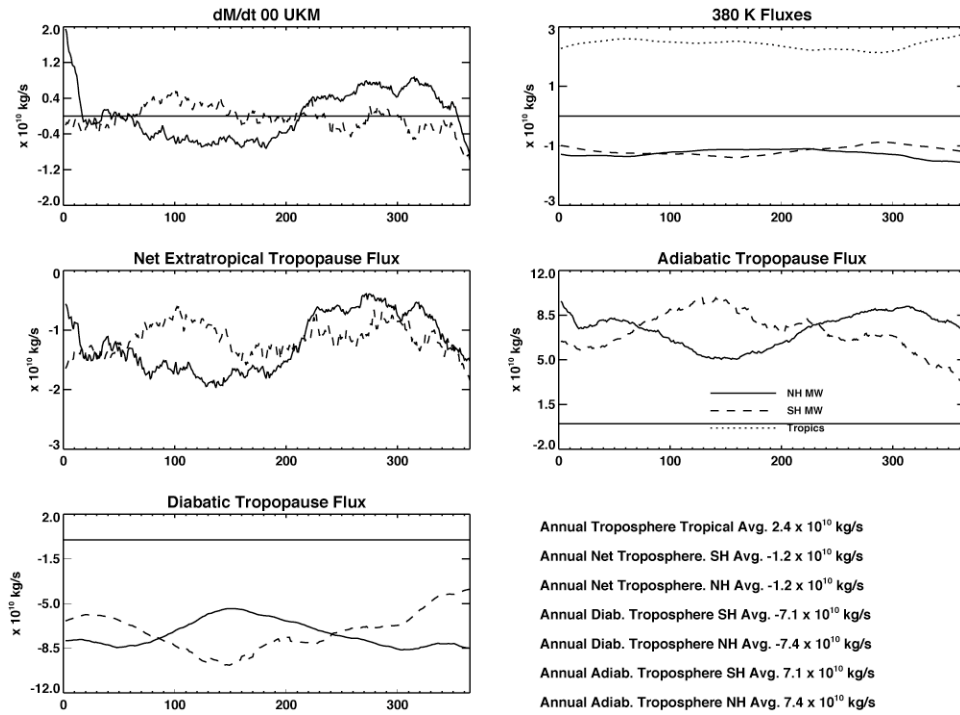


Figure 2.2.1.3 Mass fluxes and mass variations of the middle world computed using the off-line radiative transfer model and the UKMO assimilation for 2000. Solid lines are the NH, the dashed lines are SH, the dotted lines are (minus) the tropics.

Figure 2.2.1.4 shows the year-to-year variations in the annually averaged fluxes from the UKMO DAS and from the FVDAS (only 2000). At 380K the fluxes for FVDAS and UKMO agree. This figure shows that from the UKMO data adiabatic inflow into the middle world is a persistent feature; however, the FVDAS estimate of the magnitude of the adiabatic flux is very different and significantly smaller (by more than a factor of 2). The discrepancy lies in the estimate of the tropopause diabatic flux as indicated in Figure 2.2.1.4.

The source of these differences probably arises from the presence of cloud radiative heating near the tropopause although other differences in the assimilation procedure could also contribute to biases in the fluxes [Gettelman and Sobel, 2000].

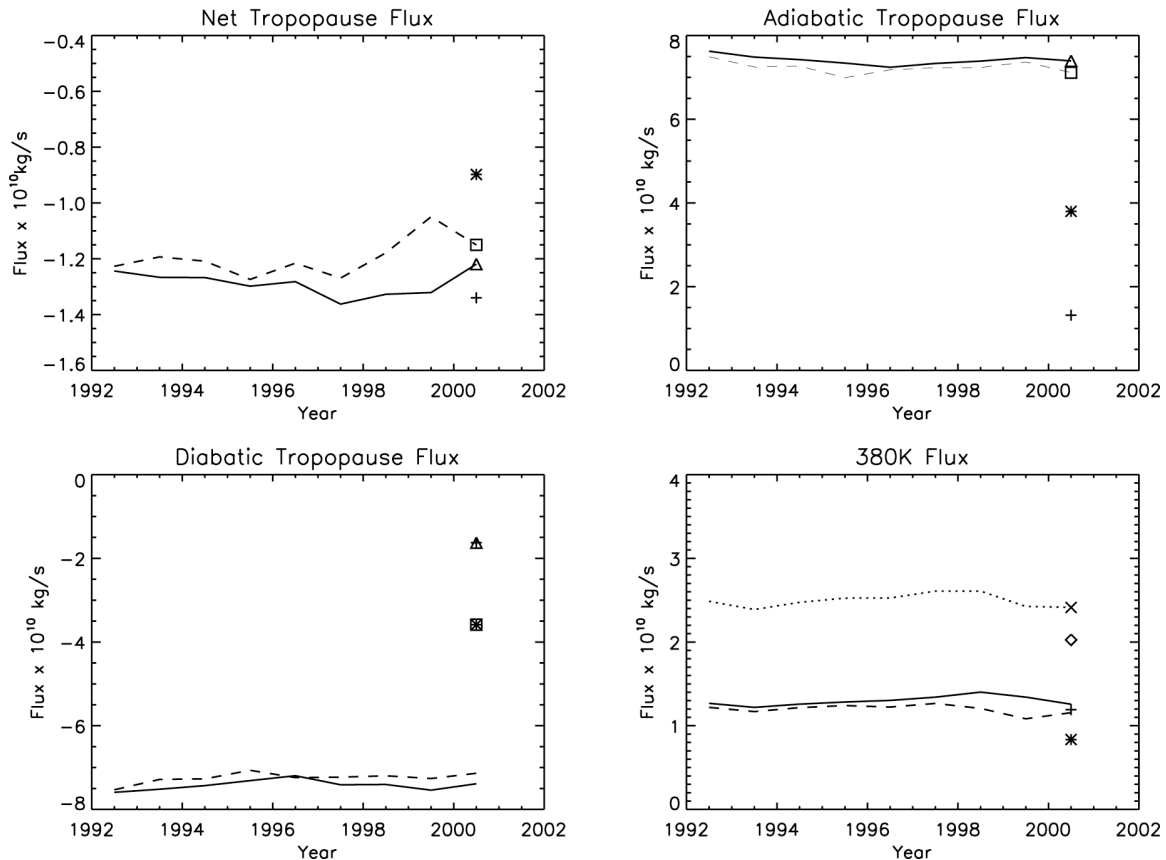


Figure 2.2.1.4 The annual variation in the fluxes across the troposphere and the 380K surface. Mass flux across the 380K surface (lower right), dotted line - tropical flux, solid line - extra tropical NH flux, dashed line - extra tropical SH flux. The + and * are NH and SH results from FVDAS, respectively. The triangle and the square are NH and SH results from FVDAS with the tropopause raised to 3.5 PVU. Upper left, the net tropopause flux computed using the Appenzeller et al. [1986] method which uses the 380K flux and the time rate of change of the middle world mass (see figure 2.2.1.3). Lower left, the diabatic cross tropopause flux computed from net radiative heating (UKMO case) and total radiative heating (FVDAS) case. Upper right, using the net tropopause flux and the diabatic flux the adiabatic flux can be computed. The x and diamond are the tropical upwelling fluxes for the 2 PVU tropopause and the 3.5 PVU tropopause cases.

The mass exchange between the troposphere and the stratosphere will no doubt be a powerful diagnostic on the capability of models to simulate that region. The current level of uncertainty – even that seen in Figure 2.2.1.4 – shows that the models have a long way to go in reconciling their analysis at the tropopause level. Additionally, constraints on the global mass flux discussed by Plumb [2002] have not been fully exploited. We propose to continue our research in this area. Just as our age spectrum inter-model comparisons provided new insights on capabilities of the DAS and GCM models, we expect that continued analysis of the mass exchange along the tropopause will provide a new diagnostic capability.

We propose to analyze the yearly variations of the FVDAS model back to 1991. The FVDAS has now been run for 1999 and 2000 but is just now completing the years 1991-1995. The analysis will also be extended to 2001-2. The FVGCM will also shortly complete a new 50-year run with greenhouse gas changes and we will apply our diagnostics to that run as well. Improved temperature retrievals from AIRS/AMSU should show up in improved FVDAS tropopause diabatic heating rates and we expect

that FVDAS analysis of the tropopause flux will change once the Aqua observations begin assimilation.

b. Ozone transport

Because of STE, the stratosphere is a significant source of ozone in the troposphere. Estimates of the stratospheric contribution to tropospheric ozone vary from 35%-10% depending on the model [Hauglustine et al., 1998]. Tropospheric ozone is a significant greenhouse gas as well [Lacis et al., 1990]. In addition, there is good evidence to believe that tropospheric ozone has increased in the northern mid-latitudes since pre-industrial times [Staehelin et al., 1994, Marengo et al., 1994]. Calculations of the radiative impact of the ozone increase vary from 0.2 to 0.6 Wm^{-2} [Houghton et al., 1995]. This wide range can be attributed to the short lifetime of tropospheric ozone (on the order of a few weeks) and a variety of natural as well as anthropogenic sources which leads to a highly variable distribution. Adding to the uncertainty in the tropospheric ozone variability is the stratospheric ozone contribution due to STE because locally STE is strongly correlated with meteorological events and varies with short-term climate change (WMO, 1986, Langford, 1999) as discussed in Section 1.2.3. It is upper tropospheric ozone which is most affected by STE and which also has the strongest climate forcing [Lacis et al., 1990]. Thus, even though the percentage contribution of stratospheric ozone to the total tropospheric ozone burden is expected to decrease as pollution-driven surface ozone sources increase, the stratospheric impact on the tropospheric ozone-forced climate change will probably remain significant.

We propose to use the Olsen et al. [2002a] algorithm with meteorological fields from the new FVDAS fields (1991-2002) to investigate seasonal and interannual variability and trends in cross-tropopause ozone flux. Since the flux locations are determined, both temporal and spatial trends and variability can be examined. These results will be interpreted in the context of stratospheric ozone trends and the relationship between STE and climate.

In addition to ozone transport into the troposphere we propose to look at unconventional regions for water vapor entry into the stratosphere. Convection and net radiative heating in the tropics are probably primary mechanism for transport of water vapor from the troposphere to the middle atmosphere [e.g., H95, Sherwood and Dessler, 2000]. However, other stratospheric injection sources have been recognized, including convection associated with monsoon activity [SPARC, 2000]. The extent to which the Asian and North American monsoons increase the water vapor in the lower and middle stratosphere remains unknown. Mote et al. [1996] describe the seasonal variability of the stratospheric water vapor as a "tape recorder" of tropical tropopause temperatures. In their work a discrepancy exists between middle stratospheric water vapor mixing ratios and the stratospheric entry mixing ratios found using back trajectories. Their 2-D back trajectories do not exhibit air originating from the Asian monsoon. The tropics are considered zonally symmetric in the transformed Eulerian mean formulation and the asymmetric monsoon outflow into the tropics cannot be resolved. However, Mote et al. note that the water vapor mixing ratios in the monsoon region are similar to the mixing ratios found later in the middle stratosphere. Dethof et al. [1999] show that water vapor may be transported to the stratosphere from the northern flank of the Asian monsoon. The Goddard kinematic trajectory model will be used to investigate the role the Asian and North American monsoons play as a source of stratospheric water vapor. Back trajectories of stratospheric air parcels will be calculated with 3-D wind fields from the FVGCM to determine the tropospheric source. Parcels of a monsoon origin may be transported directly to the extratropical lower stratosphere or may be advected to the tropics before convection lofts them to tropopause heights. The parcels' histories can be

examined to determine the relative importance of the seasonal monsoons to the midlatitude lower stratosphere and tropical stratosphere humidity. This activity is coordinated with the Dessler IDS (Appendix B).

2.3 (Q3) How does the long range transport of pollutants affect local air quality and chemical processes?

2.3.1 Aerosol transport and smoke

With the development of the kinematic trajectory model and the gradual extension of the IDS effort into the troposphere, we have begun investigate the transport of tropospheric pollutants. This new effort involves the use of Terra, Aqua MODIS aerosols [Kaufman et al., 2002] and TOMS aerosol data [Torres et al., 1998] as well as MOPITT CO data along with ground based aerosol information. Somewhat fortuitously, a significant aerosol event occurred over the east coast in July 2002. This event provides an excellent study topic and a chance to exercise the analysis tools developed under the PIDS.

2.3.1.1 The East Coast Smoke Event of July 2002

On July 5, 2002 wild fires broke out just east of Hudson Bay, Canada. These fires created a thick smoke plume that was transported southward along the flank of a northward moving low pressure system off the east coast. The smoke was transported as far south as North Carolina. Aeronet observations near Goddard Space Flight Center showed an optical depth of 7 (their limit) and smoke odor was noticeable at the surface. Aircraft observations (Bruce Doddridge, personal communication) showed ozone in the plume had risen to 120 ppbv and higher. There is good evidence that air quality in New England states was bumped to Code Red by this event alone. This event was similar to the Egnell Lakes Fire of 1982 (Eg event). The Eg event was probably the first smoke event of this type to be observed by satellite, although a comparable large-scale event was occurred in the 1950's [Westphal and Toon, 1991a].

An analysis of the East Coast event using the kinematic trajectory model and FVDAS data has been very useful. Figure 2.3.1.1 shows the smoke event as observed by SeaWIFS. The gap between the fresh plumes and the older smoke is due to the diurnal nature of the fires. This diurnal nature was established by GOES (Geostationary Satellite) IR fire channels and is consistent with gap between the younger and older plumes shown in the figure.

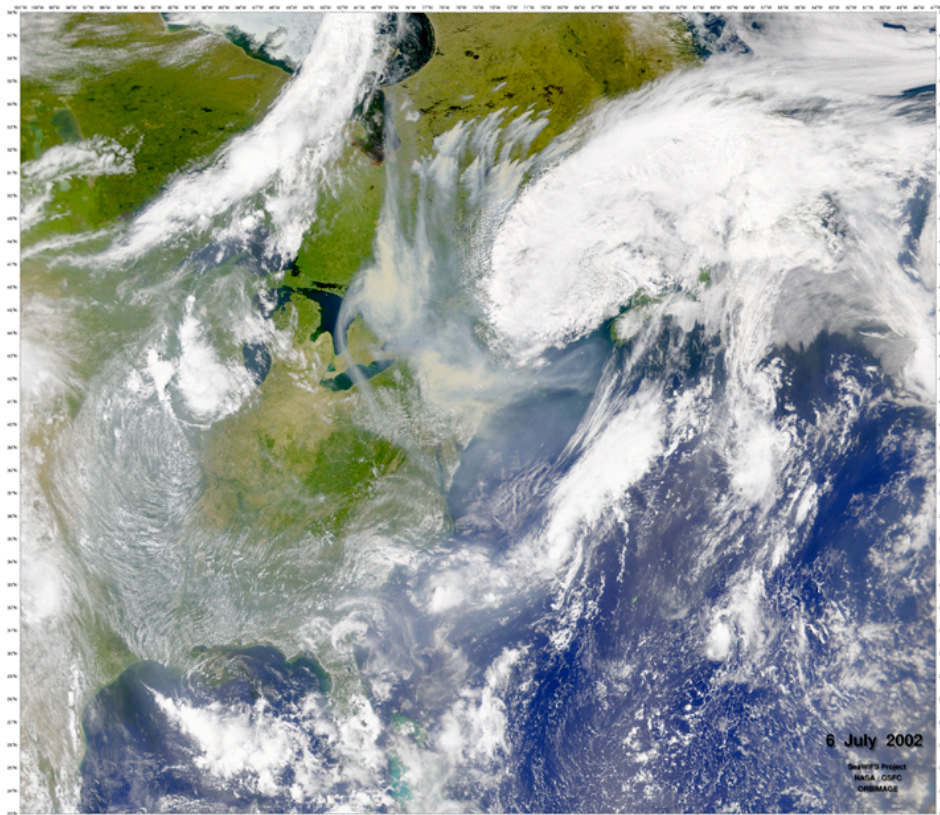


Figure 2.3.1.1 SeaWiFS image of the smoke plumes east of Hudson Bay on July 6, 2002. Smoke can be distinguished from cloud by its faint yellowish color.

Our trajectory analysis also showed that the smoke event consisted of several plumes that resulted from diurnal fire variability. (Apparently forest fires flare up during the day when they can be fanned by boundary layer winds, and then bank down at night.) The trajectory studies showed a strong correlation between the TOMS aerosol index and parcels which had passed over fire region. However, TOMS did not detect the smoke at the source region. TOMS detects the presence of smoke layers based on the interaction between aerosol absorption by carbonaceous aerosols and the large Rayleigh scattering component in the near ultraviolet region (330-380 nm). TOMS uses measurements of radiances at two near UV wavelengths to calculate an aerosol index [Torres et al., 1998]. The detection of smoke by TOMS is possible even over bright backgrounds such as cloud decks and over snow/ice covered surfaces. Our preliminary study showed TOMS detection of smoke was superior to the MODIS aerosol algorithm over land. The altitude of the plume used for the trajectories was fixed by the aircraft observations. In the future, IceSat or CALIPSO lidar observations can help us fix the height of the cloud.

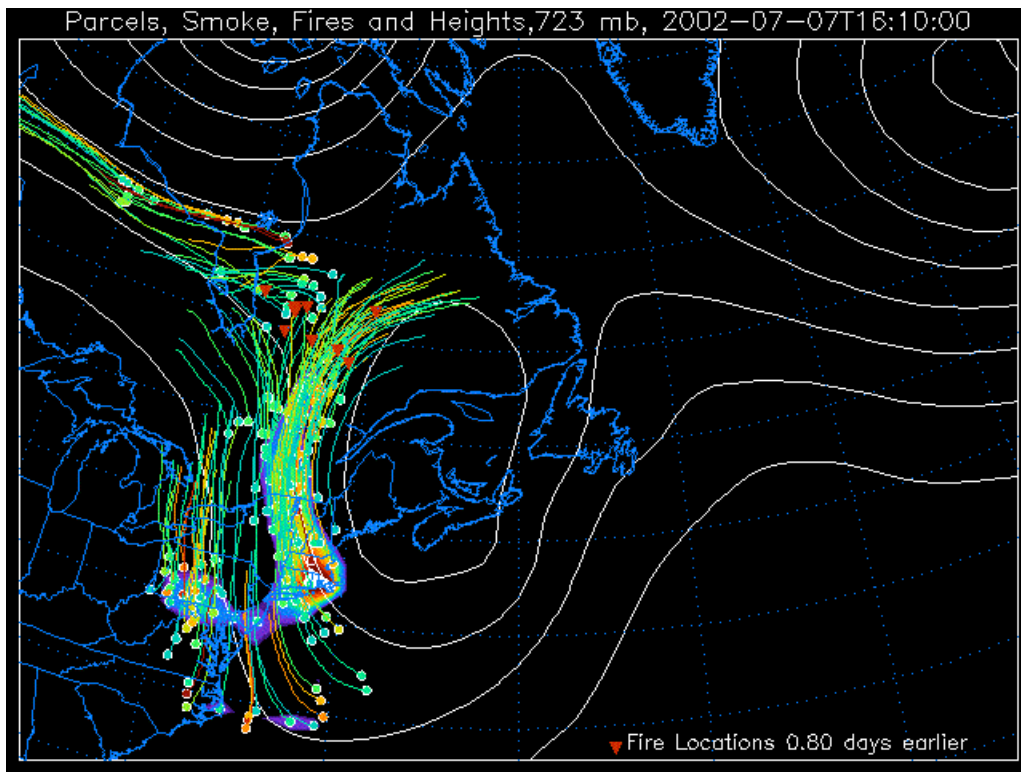


Figure 2.3.1.2 Trajectories for the smoke event of July 7 2002. Colored lines with terminating as dots show the trajectories – the dots are show the position and the tail shows the trajectory history over 24 hours. The color of the dot indicates an aerosol index value from TOMS. Red inverted triangles show the location of fires. Contours are the geopotential height of the pressure surface associated with the parcels (723 hPa). Overlaid on the parcel plots is the TOMS aerosol index value (high values are red/white – low values are blue). Note the parcels are curving around the low pressure system over eastern Canada.

Figure 2.3.1.2 shows the trajectory analysis. The trajectories are initiated from the TOMS data and run backward then forward from July 3. The tails on the trajectories are one day long. Fire locations were hand digitized from GOES data and are shown as red inverted triangles. The mean altitude of the trajectories is 723mb. The parcel tails show that the TOMS smoke initiated trajectories passed near or over the fires. The correlation between the distance between the trajectories and the fires is shown in Fig. 2.3.1.3. This figure shows that high aerosol amounts generally correlate with close proximity to the fire while lower aerosol amount is found further from the fire. However, unexpectedly low aerosol amounts are found for trajectories that passed very close to the fire. This suggests that some fires were not able to loft significant material into the free troposphere.

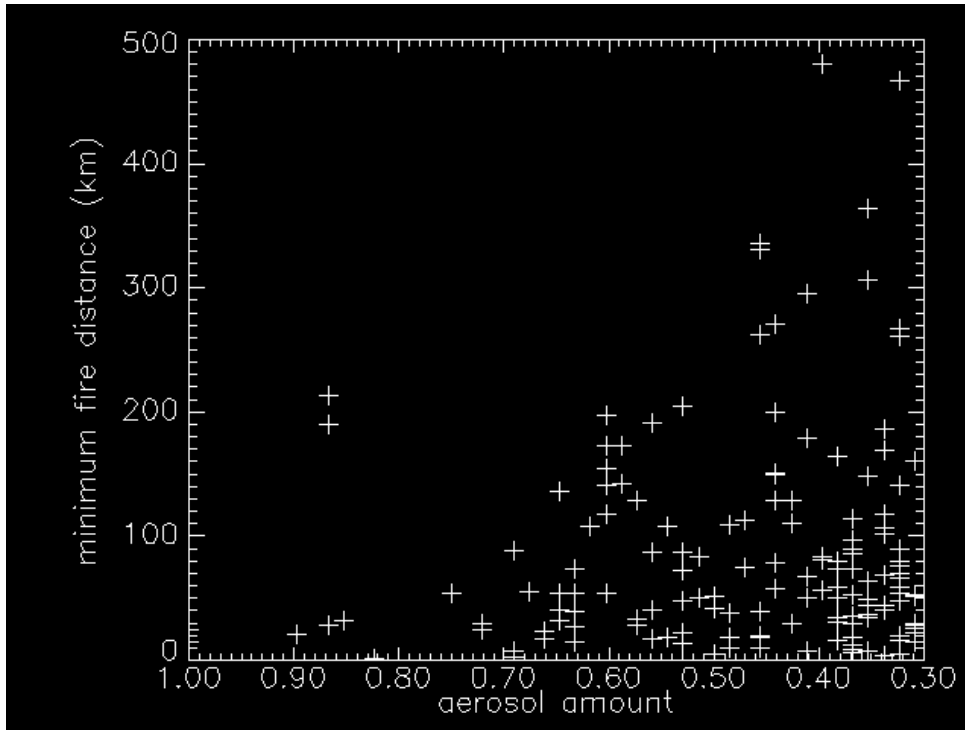


Figure 2.3.1.3 shows the correlation between the aerosol amount (from TOMS – the aerosol index) and the minimum distance from the trajectory to the fire.

The coupling of the free troposphere to the pollution source is a key issue in the transport of pollution from the source. How does the pollution get into the free troposphere? How does the pollutant, once in the free troposphere, couple back to the surface? In the case of the smoke event, this latter question can be addressed using MPL (Micropulse Lidar) data taken over Goddard. Figure 2.3.1.4 shows the MPL data for the smoke event. Superimposed on the image is the boundary layer height calculated using the FVDAS. The white arrow shows where the boundary layer is predicted to intercept the smoke plume. At roughly that point in time the aerosol is seen throughout the boundary layer indicating that the plume has been coupled to the surface.

This observation demonstrates an important process by which material in the free troposphere moves to the surface under non-frontal conditions. Namely, the boundary layer turbulence has to reach the plume in the free troposphere. This tells us not only the minimum height of important plumes (they must be near 2 km in this case) but also the time of day the material will be transported to the surface (during the late morning and afternoon, but not at night).

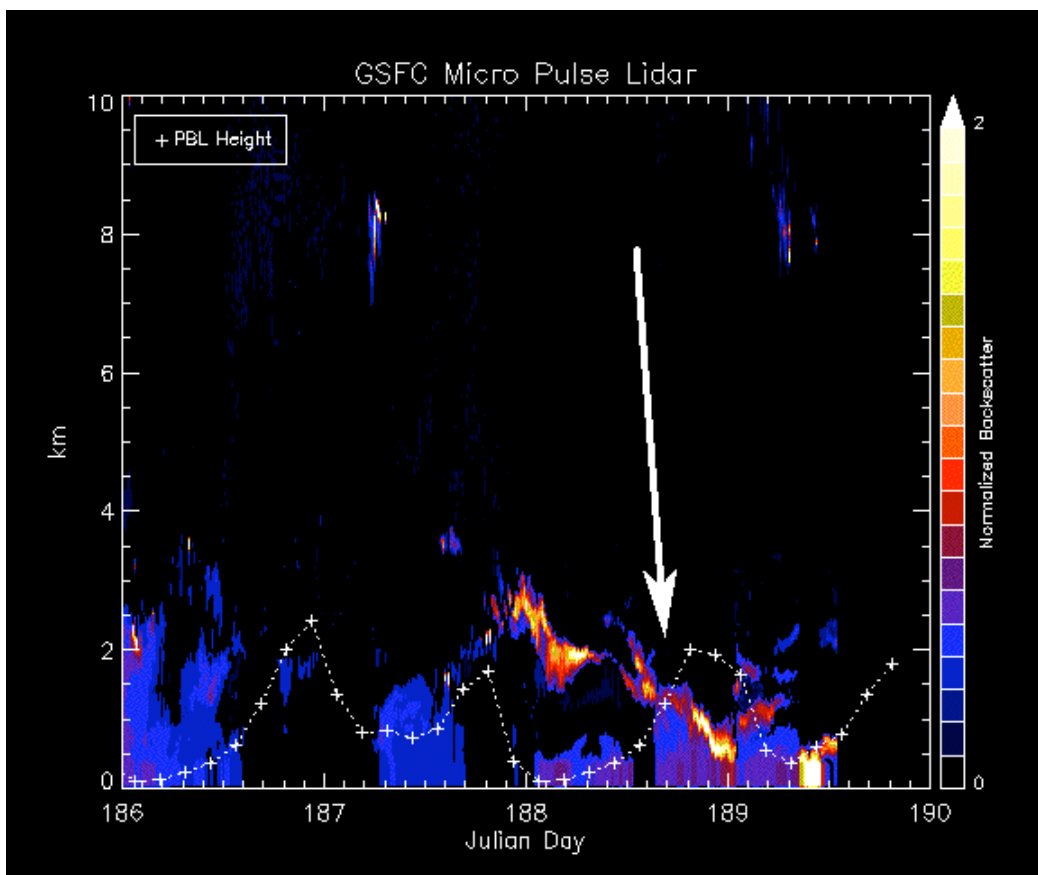


Figure 2.3.1.4 MPL data from GSFC showing the aerosol layer for the smoke event of early July 2002. The dotted line is the analyzed boundary layer height. The arrow shows where the plume couples to the surface through boundary layer turbulence.

2.3.2.1 Proposed Research on Smoke Plumes

Smoke plumes from large fires are observed to affect the surface temperature through the attenuation of solar radiation as a result of both absorption and reflection. As the smoke particles coagulate, their radiative impact increases. For example, Westphal and Toon [1991a] computed that the increase in particle size after 42 hours could increase the radiative forcing by 11%, and the Eg fire appeared produced a cooling of about 5K at the surface [Robock, 1988].

There are currently large uncertainties associated with the importance of black carbon to both direct and indirect climate forcing. Additionally, aerosol and chemical species associated with smoke plumes have uncertain, but probably large effects on pollution downwind of source regions. The extent to which pollutants transported in smoke plumes may affect downwind air quality and have regional health effects depends not only on the plume composition, but also on its transport pathway. In particular, the altitude the plume is emitted and subsequently transported at has large implications for where it is transported to and how long it resides in the atmosphere. Complicating factors include the chemical evolution of the aerosol particles and the radiative effects on the plume [Westphal and Toon, 1991a,b]. The NO_x emission from the fires means that elevated ozone often accompanies the plumes ($\text{NO}_2 + h\nu$ ($\lambda < 420 \text{ nm}$) $\rightarrow \text{NO} + \text{O}(^3\text{P})$) followed by $\text{O}_2 + \text{O}(^3\text{P}) + \text{M} \rightarrow \text{M} + \text{O}_3$.

Current climate models will typically mix smoke from biomass burning uniformly throughout the model planetary boundary layer. Smoke from boreal forests, however, may be emitted at a much higher effective altitude and subsequently transported much further [Lavoue et al., 2000]. We propose to investigate the altitude of smoke injections through use of a chemical transport models, trajectory studies and satellite observations. Large scale simulations may be carried out using GOCART (Appendix D). More focused studies, including an analysis of the summer 2000 Canadian smoke transport, are being conducted with the NASA/University of Colorado Community Aerosol and Radiation Model for Atmospheres (CARMA) [Toon et al., 1988]. Earlier versions of CARMA were employed in the analysis of the Eg fire [Westphal and Toon, 1991b]. More recently, CARMA has been coupled to NCEP/NCAR reanalyses to study dust [Colarco et al., 2002]. CARMA contains a full microphysical package, so that it is possible to model the smoke aerosol particle size distribution with any desired level of detail. This allows us to study coagulation and water uptake on the smoke particles and then study the subsequent effects on light scattering and absorption. CARMA is computationally inexpensive because it is run over a limited domain using archived meteorological fields.

The ability of the current array of satellite sensors to monitor smoke plumes has expanded enormously [Kaufman, et al., 2002] since the Eg study. IceSat lidar data, which provides aerosol altitude information, should be available in early 2003, may be used to estimate the smoke injection altitude. Data from MPLNet (micro-pulse lidar network) will be useful for validating emission altitudes and for looking at smoke plume transport into the boundary layer downwind from sources, while GLAS will allow us to probe the plume altitude closer to source regions. An improved understanding of smoke injection heights will allow us to better constrain downwind pollution and the effects of biomass smoke on climate forcing.

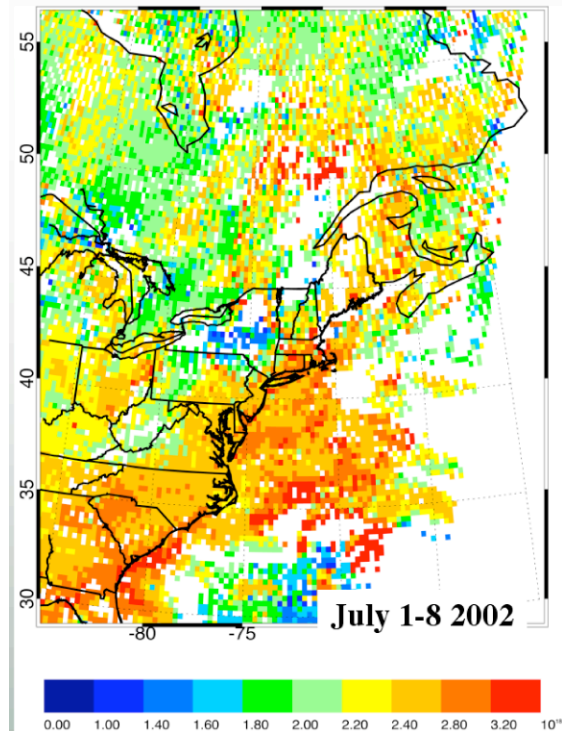


Figure 2.3.2.1 CO observations of the East Coast fire event from MOPITT averaged over 8 days. Units are 10^{18} mol/cm² (From Dave Edwards and the MOPITT team.)

Work by Lavoue et al. [2000] shows that ground based intensity and the height of injection form a linear relationship for Canadian crown fires. With the MODIS 4 μ and 11 μ fire algorithm [Kaufman et al., 1998] it should be possible to develop a satellite based intensity measure from which the fire injection height can be computed. This height can be verified with IceSat lidar data or from subsequent computations of plume evolution [Allen and Schoeberl, 1999]. CO observations should also be helpful in diagnosing the fire impact (see Figure 2.3.2.1) GOES observations will allow us to track the time dependence of the fire intensity – this time dependence is critical for defining the plume structure as was found in the East Coast fire event. Once the plume reaches the free troposphere, we can use trajectory calculations to estimate the plume structure with high time resolution. We can then use the boundary layer height information to assess the impact on surface air quality, especially PM_{2.5} and ozone, as monitored by the Environmental Protection Agency (EPA) [Finlayson-Pitts and Pitts, 1997]. If this capability of predicting surface air quality is found to be effective, it may provide a global capability to directly assess air quality effective due to natural and man-made point sources of intense aerosol pollution.

MOPITT observations have recently revealed spectacular examples of global CO plumes as shown in Figure 2.3.2.2. The origin of the plume is not clear since high CO data is seen over the whole south central African biomass burning region, and the MOPITT observations do not give us any clue as to the altitude or exact origin of the plume.

We can estimate the origin and altitude of the plume shown in Figure 2.3.2.2 using the trajectory model and the procedure described by Allen and Schoeberl [1999]. Figure 2.3.2.3 shows a sixteen-day back trajectory calculation at 320 K (developed as a reverse domain fill experiment). Parcels are tagged if they move over the square shown in the figure, best agreement with observations are obtained by advecting the parcels at the 320K surface. What is evident in the simulation is that the trans-Pacific plume is originating from the 10°-20° S region. Furthermore, the enhancement over South Africa may be due to a plume as well.

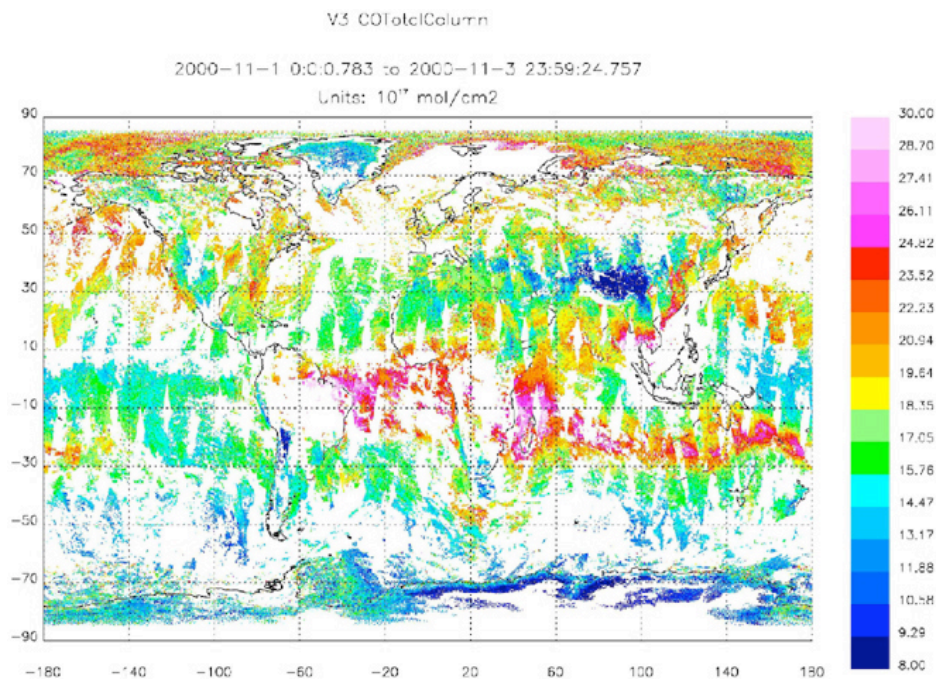


Figure 2.3.2.2 MOPITT data for November 2000. Note the plume of high CO extending eastward from southern Africa across the date line. Provided by Dave Edwards (NCAR) of the MOPITT Team.

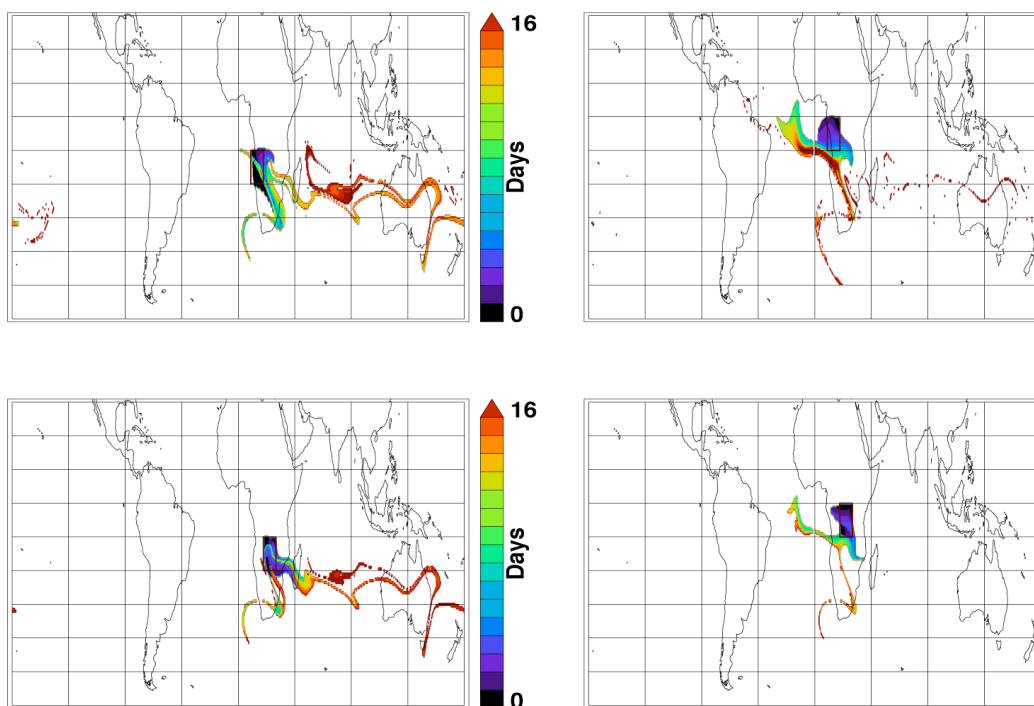


Figure 2.3.2.3 Simulation of MOPITT data for November 3 2000. RDF trajectory calculation was run for 16 days over the tropical region. Parcels were tagged with the date when they passed over the square regions shown in each figure. (Squares are 10° wide (latitude & longitude). The age of the plume is shown in color. Compare with Figure 2.3.2.2

Back trajectory studies combined with CO and aerosol measurements will allow us to better characterize global transport in the tropics and ultimately help understand the tropospheric ozone distribution and its anomalies [Thompson et al., 2000]. As we refine our proposed simulation of smoke plumes, we intend to expand our studies to the biomass burning regions of the tropics. The focus of concern is the buildup of tropospheric ozone over the South Atlantic that has been diagnosed from both tropospheric ozone residual methods and SHADOZ sondes [Thompson et al., 2002] (Figure 2.3.2.4). Moxim and Levy [2000] using GFDL models suggest that the anomaly is primarily due to lightning rather than biomass burning. This conclusion is supported by preliminary analysis of the MOPITT data that shows the lack of a CO plume in the ozone anomaly region (Edwards et al., 2002). NO_x generated by lightning will not show a CO signature unlike NO_x generated from biomass burning, (NO_x is a precursor to ozone.) However, the SHADOZ ozonesonde data shows the tropospheric ozone anomaly penetrates nearly to the surface suggesting multiple sources of ozone since a lightning source would produce a high altitude anomaly. Indeed, Thompson et al. [2001] suggested multiple sources for tropospheric ozone in the Indonesian fires that occurred during the last El Niño. There are several hypotheses to test here: Could the ozone anomaly be due to multiple sources? Why doesn't the anomaly disperse along the subtropics – what maintains the anomaly? What are the relative roles of biomass burning and lightning? An intriguing finding from a preliminary data assimilation of early 1998 SBUV ozone in the FVDAS [Hayashi et al., 2002] is advection of middle and upper troposphere ozone from higher latitudes toward the tropical Atlantic. The variability observed over the south Atlantic compares well with ozonesondes from Ascension Island (8S, 15W) during the early 1998 period. Likewise, comparisons between assimilated ozone and sonde profiles at Fiji (18S, 178E) at that time are very good. Meridional advection has not been considered as a possible contributor to the south tropical Atlantic ozone maximum and needs to be studied further.

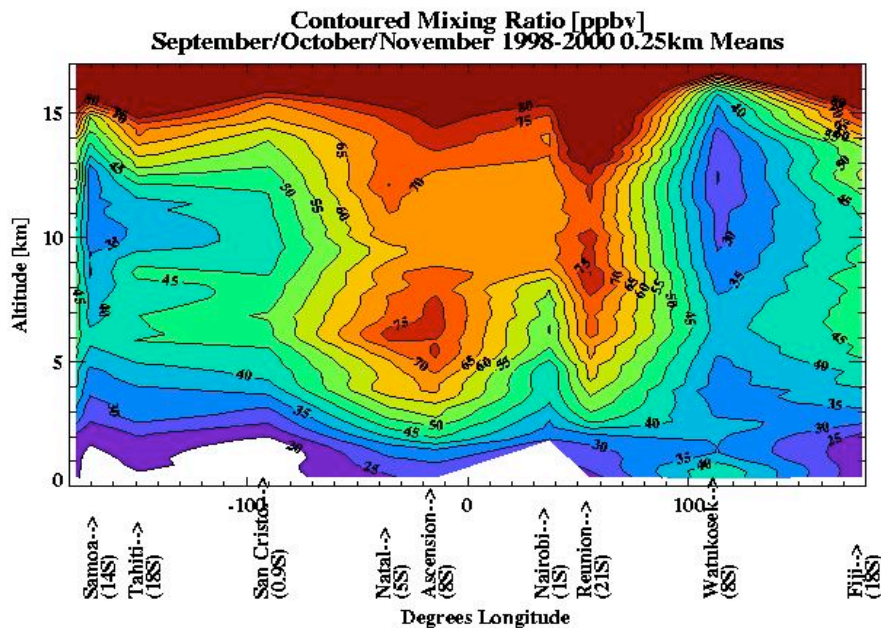


Figure 2.3.2.4 SHADOZ analysis of tropospheric ozone from sondes stations indicated in figure. The high values of ozone shown in the center of the figure indicate are due to the South Atlantic ozone anomaly.

For tropical plumes of aerosol, CO and ozone, the goal of the trajectory studies will be to compare the transport properties of GOCART with observations. The transport questions must be resolved before an assessment of the ozone anomaly simulation can be determined. We propose to make such transport assessments in this proposal. In the next section we describe in more detail the role of modeling studies in our overall effort.

2.4 (Q4) How do chemical changes in the atmosphere affect climate?

To answer (Q4) we will be using a number of models that are described in Appendix C and D. The models are appropriate for different applications, as there are trade-offs between speed and complexity, and different types of experiments that will be proposed. Figure 2.4.1 shows a cartoon of the various models discussed below with a rough assessment of their relative computational speed. Clearly the computationally cheaper models are more useful to “explore parameter space” and to gain insight into feedbacks. The more complex models are useful in assessments and increasing our confidence that the interactions seen in the simpler models provide insight into actual atmospheric processes. We do not propose development of any of these models – it is beyond both our budget and scope, but our proposal includes improvements to some of them.

IDS Models

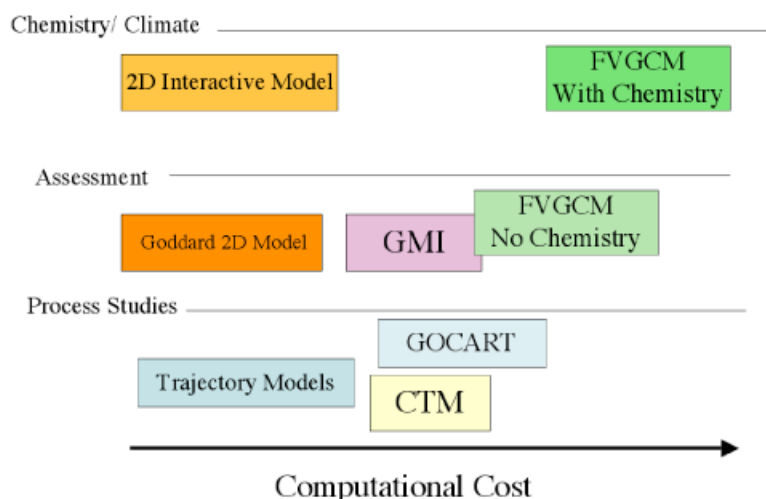


Figure 2.4.1 The relationship between the various models described in this proposal. The models can be categorized roughly by uses. The trajectory models and the stratospheric CTM (chemical transport model) are used primarily for process studies. Results from these process studies support assessment applications. The Goddard 2D model, the GMI (Global modeling Initiative Model) and GOCART aerosol model (Appendix D.4.1) are used in processes studies and assessment calculations. Like the GSFC CTM, the GMI calculates constituent evolution using meteorological fields from assimilation systems or general circulation models. FVGCM can be used in a climate assessment mode but has no interactive chemistry. The Interactive 2D model is used for climate/chemistry studies. Eventually the chemistry elements of GMI will be incorporated into the FVGCM. This fully coupled 3D model does not exist yet.

2.4.1 The Interactive 2D model

The interactive 2D model has proven to be a useful tool for investigating the links between climate change and chemistry in the stratosphere. For this investigation we propose to study is the impact of long-term increases in stratospheric water vapor on stratospheric dynamics and chemistry. Rosenlof et al. [2001] combined existing water vapor data sets to show a 1%/year increase in stratospheric water vapor over the 1954-2000 period. In preliminary work with our 2D model, a water vapor trend of 1%/year was imposed in the stratosphere. Figure 2.4.1.1 shows that this trend might have a major impact on global ozone, delaying recovery by more than twenty years. Dvortsov and Solomon [2001] found a delay in ozone recovery at a northern midlatitude with a 2D model as well due to water vapor increases mainly as a result of increased HO_x losses.

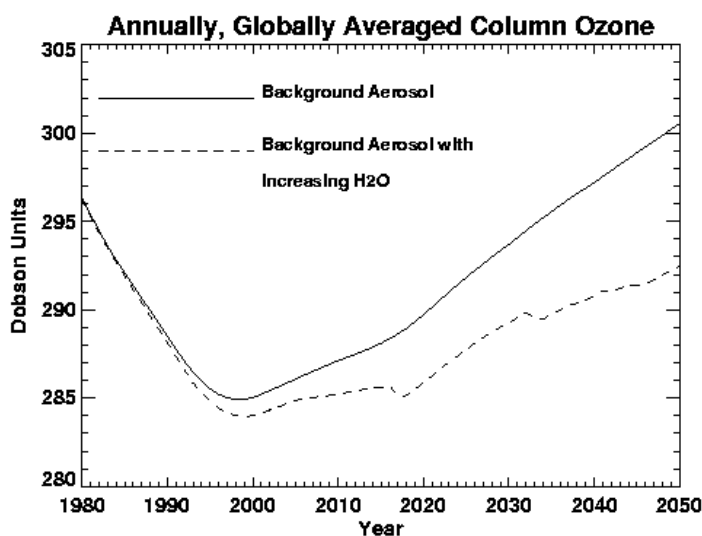


Figure 2.4.4.1 Globally and annually averaged column ozone from the 2D model showing the delay in recovery of ozone if 1%/year increase in water vapor is included.

Our mode is more complex. We find that the increased water vapor affects the PSC's in our model leading to more polar ozone loss, thus our preliminary results show a larger impact on ozone recovery. We propose to examine the effects of increasing water vapor more extensively, including possible feedbacks on circulation and other chemical species. Because the results are sensitive to the PSC algorithm [Considine et al., 2000], we will compare its performance in 3D simulations with its performance in the 2D framework.

2.4.2 The Three Dimensional Constituent Modeling: Development and Applications

2.4.2.1 Troposphere-Stratosphere CTM

Ozone in the upper troposphere is an important greenhouse gas, and its evolution is affected by local photochemistry and by transport both within the troposphere and from the stratosphere. Although many photochemical processes of importance to the troposphere are not important to the stratosphere, and vice versa, the linkage between the stratosphere and troposphere makes it necessary to develop modeling capability to address the entire region. We will continue to develop such an in-house modeling capability by capitalizing on our involvement with the Global Modeling Initiative (GMI) as detailed in Appendix C. A near-term goal of GMI is identification of a minimum photochemical mechanism to represent the photochemical processes that contribute most strongly to ozone evolution in the upper troposphere and lower stratosphere. The chemical mechanism will be defined, evaluated, implemented in the GMI CTM framework, and made available to all GMI team members. In addition to our participation in evaluation of this combined stratosphere/troposphere version of the GMI CTM, we will implement the combined mechanism in our CTM framework (Appendix D.2) and use this capability in process studies.

The current CTM capability will be extended downward into the free troposphere and at some point linked to the GOCART model system. This merging of models will take place over the next few years, but it is not part of our proposal activity. What we do

propose to do is use the merged model (eventually) and GOCART initially to look at biomass burning events as described in the smoke research (Section 2.3.2.1) and extend this research to looking at ozone and ozone transport – first as a result of boreal fires and then inside the tropical region. The goal here is to look at ozone generation as a contribution to greenhouse gas increases. Previous studies (e.g., Mickley et al, 2001) have been limited in that the models used could not correctly assess the flux of ozone from the lower stratosphere into the upper troposphere. Our efforts to quantify ozone STE and evaluate modeled STE for meteorological fields from the FVGCM and FVDAS (section 2.2.1) will contribute to this application.

Aura and Envisat instruments will provide detailed information on the upper troposphere and lower stratosphere (See Table 2.3). We propose to evaluate the importance of short-lived halocarbons to the stratospheric burden of chlorine and bromine using Aura data to evaluate relevant aspects of model transport. The HIRDLS instrument will provide profiles of ozone, H₂O, N₂O and other constituents at about 1.5 km vertical resolution into the upper troposphere in the absence of clouds. This data set will enable a thorough evaluation of model processes that contribute to transport between the upper tropical troposphere and the lowermost stratosphere [e.g., Ray et al., 1999; Nielsen and Douglass, 2001]. Accurate representation of such transport, including its seasonal and longitudinal variability, is key to evaluating the importance of the short-lived halocarbons. Results from Schoeberl et al. [2002] and Douglass et al. [2002] show excessive ventilation of the tropics produced by winds from various data assimilation systems. We propose to make comparisons of observed and modeled constituents in this key region of the atmosphere. Such comparisons will provide information to improve the representation of processes in the FVGCM, and also lead to improvements in the transport associated with the FVDAS fields.

2.4.2.2 The Fully Coupled General Circulation Model with Chemistry

A central focus for atmospheric research has long been development of the capability to evaluate the response of atmospheric composition and climate to natural and anthropogenic forcing. The ideal assessment model will represent the dynamic, radiative, and photochemical processes and coupling between them. Such efforts have a long history. The FVGCM, which was developed in collaboration with the National Center for Atmospheric Research (NCAR), uses a flux-form semi-Lagrangian transport scheme [Lin and Rood, 1996, 1997] and a quasi-Lagrangian vertical coordinate system [Lin, 1997] to ensure accurate representation of transport by the resolved-scale flow. We have used the daily averaged meteorological fields from FVGCM in our CTM framework. Physical parameterizations in the current version of the FVGCM come from the Version 3 NCAR Community Climate Model [Kiehl et al., 1998]. The FVGCM is described in Appendix D.

Analysis of the results of CTM calculations using meteorological fields from the FVGCM have prepared us to participate in the development of this fully coupled model. Computational resources are available to include the full photochemical calculation that replaces the climatological ozone currently used in the FVGCM. This effort is being accomplished in collaboration with the primary developer of the dynamical core of the FVGCM, S. J. Lin of the GSFC Data Assimilation Office (DAO). Evaluation of the coupled model using comparisons of constituents with observations will benefit from our broad experience in analysis of off-line transport.

As the fully coupled model is developed by the DAO, we propose to analyze its output. The differences between observed and modeled constituent behavior will provide an independent source of information for evaluating model performance, particularly in the

tropics where most observations are of temperature and where the temperature and wind fields are not strongly constrained. This evaluation will follow our GMI experience, and emphasize development of quantitative diagnostics from constituent observations. Evaluation of this model will be used to identify the consequences of the zonal-average approximation for applications of the interactive 2D model to issues such as the impact of a trend in water vapor on the future behavior of stratospheric ozone. The ultimate goal of the process studies and the comparisons of the representation of processes in 2D and 3D models is to improve the physical basis of assessment models thereby reducing uncertainty and increasing confidence in the results. The actual assessment calculations will most likely be undertaken through the GMI effort (Appendix C).

2.5 Statistical Analysis of Data Sets and Aura Validation

Inhomogeneity in atmospheric chemical fields makes validation of satellite measurements complex. Work under the PIDS on validation issues included an estimate of the contribution of geophysical variability to differences between local (in situ) and satellite measurements. The motivation for these investigations comes our link to the EOS missions, especially Aura, and our participation in validation and other field campaigns associated with missions. Figure 2.5.1 shows the result of a statistical analysis of over 10^6 high-resolution measurements of ozone taken over two decades of NASA ER-2 measurement campaigns in the lower stratosphere. The data was used to estimate the statistics of differences between point measurements and satellite measurements separated by a horizontal distance G . Satellite measurements were simulated by locally averaging over a distance L on the order of the satellite footprint. The Fig 2.5.1 is an estimate of the seasonal and latitudinal dependence of the contribution of geophysical variability to in situ/satellite measurement differences. In the northern hemisphere for example, we can expect differences on the order of 5-10% during the summer, but these increase to about 20% during the winter. A similar analysis will be performed with aircraft measurements of tropospheric chemical species. We also propose to extend this work in several ways. First, the same type of analysis will be applied to ozonesonde data to estimate the contribution of vertical layering. Second, we will investigate horizontal anisotropy to assess whether coincidence criteria should distinguish between zonal and meridionally oriented separations between measurements. Third, we will use scale dependent two-point statistics of differences between two points to define seasonal and latitude dependent coincidence criteria from the correlation length of the chemical field. The results of these studies will aid in interpreting differences in correlative measurements on different platforms, and will provide direction in the development of validation strategies that minimize the impact of natural variability.

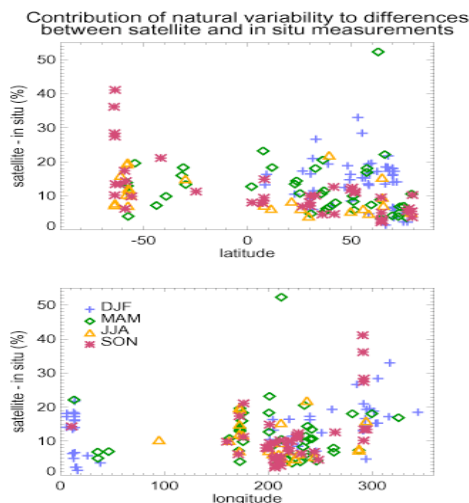


Figure 2.5.1 The contribution to geophysical variability from a statistical analysis of over 1 million high resolution measurements of ozone taken over two decades of NASA ER-2 measurement campaigns in the lower stratosphere. Colors indicate seasons.

Another goal of this statistical analysis effort is the formulation of meaningful tests of model/measurement consistency under conditions of extreme spatiotemporal variability. We will make use of the GOCART aerosol transport model and the smoke trajectory calculations described above. In both cases it is important to evaluate the extent to which the model simulations are consistent with the observations. The aerosol field is highly inhomogeneous due to the small scale and temporally intermittent nature of the surface aerosol sources and their short atmospheric residence time. Figure 2.5.2 shows a comparison of statistics of 550 nm total extinction a_{550} from the Goddard GOCART model and 10 min. averaged aircraft measurements taken during the ACE-ASIA campaign. Below the boundary layer, the overall range of the variability in model total extinction agrees very well with the measurements, indicating that the model simulation of sources and boundary layer processes is reasonable. Both are biased high relative to the regional distribution, which reflects the mission objectives in sampling high aerosol sources. Above the boundary layer, the measurements agree with the model regional distribution, but the mission-sampled model (model interpolated to flightpaths) was clearly biased high. This may indicate a problem with the model convection and aerosol removal.

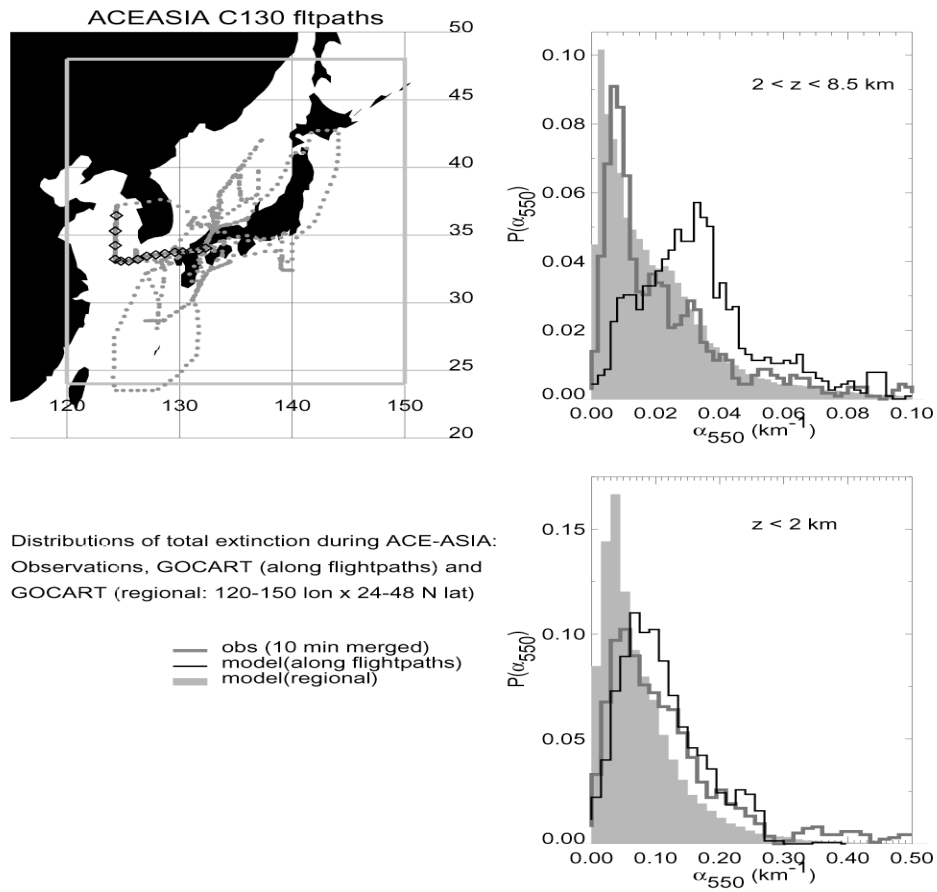


Figure 2.5.2 See figure for caption

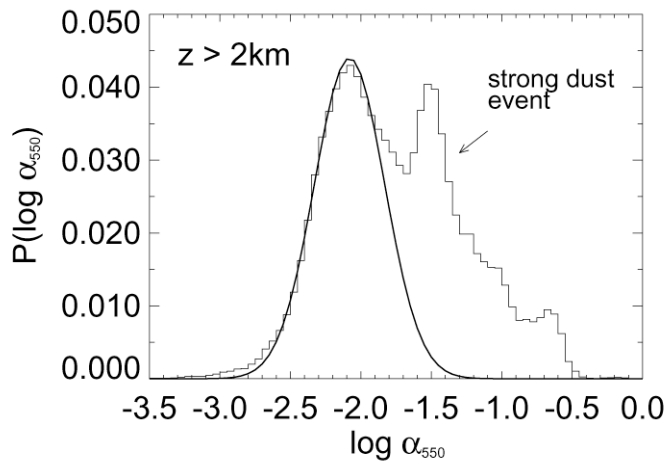


Figure 2.5.3 The distribution of aircraft measurements of total extinction above the boundary layer.

Quantitative assessments of climate perturbations in, for example, aerosol radiative forcing are not possible without a clearly defined background reference state. Research under this IDS also includes an investigation of the problem of defining quantitatively changes or perturbations to the climate. Variability in atmospheric chemical constituents tends to be non-Gaussian [Sparling and Bacmeister, 2001], thus large departures from the most probable value can in fact be part of the normal range of variability. Analysis of upper level aerosol variability measured during ACE-ASIA illustrates this point. Figure 2.5.3 shows the distribution of aircraft measurements of total extinction above the boundary layer. The distribution of $\log a_{550}$ shows an embedded Gaussian distribution around the most probable value which we identify as the background distribution. Because the distribution $P(a_{550})$ is lognormal, values of total extinction several times the most probable value are within the typical range of variation. This idea will be tested with other aerosol and chemical data sets to see whether background distributions can generally be defined by this method.

We propose to continue this kind of statistical analysis with regard to Aura validation measurements – applying our approach to the measurements made by Aura and by other elements in the Aura – Aqua formation that includes CALIPSO and CloudSat.

2.6 Other Relevant Activities

Although the activities described above will be the main focus of our investigations over the next three years, we would like to note here the involvement of the IDS team in scientific leadership and validation activities.

2.6.1 Leadership in orbital missions

The PI and one of the COI's (Douglass) continue in their role in Aura Project Management. The science activities performed here have lead to insights into mission strategies and aided us in developing the Aura validation plan. (<http://eos-chem.gsfc.nasa.gov/mission/validation.html>). This includes development of aircraft mission plans that will use some of the statistical approaches discussed in Section 2.5.

2.6.2 Leadership on sub-orbital missions

The PI and a CoI (Newman) will be Co-Project Scientists for the SOLVE II DC-8 Mission. The participation in these missions includes the use of the flight planning and modeling tools developed within the IDS. Newman is leading the development of the AVE (Aura Validation Experiment) mission plan as well.

3.0 Timeline and Expected Results

First proposal year (FY04):

Analysis of STE in new 50 year run of FVGCM and re-analysis of 1991-2002 DAO data. This model includes some trace gas changes with year. CTM runs with full chemistry along with age-spectrum analysis will be used to diagnose the runs. Compare STE in GCM with estimates from observations and DAS models.

Analysis of Sage III Ozone Loss and Validation Experiment II (SOLVE II) observations. Begin MATCH type analysis of SAGE III and POAM satellite observations

Analysis of additional Boreal smoke events. Simulations include CO and ozone from GOCART. Begin analysis of tropical processes from GOCART – compare to MOPITT observations.

Begin trajectory analysis of tropical biomass burning events. Begin looking at IceSat lidar data for aerosol heights.

2D model runs with increasing water vapor and short-lived halocarbons.

**Second proposal year (FY05):
(EOS Aura data becomes available – Aura is beyond commissioning phase)**

Continued analysis of Boreal smoke events using Aura data, begin extension of smoke analysis into the tropics. Look at ozone processing and NO_x from OMI. Begin activity on tropospheric ozone.

Begin analysis of extratropical STE events using Aura data.

Participation in Aura validation missions (Probably TC3 proposed mission)

Begin preliminary analysis of Aura data and CTM and GMI model intercomparisons.

Third proposal year:

Continued analysis of smoke events – include tropospheric ozone analysis from models and compare with Aura observations (using TES and difference techniques)

Continued model analysis. At this point, FVGCM should include some interactive chemical processes. We will apply our analysis tools to this new model.

Continue other activities as appropriate.

4.0 Management Plan

The PI will manage the proposal. Since all but one of the co-investigators are on site at GSFC at least one day per week, we do not see any issues with travel. Gary Morris typically spends the summer at GSFC. Monthly meetings have been used in the past to coordinate overall activities.

Project Responsibilities

Q1 - Is the ozone layer recovering?

This area will be coordinated by the PI. G. Morris is responsible for the MATCH type analysis and P. Newman will analyze the 3D model CTM and OMI observations. Stolarski will also be looking at ozone trends between instrument types.

Q2 - Do we understand the processes that control mid-latitude STE?

This area will be coordinated by the PI and A. Douglass. M. Olsen will work on ozone STE. He will be extending his analysis to Aura data. Schoeberl will be looking at STE in the new FVGCM and the reanalysis.

Q3 - How does the long range transport of pollutants affect local air quality and chemical processes?

The PI will lead this team along with M. Chin. P. Colarco will work in smoke analysis. M. Chin is responsible for GOCART runs. Thompson will compare tropospheric ozone from SHADOZ and modified residual method with model analyses and Aura data. Torres is responsible for TOMS smoke analysis. Hollandsworth-Firth will work with Stolarski on tropospheric ozone residual methods.

Q4 - How do chemical changes in the atmosphere affect climate?

A. Douglass will lead this team. Gupta will work on the FVGCM. M.Chin (GOCART) and J. Rosenfield (2D model). Schoeberl will run the age-spectrum analysis. Douglass will be make chemical comparisons. S. Pawson is the interface to the Data Assimilation Office and has been running the reanalysis. Stolarski will be the primary interface to the GMI effort.

Tools –

Rosenfield maintains and runs the radiative transfer model and the interactive 2D model. Schoeberl maintains the trajectory models. Lait maintains the trajectory web page interface and the Science System data set. Douglass is responsible for the CTM. Chin maintains the GOCART model. Pawson is producing the reanalysis.

Data sets -

L. Lait will be responsible for porting data sets from the EOS observatories to the Science System. We have already begun to port MODIS aerosol data onto the system. Data sets we will be using when they are available are listed in Tables 1-3.

S. Pawson will coordinate the DAO modeling efforts and the availability of data for the science system.

5.0 Personnel

Vitae are attached.

6.0 Facilities and Equipment

Most of the data analysis and research will be carried out on the Code 916 workstation cluster. This system consists of 39 SGI workstations and 8 Linux boxes with over a terabyte of attached disk space. The science system allows any user within the cluster to transparently access any data file. One workstation has been assigned the task of running the GSFC trajectory model for outside users. The SGI workstations have become less cost competitive with the advent of inexpensive Linux boxes (basically multi-processor PC's running Linux). Due to the high cost of SGI maintenance, it is more cost effective to remove the machines from maintenance as the maintenance costs increase and spend the money on Linux boxes. We have now integrated a few of these Linux boxes into our cluster without problems. Our budget includes one man-year (Honey) support for the Science System cluster.

FVGCM and GMI calculations will be carried out on the Data Assimilation Office computer systems at no charge to the proposal. The results will be transferred to the Science System for analysis by the investigators. We have begun to move data from the EOS DAAC's to the science system as well.

Part of this proposal includes planned upgrades to the science system and the trajectory models. (see Appendix D for a description). Appendix E details the planned equipment upgrades proposed.

6.1 Upgrading the Trajectory models

Much of the current and proposed science activities depend upon the Goddard trajectory models. Currently, these are written in IDL, an interpreted language. Re-coding this software in C should make it more efficient, thus making it possible to calculate the trajectories of more parcels over a longer period of time. It would also allow us to implement a parallel version of the code that would run efficiently on multi-processor machines. This activity has begun with a set of low-level C routines to read gridded 4-D meteorological analyses; these routines can then be called from within the current trajectory model. As the activity proceeds, higher-level IDL routines will be re-written in C and made callable from the remaining IDL software, until the entire model has been re-implemented in C.

6.2 Improved Data Set Management

A vast amount of data from satellite, ground-based, and aircraft instruments is needed to carry out the interdisciplinary analysis and intercomparison being proposed. Even with the development of the Distributed Active Archive Centers (DAACs), these locally resident data collections must be organized and managed effectively.

Under the PIDS, we developed a data system which organizes data, software, and documentation. Designed around a collection of Unix workstations and servers which share files among each other, this "Science System" encourages collaboration by putting a wide variety of data sets into standardized locations which are accessible by anyone, along with software to read the data sets. Most of the data follow a standardized naming convention and are written in a compact, platform-independent, self-documenting format. Table 1 lists some of the datasets that are available. In addition to the data reader subroutines, an extensive toolkit of routines for modeling, analysis, and plotting have been developed by the system's users and made available to all. The open source programming codes can be modified or improved by any user (under a revision control system); all changes are promulgated to all computers in our data system, so that everyone uses the same version of the software.

As the number and size of the data sets have grown, performance demands have increased. New computer servers and upgrades to existing machines will be needed. In addition, a significant bottleneck exists in simply looking up what data are available. Under this IDS, programming support will be used to install and configure database software to help manage data access. In addition, part of our proposed activity is to transfer the relevant EOS and other important data sets to the current science system. The most relevant data sets from the EOS platforms are listed in Tables 2 and 3.

7.0 Current Support

The principal investigator is a civil servant and NASA covers costs. He also gets support as Aura Project Scientist.

Appendix A Publications funded or partially funded by the IDS over the last proposal period.

1. Choi, W., S. Kim, W.. Grant, M. Shiotani, Y. Sasano, and M. Schoeberl, Transport of methane in the stratosphere associated with the breakdown of the Antarctic polar vortex, *J. Geophys. Res.*, (in press) 2002.
2. Considine, D.B., J.E. Rosenfield, and E. Fleming, An interactive model study of the influence of the Mount Pinatubo aerosol on stratospheric methane and water trends, *J. Geophys. Res.*, *106*, 27,711-27,727, 2001.
3. Douglass, A. R., R. B. Rood, M. R. Schoeberl, and S. Pawson, Evaluation of transport in the lower tropical stratosphere in a global chemistry and transport model, *J. Geophys. Res.*, (in press) 2002.
4. Douglass, A. R., M. R. Schoeberl, S. R. Kawa and E. V. Browell, 2001: A composite view of ozone evolution in the 1995-96 northern winter polar vortex developed from airborne lidar and satellite observations. *JGR (Atmospheres)*, *106*, 9879-9895.
5. Drdla, K., M. Schoeberl and E. Browell, Microphysical modeling of 1999-2000 Arctic winter: 1. Polar stratospheric clouds, denitrification and dehydration, *J. Geophys. Res.*, *108*, 8312, doi:10.1029/2001JD000782, 2003
6. Fleming, E.L., C.H. Jackman, D.B. Considine, J.E. Rosenfield, Two-dimensional model simulations of the QBO in ozone and tracers in the tropical stratosphere, *J. Geophys. Res.*, 2002, in press.
7. Gao, R. S., E. C. Richard, P. J. Popp, G. C. Toon, D. F. Hurst, P. A. Newman, J. C. Holocek, M. J. Northway, D. W. Fahey, M. Y. Danilin, B. Sen, K. Aikin, P. A. Romashkin, J. W. Elkins, C. R. Webster, S. M. Schauffler, J. B. Greenblatt, C. T. McElroy, L. R. Lait, T. P. Bui and D. Baumgardner, 2001: Observational evidence for the role of denitrification in Arctic stratospheric ozone loss. *Geophys. Res. Lett.*, *28* (15), 2879-2882.
8. Hoppel, K., R. Bevilacqua, G. Nedoluha, C. Deniel, F. Lefevre, J. Lumpe, M. Fromm, C. Randall, J. Rosenfield, and M. Rex, POAM III observations of Arctic ozone loss for the 1999/2000 winter, *J. Geophys. Res.*, *107*, 10.1029/2001JD000476, 2002.
9. Lait, L., 2000: Effects of satellite scanning configurations on derived gridded fields. *J. Geophys. Res.-Atmos.*, *105*, 9063-9074.
10. Lait, L. R., et al., Ozone loss from quasi-conservative coordinate mapping during the 1999-2000 SOLVE/THESEO 2000 campaigns, *J. of Geophys. Res.*, 10.1029/2001JD000998, 2002
11. Lait, L. R., Systematic differences between radiosonde instruments, *Geophys. Res. Lett.*, 10.1029/2001GL014337, 2002

12. Morris, G. A., J. Ziemke, J. F. Gleason and M. R. Schoeberl, 2000: Trajectory mapping: A tool for validation of trace gas observations. *J. Geophys. Res.*, 105, 17,875-17,894.
13. Morris, G. A., M. R. Schoeberl, J. E. Rosenfield, and C. HY. Jackman, The potential impact of subsonic and supersonic aircraft exhaust on water vapor in the lower stratosphere assessed by a trajectory model *J. Geophys. Res.* (in press) 2002.
14. Morris, G. J. Gleason, J. Russell, III, M. Schoeberl, and M. P. McCormick, A comparison of HALOE V19 with SAGE II V6.00 ozone observations using trajectory mapping, (*JGR*, in press), 2002.
15. Nedoluha, G.E., R.M. Bevilacqua, K.W. Hoppel, M. Daehler, E.P. Shettle, J.H. Hornstein, M.D. Fromm, J.D. Lumpe, and J.E. Rosenfield, POAM III measurements of dehydration in the Antarctic lower stratosphere, *Geophys. Res. Lett.*, 27, 1683-1686, 2000.
16. Newman, P.A., E.R. Nash, and J.E. Rosenfield, What controls the temperature of the Arctic stratosphere during the spring?, *J. Geophys. Res.* 106, 19,999-20,010, 2001.
17. Newman, P. A., J. C. Wilson, M. N. Ross, C. Brock, P. Sheridan, M. R. Schoeberl, L. R. Lair, T. P. Bui and M. Loewenstein, 2001: Chance encounter with a stratospheric kerosene rocket plume from Russia over California. *JGR*, 28, 959-962, 2001.
18. Newman et al., An overview of the SOLVE/THESEO 2000 campaign, *J. Geophys. Res.*, (in press), 2002
19. Olsen, M. A., and J. L. Stanford, Evidence of stratosphere-to-troposphere transport within a mesoscale model and Total Ozone Mapping Spectrometer total ozone, *J. Geophys. Res.*, 106, 27323-27334, 2001.
20. Olsen, M. A., A. R. Douglass, and M. R. Schoeberl, Estimating downward cross-tropopause ozone flux using column ozone and potential vorticity, *J. Geophys. Res.*, in press/2001JD002041, 2002.
21. Olsen, M. A., An. R. Douglass, and M. R. Schoeberl, A Comparison of Northern and Southern Hemisphere Cross-tropopause Ozone Flux, *submitted to Geophys. Res. Let.*, 2002b.
22. Pfister, L. , H. Selkirk, E. Jensen, M. Schoeberl, O. Toon, E. Browell, W. Grant, B. Gary, M. Mahoney, T. Bui, E. Hintsa, Aircraft observations of this cirrus clouds near the tropical tropopause, *J. Geophys. Res.*, 106, 9765-9786, 2001.
23. Rosenfield, J. E., Effects of Volcanic Eruptions on Stratospheric Ozone Recovery, in "Volcanism and the Earth's Atmosphere," ed. A. Robock, AGU, 2003, submitted.
24. Rosenfield, J.E., and M.R. Schoeberl, On the origin of polar vortex air, *J. Geophys. Res.* 106, 33,485-33,497, 2001.

25. Rosenfield, J.E., A.R. Douglass, and D.B. Considine, The impact of increasing carbon dioxide on ozone recovery, *J. Geophys. Res.*, 107, 10.1029/2001JD000824, 2002.
26. Schoeberl, M. R., A. R. Douglass, Z. Zhu, and S. Pawson, The Age-Spectrum as a Diagnostic of Stratospheric Trace Gas Transport, *J. Geophys. Res.*, in press, 2002a
27. Schoeberl, M. R. et al., "An Assessment of the Ozone Loss During the 1999-2000 SOLVE/ THESEO 2000 Arctic Campaign," *J. Geophys. Res.*, 2002b
28. Sparling, L. C. and J. T. Bacmeister, Scale dependence of the tracer microstructure: PDF's intermittency and the dissipation scale, *Geophys. Res. Lett.*, 28, 2823-2826, 2001.
29. Sparling, L. C., 2000: Statistical perspectives on stratospheric transport. *Rev. Geophys.*, 38, 417-436, 2000.
30. Tabazadeh, A., M. L. Santee, M. Y. Danilin, H. C. Pumphrey, P. A. Newman, P. J. Hamill and J. L. Mergenthaler, 2000: Quantifying denitrification and its effect on ozone recovery. *Science*, 288, 1407-1411.
31. Tabazadeh A., E. Jensen, O. Toon, K. Drdla, M Schoeberl, Role of the stratospheric polar freezing belt in denitrification, *Science*, 291, 2591-2593, 2001
32. Tabazadeh, A., K. Drdla K., M. Schoeberl, P. Hamill, O. B. Toon, Arctic "ozone hole" in a cold volcanic stratosphere, *Proc. of the Natl. Acad.*, 99, 2609-2612, 2002.

Appendix B: Related IDS and ACMAP Proposals

Proposals being coordinated with this IDS are listed below.

M. Chin (ACMAP): From regional pollution to global atmospheric change: Modeling and data analysis in a global-regional atmospheric modeling system

This proposal focuses on (1) understanding the regional processes that determine the aerosol and ozone distributions, (2) quantifying the intercontinental transport of aerosols, ozone, and their precursors, and (3) assessing the climate and chemical impact of regional pollution on regional and global atmosphere.

M. Chin (RSP): Global and regional aerosol modeling studies (GRAMS): Sources, distributions, near-term to long-term climate effects

This proposal focuses on determining the near-term to long-term global and regional distributions of aerosols and understanding the relationships among the aerosol sources, processes, distributions, and global and regional climate and air quality effects.

A. Dessler (IDS): Investigations of the tropical tropopause region

This proposal investigates the tropical tropopause region (TTR), that volume of the atmosphere extending from about 25°S to 25°N and from approximately 200 hPa (~12 km) to 50 hPa (~20 km).

A. Douglass (ACMAP): Continued Funding of the Stratospheric General Circulation with Chemistry Project

This proposal uses the CTM with winds and temperatures from the FVGCM and from various versions of GEOS-DAS to interpret observations of ozone and other stratospheric constituents from various platforms, including satellite, aircraft, and balloon. The central focus of this proposal is a hindcast of observed ozone behavior 1975 - present and forecast of ozone recovery through analysis of long simulations with variable meteorology from the FVGCM and changing boundary conditions for trace gases.

Y Kaufman (IDS): The global aerosol system and its direct and indirect forcing of climate

This proposal integrates the multiple satellite aerosol and cloud data, AERONET measurements, and GOCART model to quantify the "global aerosol system", estimate the aerosol direct radiative forcing and the aerosol effects on cloud properties.

P. Newman (ACMAP): Continued Funding for Analysis of Spatial and Temporal Variability of Stratospheric Dynamics and Trace Constituents

This proposal is to use data assimilation data sets (DAO, NCEP/NCAR, UKMO, and NCEP/CPC) covering the last two decades to investigate how planetary wave driving of the stratosphere is connected to polar stratosphere, and to determine the response of the NASA/NCAR GCM to the heating of the tropical upper troposphere in the double 2xCO₂ atmosphere. This proposal will focus on the changes of linear wave propagation in the stratosphere under a 2xCO₂ environment.

L. Sparling (ACMAP): An investigation of the statistical properties of sub-grid scale variability in chemical tracers in the UT/LS: Applications to chemical modeling, data validation and constituent data assimilation

This proposal is to use a combination of aircraft and balloon data collected over the past decade to develop a statistical synthesis of sub-grid scale variability in chemical tracers. The research includes an investigation of fundamental problems related to sub-grid scale transport and chemical mix-down. The results of this research are directly applicable a number of practical problems in the areas of model evaluation, satellite data validation and constituent data assimilation.

A. Thompson (ACMAP) - Climatological and Process Studies of Tropical Tropospheric Ozone using Ozonesonde and Satellite Data

This proposal focuses on: (1) climatology of southern hemisphere tropospheric ozone at tropical and subtropical stations; (2) refinement of modified-residual TTO data, using 1997-1999 ozonesonde data; (3) analysis of ozone data over southern Africa and the adjacent oceans, including profiles collected during the R/V R H Brown 1999 Aerosols and INDOEX cruises. In conjunction with ACPMAP funding to R D Hudson at U MD, modified-residual maps of tropical tropospheric ozone are produced under this support.

(This proposal is will provide tropospheric ozone estimates for validation of our data product.)

Steven Pawson (Pathfinder Data Sets)- Reanalysis for Stratospheric Trace Gas Studies

In this proposal, a 4-year reanalysis (May 1991--April 1995) of the troposphere and stratosphere is being undertaken and evaluated. The proposer has just completed three years of reanalysis as of Nov. 2002. The current plan is to extend the reanalysis through to the present.

Torres, O., L.Remer, and P.Ginoux,: A climatological record of aerosol absorption optical depth.

This proposal will use TOMS, MODIS, MISR and AERONET observations during a two ear overlap period, to optimize the TOMS retrieval algorithm. The improved TOMS algorithm will be applied to the historical TOMS record back to 1979.

Toon, O. et al.: Interdisciplinary Studies of Aerosols and Clouds: Aerosol chamber, radiation observation site, and numerical modeling focused on understanding biomass combustion aerosols

This proposal is to improve microphysical modeling of smoke using both observations and an experimental laboratory system.

Appendix C: Participation in the Global Modeling Initiative (GMI)

The purpose of the Global Modeling Initiative (GMI) is to provide a state-of-the-art three dimensional model that is appropriate for assessment of the effects of natural and anthropogenic perturbations on the composition of the stratosphere and troposphere, and that can be used to quantify the uncertainty in assessment. The present GMI model is best thought of as a modular framework that allows various elements that are make up a CTM to be interchanged. An early version of the GMI CTM was used to simulate the effects of a fleet of supersonic aircraft flying in the lower stratosphere [Kinnison et al., 2001]. During the development of the CTM, Douglass et al. [2000] used data from several instruments on UARS and from instruments on NASA's ER-2 to develop quantitative metrics of model performance.

At present there are versions of the GMI CTM that are appropriate for either the stratosphere (GMI-STRAT) or the troposphere. (GMI-TROP) The present version of GMI-STRAT uses meteorological fields from the FVGCM and from the FVDAS. The change in ozone between 1995 and 2030 assuming decreases in chlorofluorocarbons and increases in methane and nitrous oxide was calculated using each set of wind fields. One co-investigator of this proposal (ARD) presented an analysis of the high latitude summer ozone decrease using results from these two simulations and data from UARS HALOE and MLS at the November American Meteorological Society Middle Atmosphere Meeting. The analysis relied on the two simulations to eliminate transport problems as the cause of the difference between the model results and observations. This presentation emphasized the value of having the capability to vary single modules in the CTM framework.

The GMI-STRAT will next be used to simulate the period 1975 – 2005, an effort that is led by another co-investigator of this proposal (RSS). This effort will compare results from simulations driven by wind fields with very different meteorological characteristics. RSS will lead the analysis of the simulations, emphasizing comparisons with observations from various satellite instruments including TOMS, SAGE, POAM, SBUV, LIMS, HALOE, and MLS and also comparisons with observations from ground-based instruments, including but not limited to those taken through the NDSC.

A development effort currently underway in GMI is to identify a chemical mechanism that captures the most important processes for upper tropospheric and lower stratospheric ozone behavior. Once this "combined" mechanism has been identified and implemented in the CTM (GMI-Combined), global simulations will be produced. As for the GMI-STRAT, evaluation of the GMI-Combined will rely on comparisons with observations. Members of this investigation will provide expertise through their knowledge of the value and limitations of tropospheric ozone products that have been derived from TOMS data (Hudson and Thompson, 1998; Ziemke et al., 1998). The analysis of STE processes as detailed in this proposal will also be brought to bear in the analysis of the GMI combined results. The combined mechanism will be available to us for integration in our local CTM's. The use of the combined mechanism in process studies will be invaluable in interpretation of data from Aura, will provide information about the budget and behavior of the upper tropospheric and lower stratospheric ozone, and will benefit the assessment effort of GMI by providing strong validation of the model behavior.

Appendix D Model Descriptions

D.1 The FVGCM

The FVGCM or FVCCM model, developed in collaboration between the DAO and NCAR, will be used as the core general circulation model for this investigation. The dynamical core is based on the work of Lin [1997] in which the 'finite-volume semi-Lagrangian' technique was developed. The FVGCM uses a regular latitude-longitude grid with Lagrangian vertical coordinate. Meteorological variables are re-mapped to a hybrid vertical grid at regular intervals (currently 30 minutes) when the physical tendencies are recalculated. The model currently uses the complete NCAR CCM3 physics package (representing radiative transfer, clouds and the hydrological cycle, and turbulent exchange of moisture and momentum with the surface). The FVGCM is the core of the DAO's GEOS-4 data assimilation system (DAS) and has also been integrated in "free-running" or climate mode. A 50-year integration using observed SSTs between 1950 and 2000 has been performed in the climate-mode at 2.5lat by 2lon by 55 level resolution.. Shorter integrations are available at horizontal resolution as small as 0.5-degrees. The model resolution is flexible, meaning that it can be readily adapted to the problem under investigation. A number of short model simulations have also been made with 96 levels, in place of the standard 55-level configuration: this impacts vertical gradients of water vapor in the lower stratosphere. Even the 2.5*2-degree, 55-level model configuration is at the high end of the range used in present climate simulations (e.g., Gates, 1999). Quantitative measures of the model performance place it at the superior end of the range of models in the GCM-Reality Intercomparison Project for SPARC (GRIPS) initiative (Pawson et al., 2000). However, one aspect of the model performance that is less realistic is the space-time distribution of convective precipitation (Horinouchi et al., 2002), which can be traced to the use of the Zhang-McFarlane convection scheme. While Horinouchi et al. (2002) note the impact on the spectrum of resolved, upward-propagating gravity waves, this will also affect the convective transport of trace species in the troposphere, especially those with a strong diurnal cycle (because of an overly strong locking of the convection to overhead sun). On the positive side, Schoeberl et al. [2002a] showed that the FVGCM showed excellent age spectral characteristics and very little tropical ventilation in the stratosphere. This is due to the large-scale transport, which will not be affected by future improvements in tropospheric processes, which are ongoing both in the DAO and in collaboration with NCAR.

The FVGCM as presently implemented in the operational GEOS-4 analysis system has a resolution of 1.25 x 1°. Additionally, as part of the "Reanalysis for Stratospheric Trace Gas Studies" a 2.5° x 2° version of GEOS-4 has been run from May 1991 until September 1994; this reanalysis will proceed until April 1995. This is the longest continuous analysis using a stable configuration of the DAS, that has existed in the DAO since the 1982-1994 GEOS-1 reanalysis (Schubert et al., 1994). Within the time-frame of the current proposal, a 1.25x1-degree ReSTS reanalysis will be made, beginning in May 1991 and running until the present.

D.2 Troposphere - Stratospheric Chemical Transport Model (CTM)

D.2.1 Stratosphere

The stratospheric chemical model, which combines advection and photochemical algorithms, is described in detail in Douglass and Kawa [1999]. Briefly, the advection scheme [Lin and Rood, 1996] calculates constituent transport on a 2.5 x 2 lon-lat grid, with 28 vertical levels using a hybrid sigma coordinate for 7 tropospheric levels and pressure for 21 stratospheric levels. The interface pressure is at 247 hPa. The spacing is about 1 km near the tropopause and increases to 4 km near the upper boundary. This scheme maintains sharp gradients and appropriate correlations for long-lived constituents.

The photochemical scheme contains all gas phase and heterogeneous reactions thought to be important in the stratosphere; input data for reaction rates are taken from the current JPL evaluation [DeMore et al., 1997]. The photolysis rates are calculated using temperature dependent cross sections [DeMore et al., 1997] and reduced fluxes interpolated from a table lookup based on the detailed radiative transfer calculations from the model of Anderson and Lloyd [1990]. The photolysis rates calculated in this way compare favorably with the photolysis benchmark that was developed as part of the AEAP program [Stolarski et al., 1995]. This photochemical scheme is used in the CTM and also in the trajectory photochemical model. The approach of using assimilated winds and temperatures in an off line chemistry and transport model has been used by ourselves and others in analysis of observations from aircraft (e.g., Douglass et al., 1991; Lefevre et al., 1994); balloon (e.g., Kondo et al., 1996); ozonesonde (e.g., Weaver et al., 1999); and satellites included Nimbus 7 TOMS (e.g., Douglass et al., 1996; Jiang et al., 1998), UARS (e.g., Chipperfield et al., 1996; Douglass and Kawa, 1999), and POAM (Deniel et al., 1998). There have been improvements in the transport characteristics of assimilated wind fields during the past decade [Douglass et al., 2002]. Recent analysis by Douglass et al. and by Schoeberl et al. [2002] reveal problems in transport with assimilated wind fields that are not unique to the Goddard DAS products. For some applications it is more realistic to use meteorological fields from a general circulation model in the CTM framework. Either DAS or GCM winds can be used in this CTM.

D.2.2 The troposphere - lower stratosphere chemical model

Although we have not developed a chemical mechanism and solver appropriate for tropospheric applications, we have access to the Harvard GEOS-CHEM model (Bey et al., 2001a). GEOS-CHEM has the same grid resolution model and uses the same meteorological fields and transport algorithms as the GOCART model (following section). The tropospheric chemical mechanism in GEOS-CHEM includes about 120 species. 24 tracers are transported, including O₃, NO_x, total nitrogen (NO_y), H₂O₂, CO, and several types of hydrocarbon (Bey et al., 2001). The chemical solver used in the GEOS-CHEM model is a highly accurate sparse-matrix vectorized Gear solver (SMVGEAR) (Jacobson, 1995). This solver is also used in GMI-TROP, and one avenue to development of GMI-combined entails modifications to GMI-TROP. The GEOS-CHEM model has been applied to a wide range of tropospheric problems, including the chemical evolution of Asian outflow, the biogenic source inferred from satellite observations, the tropical tropospheric ozone budget, and the intercontinental transport of ozone and pollutants. The aerosol effects on ozone production have been investigated recently in the GEOS-CHEM by using the monthly averaged aerosol fields from the GOCART model (Martin et al., 2002a, b). It is shown that aerosols could have large effects on tropospheric chemistry by reducing the most important oxidants concentrations, such as OH, HO₂, NO₂, and O₃, especially in the pollution and biomass burning regions (Martin et al., 2002b; Duncan et al., 2002b). The inclusion of aerosols in the atmospheric chemistry model has improved the model agreement with observations. (For more on the GEOS-CHEM model and related publications, see <http://www-as.harvard.edu/chemistry/trop/geos/index.html>.)

D.3 The GOCART microphysics and aerosol model

The Georgia Tech/Goddard Global Ozone Chemistry Aerosol Radiation and Transport (GOCART) model is a global model driven by assimilated meteorological fields from the Goddard Earth Observing System Data Assimilation System (GEOS DAS). The spatial

resolution of the GOCART model is 2° latitude by 2.5° longitude or 1° by 1.25° , and 20–55 vertical layers depending on the version of GEOS DAS. The GOCART model simulates tropospheric aerosols, including sulfate, dust, black carbon, organic carbon, and sea-salt. The GOCART model contains the following modules in aerosol simulation: emission, which includes sulfur, dust, black carbon and organic carbon, and sea salt emissions; chemistry, which currently uses prescribed OH, H_2O_2 , and NO_3 fields for gaseous sulfur oxidations; advection, which is computed by a flux-form semi-Lagrangian method; boundary layer turbulent mixing, which uses a second-order closure scheme; moist convection, which is calculated using archived cloud mass flux fields; dry deposition, which uses a resistance-in-series algorithm as a function of surface type and meteorological conditions; and wet deposition, which accounts for the scavenging of soluble species in convective updrafts and rainout/washout in large-scale precipitation. We consider 8 size bins for dust and 4 size bins for sea-salt ($r=0.1 - 10 \mu\text{m}$). We assume lognormal size distributions for sulfate, organic carbon, and black carbon, and for each size bin of dust and sea-salt. The hygroscopic growth of aerosol size with ambient relative humidity is parameterized. More detailed description and summary can be found in Chin et al. [2002a] and references therein (<http://code916.gsfc.nasa.gov/People/Chin/jas.all.pdf>), and the model results of monthly averaged aerosol optical thickness can be found at <http://code916.gsfc.nasa.gov/People/Chin/aot.html>.

The model has been used to support field experiments (Chin et al., 2002b), to analyze observations from field programs and satellite (Chin et al., 2000a, b; Ginoux et al., 2001), and to assess future climate change (Penner et al., 2001). We have compared our results with the TOMS and AVHRR retrievals on global aerosol distributions, and with the AOT from the AERONET at different geographic locations for model evaluations (Chin et al., 2002a). The dust source in the GOCART model is determined at the topographic depression areas with bare soil surface, and dust uplifting probability is defined according to the degree of depression. The model simulation of dust aerosol with this parameterization has been found to be consistent with the surface, lidar, and satellite observations (Ginoux et al., 2001). The biomass burning emissions of BC and OC are based on the burned biomass inventory which is estimated using the satellite observations of fire counts and aerosol index (Duncan et al., 2002a; Chin et al., 2002a). The new biomass burning emissions have significantly improved the modeled seasonal variations of biomass burning and have made the interannual biomass burning simulation possible. Figure D.3.1 compares MODIS aerosol data with GOCART a GOCART simulation.

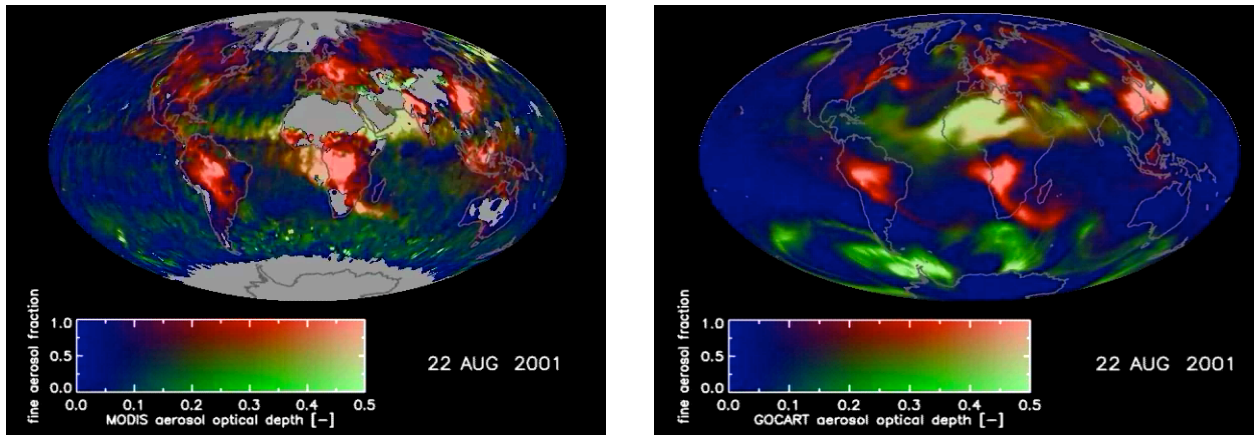


Figure D.3.1 Total aerosol optical thickness at 550 nm and the fraction of fine model aerosols ($D_p < 1 \mu\text{m}$) for August 22, 2001 from the satellite retrieval of MODIS (left) and the model (right). The high fraction of small particles (mostly sulfated, BC, OC, with some dust and sea-salt) is indicated in red, and low fraction of small particles (or high fraction of large particles, $D_p > 1 \mu\text{m}$, mostly dust and sea-salt) is in green.

D.4 Radiative Transfer Model

The current radiation model is as described in Rosenfield et al. [1994] with the addition of an infrared transmission parameterization which allows for varying amounts of CO₂ [Chou and Kouvaris, 1991]. The shortwave absorbers are O₃, H₂O, and CO₂, and the longwave absorbers are CO₂, O₃, and H₂O. We have an updated version of the near infrared solar heating due to H₂O. This replaces the old Lacis and Hansen [1974] parameterization in which the entire 0.7-4.0 micron region is treated as one wide band. The new parameterization is that of Chou and Lee [1996], which divides the region into three bands, allowing a better treatment of the scattering due to aerosols.

D.5 The trajectory model group

There are four trajectory models in the group, all derived from the original Schoeberl code (trajdriver) often referred to as the Goddard Trajectory Model. These models have been used in a variety of studies associated with satellite and aircraft measurements. Three are available through the auto-mailer system

http://code916.gsfc.nasa.gov/Data_services/automailer/index.html

Trajdriver – isentropic trajectories and limited diabatic trajectories. Fastest code for adiabatic runs.

Ftraj – diabatic trajectory code (also adiabatic). Uses a fastr vertical interpolation scheme and precomputes the fields on isentropic surfaces. Fastest code for diabatic runs.

Ktraj – kinematic trajectory code (uses vertical velocities). Ktraj runs are automatically and its output is provided with the SHADOZ data.

Not available through the automailer-

Mtraj – single level code for use in field missions – requires pre-computed fields on an isentrope.

D.6 The Interactive 2D Model

The interactive 2D (latitude-pressure) model has been described in Rosenfield et al. [1997]. Subsequent modifications are given in Rosenfield et al. [1998] and Rosenfield and Douglass [1998]. The model is interactive in the sense that computed temperatures, ozone, water vapor, and carbon dioxide are used in the calculation of the radiative heating rates. The residual circulation, which drives the transport of momentum, heat, and constituents, is determined from the computed heating rates. The model has a full chemistry scheme, with ~130 gas phase reactions. A detailed parameterization of heterogeneous chemical reactions occurring on the surfaces of sulfate aerosols, and Type 1 and Type 2 polar stratospheric clouds is included [Considine et al., 1994].

Appendix E Equipment Costs and Upgrades under this Proposal

Maintaining the science system and on-line data sets requires a continuous investment in disk storage and processing equipment. Below are our proposed enhancements and upgrades to the science system with this proposal. The costs are summarized in the table and paragraph below it.

Disks:

Three 8-bay racks and 24 146-GB disk drives would fill up the rack space used for scratchy and auster, allowing us to replace the larger RAIDS. At least 1 new enclosure with 8 drives would be moderately high priority; additional enclosures allow for relatively quick expansion of disk space as needed by purchasing drives as need arises.

Desktop Linux boxes:

Replacing the old SGI R4400 machines is needed; there are seven in the cluster.

Linux server machines:

Replacing scratchy and auster would do a couple things. First, it would eliminate the cost of the SGI maintenance on those machines. It would also allow us to expand the number of SCSI channels and thus the number of drives we hang off of them.

DLT-8000 tape drive:

tape drive for backups

| Computer Equipment | Quantity | Cost | Subtotal |
|---|----------|-------------|-----------|
| 8-bay rack-mount disk enclosures with cabling | 3 | \$1,500 ea | \$ 4,500 |
| 146 GB Seagate Cheetah SCSI drives | 24 | \$1,000 ea | \$ 24,000 |
| Dual-processor linux boxes to replace low-end SGI's | 4 | \$3,500 ea | \$ 14,000 |
| 4-processor Intel Xeon MP linux systems to replace Power Challenges (scratchy,auster) | 2 | \$22,000 ea | \$ 44,000 |
| Shelving/racks | | | \$ 5,000 |
| DLT-8000 tape drives | 1 | \$ 2000 | \$ 2000 |
| Total | | | \$ 93,500 |

In addition we have estimated that misc equipment costs for software, small IDE hard drives, processor upgrades and other equipment for the group runs about \$10,000/year. Spreading these costs over three years gives \$41 K/ year.

References

- Ackerman, A.S., O. B. Toon, and P. V. Hobbs, Dissipation of Marine Stratiform clouds and collapse of the marine boundary layer due to aerosol depletion by clouds, *Science*, 262, 226-229, 1993.
- Ackerman, A.S., O. B. Toon, and P. V. Hobbs, Reassessing the dependence of cloud condensation nucleus concentrations on formation rate, *Nature* 367, 445-447, 1994.
- Ackerman, A.S., O. B. Toon, and P. V. Hobbs, A model for particle microphysics, turbulent mixing, and radiative transfer in the stratocumulus-topped marine boundary layer and comparisons with measurements, *J. Atmos. Sci.*, 52, 1204-1236, 1995a.
- Ackerman, A.S., O. B. Toon, and P. V. Hobbs, Numerical modeling of ship tracks produced by injections of cloud condensation nuclei into marine stratiform clouds *J. Geophys. Res.*, 100, 7121-7134, 1995b.
- Allen, D. and M. Schoeberl, Trajectory modeling of aerosol clouds observed by TOMS, *J. Geophys. Res.* 104, 27461-27471, 1999
- Ancellet, G., M. Beekmann, and A. Papayannis, Impact of a cut-off low development on downward transport of ozone in the troposphere, *J. Geophys. Res.*, 99, 3451-3468, 1994.
- Anderson et al., 2002? Submitted.
- Anderson, D. E., Jr., and S. A. Lloyd, Polar twilight UV-visible radiation field: perturbations due to multiple scattering, ozone depletion, stratospheric clouds, and surface albedo, *J. Geophys. Res.*, 95, 7429-7434, 1990.
- Appenzeller, C., J. R. Holton and K. Rosenlof, Seasonal variation of mass transport across the tropopause, *J. Geophys. Res.*, 101, 15071-15078, 1996.
- Avallone L. M., and M. J. Prather, Photochemical evolution of ozone in the lower tropical stratosphere, *J. Geophys. Res.*, 101, 1457-1461, 1996.
- Bacmeister, J., M. Schoeberl, M. Summers, J. Rosenfield, and X. Zhu, Descent of Long-Lived Trace Gases in the Winter Polar Vortex, *J. Geophys. Res.*, 100, 11669-11684, 1995.
- Bamber, D. J., P. G. W. Healey, B. M. R. Jones, S. A. Penkett, A. F. Tuck, and G. Vaughan, Vertical profiles of tropospheric gases: Chemical consequences of stratospheric intrusions, *Atmos. Environ.*, 18, 1759-1766, 1984.
- Beekman, M., et al., Regional and global tropopause fold occurrence and related ozone flux across the tropopause, *J. Atm. Chem.*, 28, 29-44, 1997.
- Bekki, S., and J. A. Pyle, A two-dimensional modeling study of the volcanic eruption of Mount Pinatubo, *J. Geophys. Res.*, 99, 18,861 - 18,869, 1994.
- Bey I., D. J. Jacob, R. M. Yantosca, J. A. Logan, B. Field, A. M. Fiore, Q. Li, H. Liu, L. J. Mickley, and M. Schultz, Global modeling of tropospheric chemistry with assimilated meteorology: Model description and evaluation, *J. Geophys. Res.*, 106, 23,073-23,096, 2001a.

Bluth, G. J., S. D. Doiron, C. C. Schnetzler, A. J. Krueger, and L. S. Walter, Global tracking of the SO₂ clouds from the June, 1991 Mount Pinatubo eruptions, *Geophys. Res. Lett.*, 19, 151 - 154, 1992.

Brasseur G. and C. Granier, Mount Pinatubo aerosols, chlorofluorocarbons, and ozone depletion, *Science*, 257, 1239 - 1242, 1992.

Chipperfield, M. P., M. L. Santee, L. Froidevaux, G. L. Manney, W. G. Read, J. W. Waters, A. E. Roche, and J. M. Russell, Analysis of UARS data in the southern polar vortex in September 1992 using a chemical transport model, *J. Geophys. Res.*, 101, 18,861-18,881, 1996.

Chin, M., R.B. Rood, S.-J. Lin, D.J. Jacob, J.-F. Muller, and A.M. Thompson, Atmospheric sulfur cycle in the global model GOCART: 1. Model description and global properties, *J. Geophys. Res.*, 105, 24,671-24,687, 2000a.

Chin, M., et al., "Tropospheric aerosol optical thickness from the GOCART model and comparisons with satellite and sunphotometer measurements", *J. Atmos. Sci.*, 59, 461-483, 2002a.

Chin, M., Ginoux, P., and Lucchesi, R., A global model forecast for the ACE-Asia field experiment, submitted to *J. Geophys. Res.*, 2002b.

Chin, M., Savoie, D. L., Huebert, B. J., Bandy, A. R., Thornton, D. C., Bates, T. S., Quinn, P. K., Saltzman, E. S., and De Bruyn, W. J., "Atmospheric sulfur cycle in the global model GOCART: Comparison with field observations and regional budgets," *J. Geophys. Res.*, 105, 24,689-24,712, 2000b.

Choi, W., S. Kim, W. Grant, M. Shiotani, Y. Sasano, and M. R. Schoeberl, "Transport of methane in the stratosphere associated with the breakdown of the Antarctic polar vortex", *J. Geophys. Res.* (in press) 2002.

Chou, M.-D., and K.-T. Lee, Parameterizations for the absorption of solar radiation by water vapor and ozone, *J. Atmos. Sci.*, 53, 1203-1208, 1996.

Chou, M.-D., and M.J. Suarez, An efficient thermal infrared radiation parameterization for use in general circulation models, NASA Technical Memo. 104606, Vol.3, 1994.

Chou, M.-D., and L. Kouvaris, Calculations of transmission functions in the infrared CO₂ and O₃ bands, *J. Geophys. Res.*, 96, 9003-9012, 1991.

Colarco, P.R., O.B. Toon, O. Torres, and P.J. Rasch, "Determining the UV imaginary index of refraction of Saharan dust particles from TOMS data using a three dimensional model of dust transport," *JGR* (107), 4289, doi:10.1029/2001JD000903 (2002).

Considine, D. G., A. R. Douglass, P. S. Connell, D. E. Kinnison, and D. A. Rotman, A polar stratospheric cloud parameterization for the global modeling initiative three-dimensional model and its response to stratospheric aircraft, *J. Geophys. Res.*, 105, 3955-3973, 2000.

Considine, D.B., A.R. Douglass, and C.H. Jackman, Effects of a polar stratospheric cloud parameterization on ozone depletion due to stratospheric aircraft in a two-dimensional model, *J. Geophys. Res.*, 99, 18,879-18,894, 1994.

Danielsen, E., R. Bleck, J. Shedlovsky, A. Wartburg, P. Haagenson, and W. Pollock, Observed distribution of radioactivity, ozone, and potential vorticity associated with tropopause folding, *J. Geophys. Res.*, 75, 2353-2361, 1970.

DeMore W. B., S. P. Sander, D. M. Golden, R. F. Hampson, M. J. Kurylo, C. J. Howard, A. R. Ravishankara, C. E. Kolb, M. J. Molina, Chemical Kinetics and Photochemical Data for Use in Stratospheric Modeling, Evaluation Number 12, JPL Publication

Deniel, C., R. M. Bevilacqua, J. P. Pommereau, and F. Lefevre, Arctic chemical ozone depletion during the 1994-1995 winter deduced from POAM II satellite observations and the REPROBUS three-dimensional model, *J. Geophys. Res.*, 103, 19,231-19,244, 1998.

Dessler, A. E., A reexamination of the "stratospheric fountain" hypothesis, *Geophys. Res. Lett.*, 25, 4165-4168, 1998.

Dessler, A. E., E. J. Hints, E. M. Weinstock, J. G. Anderson, and K. R. Chan, Mechanisms controlling water vapor in the lower stratosphere: "A tale of two stratospheres", *J. Geophys. Res.*, 100, 23167-23172, 1995.

Dessler, A. E., D. B. Considine, J. E. Rosenfield, S. R. Kawa, A. R. Douglass, and J. M. Russell, III, Lower stratospheric chlorine partitioning during the decay of the Mt. Pinatubo aerosol cloud, *Geophys. Res. Lett.*, 24, 1623 - 1626, 1997.

Dethof, A., A. O'Neill, J.M. Slingo, and H.G.J. Smit, A mechanism for moistening the lower stratosphere involving the Asian summer monsoon, *Q. J. R. Meteorol. Soc.*, 125, 1079-1106, 1999.

Dethof, A., A. O'Neill, and J. Slingo, Quantification of the isentropic mass transport across the dynamical tropopause, *J. Geophys. Res.*, 105, 12279-12293, 2000.

Douglass, A., R. B. Rood, M. R. Schoeberl, and S. Pawson "Evaluation of transport in the lower tropical stratosphere in a global chemistry and transport model." *J. Geophys. Res.*, (in press) 2002.

Douglass, A. R., M. J. Prather, T. M. Hall, S. E. Strahan, P. J. Rasch, L. C. Sparling, L. Coy and M. M. Rodriguez, Choosing meteorological input for the global modeling initiative assessment of high-speed aircraft, *J. Geophys. Res.*, in press, 1999.

Douglass, A. R., and S. R. Kawa, Contrast between 1992 and 1997 high latitude spring Halogen Occultation Experiment observation of lower stratospheric HCl, *J. Geophys. Res.*, 104, 18,739-18,754, 1999.

Douglass, A. R., R. B. Rood, S. R. Kawa, and D. J. Allen, A three-dimensional simulation of the evolution of the middle latitude winter ozone in the middle stratosphere, *J. Geophys. Res.*, 102, 19,217-19,232, 1997.

Douglass, A. R., C. J. Weaver, R. B. Rood and L. Coy, A three- dimensional simulation of the ozone annual cycle using winds from a data assimilation system, *J. Geophys. Res.*, 101, 1463-1474, 1996.

Douglass, A. R., M. P. Prather, T. M. Hall, S. E. Strahan, P. J. Rasch, L. C. Sparling, L. Coy, and J. M. Rodriguez, Choosing meteorological input for the global modeling initiative assessment of high speed aircraft, to appear in *J. Geophys. Res.*, 1999.

Douglass, A.R., M.R. Schoeberl, R.S. Stolarski, J.W. Waters, J.M. Russell III, and A.E. Roche, Interhemispheric differences in springtime deactivation of vortex ClO. *J. Geophys. Res.*, 1995.

Douglass, A. R., R. B. Rood, J. A. Kaye, R. S. Stolarski, D. J. Allen and E. M. Larson, The influence of polar heterogeneous processes on reactive chlorine at middle latitudes: three dimensional model implications, *Geophys. Res. Lett.*, 18, 25-28, 1991.

Duncan, B.N., R.V. Martin, A.C. Staudt, R. Yevich, J.A. Logan, Interannual and Seasonal Variability of Biomass Burning Emissions Constrained by Satellite Observations, *J. Geophys. Res.*, in press, 2002a.

Duncan, B. N., I. Bey, M. Chin, L. J. Mickley, D. Fairlie, R. B. Peirce, R. V. Martin, and H. Matsueda, Indonesian Wildfires of 1997: Impact on tropospheric chemistry, submitted to *JGR*, 2002b.

Dvortsov, V.L., and S. Solomon, Response of the stratospheric temperatures and ozone to past and future increases in stratospheric humidity, *J. Geophys. Res.* 106, 7505-7514, 2001.

Edwards, D. P., J.-F. Lamarque, J.-L. Attie, L.K. Emmons, A. Richter, J.-P. Cammas, L.V. Lyjak, G.L. Francis, J.C. Gille, J.R. Drummond, and the NCAR MOPITT Team, Tropospheric Ozone Over the Tropical Atlantic: A Satellite Perspective, *J. Geophys. Res.*, submitted, 2002.

Eluszkiewicz, J., D. Crisp, R. G. Grainger, A. Lambert, A. E. Roche, J. B. Kumer, and J. L. Mergenthaler, Sensitivity of the residual circulation diagnosed from the UARS data to the uncertainties in the input fields and to the inclusion of aerosol, *J. Atmos. Sci.*, 54, 1739 - 1757, 1997.

Finlayson-Pitts, B. and J. Pitts, Tropospheric Air Pollution: Ozone, Airborne Toxics, Polycyclic Aromatic Hydrocarbons, and Particles, *Science*, 276, 1045-1051, 1997.

Fishman, J., and J. C. Larsen, Distribution of total ozone and stratospheric ozone in the Tropics: Implications for the distribution of tropospheric ozone, *J. Geophys. Res.*, 92, 6627-6634, 1987.

Fishman, J., C. Watson, J. Larsen; and J. Logan, Distribution of Tropospheric Ozone Determined From Satellite Data. *J. Geophys. Res.*, 95, 3599-3617, 1990

Fishman J, K. Fakhruzzaman, B. Cros , and D. Nganga, Identification Of Widespread Pollution In The Southern-Hemisphere Deduced From Satellite Analyses, *Science* 252, 1693-1696, 1991

Fishman, J., G. Brackett, G., E. Browell, and W. Grant., Tropospheric Ozone Derived From TOMS/SBUV Measurements During TRACE A. *J. Geophys. Res.*, 101, 24,069-24,082, 1996.

Folkens, I., et al., A 14 km mixing barrier in the tropics: evidence from ozone sondes and aircraft measurements, *J. Geophys. Res.*

Gates, W. L., et al. An overview of the results of the atmospheric model intercomparison project (AMIP), *Bull. Amer. Meteorol. Soc.*, 80, 29-56, 1999.

- Gettelman, A., and A. H. Sobel, Direct diagnosis of stratosphere-troposphere exchange, *J. Atmos. Sci.*, 57, 3–16, 2000.
- Gettleman, A., J. R. Holton and A. Douglass, Simulations of water vapor in the lower stratosphere and upper troposphere, *J. Geophys. Res.*, 105, 9003-9023, 2000.
- Ginoux, P., M. Chin, I. Tegen, M. Prospero, B. Holben, O. Dubovik, S. Lin, Sources and distributions of dust aerosols simulated with the GOCART model, *J. Geophys. Res.*, 106, 20255-20273, 2001.
- Gleason, J. F., et al., Record low global ozone in 1992, *Science*, 260, 523 - 526, 1993.
- Ginoux, P., Chin, M., Tegen, I., Prospero, J., Holben, B., Dubovik, O., and Lin, S.-J., "Sources and global distributions of dust aerosols simulated with the GOCART model," *J. Geophys. Res.*, 106, 20,255-20,273, 2001.
- Hall, T. M., and R. A. Plumb, Age as a diagnostic of stratospheric transport, *J. Geophys. Res.* 99, 1059-1070, 1994.
- Hauglustaine et al., MOZART, a global chemical transport model for ozone and related chemical tracers 2. Model results and evaluation, *J. Geophys. Res.*, 28,291-28,335, 1998.
- Hayashi, H., I. Stajner, S. Pawson, and A. M. Thompson, Sensitivity of assimilated tropical tropospheric ozone to meteorological analyses, *Eos Trans. AGU*, 83 (47), Fall Meeting Supp. Abs. A71G-06, 2002.
- Haynes, P., J. Scinocca and M. Greenslade, "Formation and maintenance of the extratropical tropopause by baroclinic eddies, *J. Geophys. Res.*, 28, 4179-4182, 2001.
- Held, I. M., On the height of the tropopause and the static stability of the atmosphere, *J. Atmos. Sci.*, 39, 412-417, 1982.
- Hoogen, R., V. Rozanov and J. Burrows, Ozone profiles from GOME satellite data: Algorithm description and first validation, *J. Geophys. Res.*, 104, 8263-8280, 1999.
- Holton, J. R., P. H. Haynes, M. E. McIntyre A. R. Douglass, R. B. Rood, and L. Pfister, Stratosphere-Troposphere exchange, *Reviews of Geophys.*, 33, 403-439, 1995.
- Horinouchi, T., S. Pawson, K. Shibata, U. Langematz, E. Manzini, M. A. Giorgetta, F. Sassi, R.J. Wilson, K.P. Hamilton, J. de Granpre, A. A. Scaife, Tropical cumulus convection and upward propagating waves in middle atmospheric GCMs. *J. Atmos. Sci.*, submitted, 2002.
- Hoskins, B. J., Towards a PV-potential temperature view of the general circulation, *Tellus*, 43AB, 27-35, 1991.
- Houghton, J. T. et al. (Eds.), *Climate Change 1994, The IPCC Scientific Assessment*, Cambridge University Press, 339 pp.1995
- Hudson, R. D., and A. M. Thompson, Tropical tropospheric ozone (TTO) from TOMS by a modified-residual method, *J. Geophys. Res.*, 103, 22129-22145, 1998.

- Jackman, C. H., E. L. Fleming, S. Chandra, D. B. Considine, and J. E. Rosenfield, Past, present and future modeled ozone trends with comparisons to observed trends., *J. Geophys. Res.*, 101, 28,753-28,767, 1996.
- Jacobson, M. Z., Computation of global photochemistry with SMVGEAR II, *Atmos. Environ.*, 29, 2541-2546, 1995.
- Jensen, E. J., O. B. Toon, D. L. Westphal, S. Kinne, and A. J. Heymsfield, Microphysical modeling of cirrus 1: Comparison with 1986 FIRE IFO measurements. *J. Geophys. Res.* 99, 10421-10442, 1994a.
- Jensen, E. J., O. B. Toon, D. L. Westphal, S. Kinne, and A. J. Heymsfield, Microphysical modeling of cirrus 2. Sensitivity studies, *J. Geophys. Res.*, 99 10443-10454, 1994b.
- Jiang, Y., and Y. Yung, Concentrations of tropospheric ozone from 1979 to 1992 over tropical Pacific South America from TOMS data, *Science*, 272, 714-716, 1996
- Jiang, Y., Y. L. Yung, A. R. Douglass, K. K. Tung, The standard deviation of column ozone from the zonal mean, *Geophys. Res. Lett.*, 25, 911-914, 1998.
- JPL, Chemical kinetics and photochemical data for use in stratospheric modeling, Evaluation Number 13, Sander, S. P., et al., eds., JPL Publication 00-3, 2000.
- Kim, J. and M. Newchurch, Climatology and trends of tropospheric ozone over the eastern Pacific Ocean: The influences of biomass burning and tropospheric dynamics, *Geophys. Res. Lett.*, 23, 3723-3726, 1996.
- Kaufman, Y, D. Tanre, and O. Boucher, A satellite view of aerosols in the climate system, *Nature*, 419, 215-223, 2002.
- Kaufman, Y.J., C.O. Justice, L.P. Flynn, J.D. Kendall, E.M. Prins, L. Giglio, D.E. Ward, W.P. Menzel, and A.W. Setzer, Potential global fire monitoring from EOS-MODIS, *J. Geophys. Res.*, 103, 32215 – 32238, 1998.
- Kawa, S. R., et al., Assessment of the effects of high-speed aircraft in the stratosphere: 1998, NASA/TP-1999-209237, 1999.
- Kawa, S. R., P. A. Newman, L. R. Lait, M. R. Schoeberl, R. M. Stimpfle, J. G. Anderson, C. R. Webster, R. D. May, D. Baumgardner, J. E. Dye, J. C. Wilson, K. R. Chan, and M. Loewenstein, Heterogeneous Activation of Chlorine Along Back Trajectories from ER-2 Observations During ASHOE/MAESA, *J. Geophys. Res.*, 102, 3921-3933, 1997.
- Kim, J.H., R.D. Hudson, and A.M. Thompson, "A new method of deriving time-averaged tropospheric column ozone over the tropics using total ozone mapping spectrometer (TOMS) radiances: Intercomparison and analysis using TRACE A data", *J. Geophys. Res.* 101, 24317-24330, 1996
- Kinnison, D. E., K. E. Grant, P. S. Connell, D. A. Rotman, and D. J. Wuebbles, The chemical and radiative effects of the Mount Pinatubo eruption, *J. Geophys. Res.*, 99, 25,705 - 25,731, 1994.
- Kondo, Y., S. R. Kawa, D. Lary, T. Sugita, A. R. Douglass, E. Lutman, M. Koike, and T. Deshler, Interpretation of Nitric Oxide Profile observed in January 1992 over Kiruna, *J. Geophys. Res.*, 101, 12555-12566, 1996.

- Kratz, D.P., M.-D. Chou, M. M.-H. Yan, and C.-H. Ho, Minor trace gas radiative forcing calculations using the k distribution method with one-parameter scaling, *J. Geophys. Res.*, 103, 31,647-31,656, 1998.
- Labitzke, K., and M. P. McCormick, Stratospheric temperature increases due to Pinatubo aerosols, *Geophys. Res. Lett.*, 19, 207 - 210, 1992.
- Lacis, A., D. Wuebbles, and J. A. Logan, Radiative forcing of climate by changes in the vertical distribution of ozone, *J. Geophys. Res.*, 95, 9971-9981, 1990.
- Lait, L. R., et al., Ozone loss from quasi-conservative coordinate mapping during the 1999-2000 SOLVE/THESEO 2000 campaigns, *J. of Geophys. Res.* 10.1029/2001JD000998, 2002.
- Lamarque, J. F., and P. G. Hess, Cross-tropopause mass exchange and potential vorticity budget in a simulated tropopause folding, *J. Atmos. Sci.*, 51, 2246-2269, 1994.
- Langford, A. O., Stratosphere-troposphere exchange at the subtropical jet: contribution to the tropospheric ozone budget at midlatitudes, *Geophys. Res. Lett.*, 26, 2449-2452, 1999.
- Langford, A. O., C. D. Masters, M. H. Proffitt, E.-Y. Hsie, and A. F. Tuck, Ozone measurements in a tropopause fold associated with a cut-off low system, *Geophys. Res. Lett.*, Vol. 23, 2501-2504, 1996.
- Lary, D. Satellite validation: How coincident is coincident? *J. Geophys. Res.*, (submitted), 2002.
- Lavoue, D., C. Lioussé, H. Cachier, B.J. Stocks, and J.G. Goldammer, Modeling of carbonaceous particles emitted by boreal and temperate wildfires at northern latitudes, *J. Geophys. Res.*, 105, 26871 – 26890, 2000.
- Lefevre, F., G. P. Brasseur, I. Folkins, A. K. Smith, and P. Simon, Chemistry of the 1991-1992 stratospheric winter: three-dimensional model simulations, *J. Geophys. Res.*, 99, 8183-8195, 1994.
- Li, Z., S. Nadon, and J Cihlar, Satellite-based detection of Canadian boreal forest fires: development and application of the algorithm, *Intl. J. of Remote Sensing.*, 21, 3057-3069, 2000.
- Lin, S-J. and R. Rood, Development of the joint NASA/NCAR general circulation model, AMS 13th Conference on Numerical Weather Prediction, Denver, Col., 1999.
- Lin, S-J. A finite-volume integration method for computing pressure gradient forces in general vertical coordinates, *Q. J. Roy. Meteor. Soc.*, 123, 1749-1762., 1997.
- Logan, J. A., An analysis of ozonesonde data for the troposphere: Recommendations for testing 3-D models and development of a gridded climatology for tropospheric ozone, *J. Geophys. Res.*, 104, 16115-16149, 1999.
- Marengo, A., et al., Evidence of a long-term increase in tropospheric ozone from Pic du Midi data series: Consequences: Positive radiative forcing. *J. Geophys. Res.* 99, 16617-16632, 1994.

- Martin, R.V., D.J. Jacob, J.A. Logan, I. Bey, R.M. Yantosca, A.C. Staudt, Q. Li, A.M. Fiore, B.N. Duncan, H. Liu, P. Ginoux, and V. Thouret, Interpretation of TOMS observations of tropical tropospheric ozone with a global model and in-situ observations, *J. Geophys. Res.*, in press, 2002a.
- Martin, R.V., D.J. Jacob, R.M. Yantosca, M. Chin, and P. Ginoux, Global and Regional Decreases in Tropospheric Oxidants from Photochemical Effects of Aerosols, *J. Geophys. Res.*, 10.1029/2002JD002622, 2002b.
- Mickley, L.J., D.J. Jacob, and D. Rind, Uncertainty in preindustrial abundance of tropospheric ozone: Implications for radiative forcing calculations, *J. Geophys. Res.*, 106, 3389-3399, 2001
- Manney, G.L., et al., Formation of low ozone pockets in the middle stratosphere anticyclone during winter, *J. Geophys. Res.*, 100, 13,939 – 13,950, 1995.
- McCormick, M. P., and R. E. Veiga, SAGE II measurements of early Pinatubo aerosols, *Geophys. Res. Lett.*, 19, 155 - 158, 1992.
- McIntyre, M. E., Atmospheric Dynamics: Some fundamentals, with Observational Implications, in *The Use of EOS for the Study of Atmospheric Physics*, Proceedings of the International School of Physics, "Enrico Fermi" Course 115, G. Visconti and J. Gille, eds., North Holland, NY, 313-386, NATO Summer School, 1992.
- Morris, G. A., et al, Trajectory mapping and applications to data from the Upper Atmosphere Research Satellite. *J. Geophys. Res.*, 100, 16491-16505, 1995.
- Morris, G. A., S.R. Kawa, A.R. Douglass, M.R. Schoeberl, L. Froidevaux, and J. Waters, Low-ozone pockets explained, *J. Geophys. Res.*, 103, 3599 – 3610, 1998.
- Mote, P. W., K. H. Rosenlof, M. E. McIntyre, E. S. Carr, J. C. Gille, J. R. Holton, J. S. Kinnarsley, H. C. Pumphrey, J. M. Russell, and J. W. Waters, An atmospheric tape recorder: the imprint of tropical tropopause temperatures on stratospheric water vapor, *J. Geophys. Res.*, 101, 3989-4006, 1996.
- Mote, P. W., J. R. Holton, and B. A. Boville, Characteristics of stratosphere-troposphere exchange in a general circulation model, *J. Geophys. Res.*, 99, 16,815 - 16,829, 1994.
- Moxim, W. J., and H. Levy, A model analysis of the tropical south atlantic ocean tropospheric ozone maximum: The interaction of transport and chemistry, *J. Geophys. Res.*, 105, 17393-17415, 2000.
- Murphy, D., D. Thomson, and M. J. Mahoney, In situ measurements of organics, meteoritic material, Mercury, and other elements in aerosols at 5 to 19 kilometers, *Science*, 282, 1664-1669, 1998.
- Nash, E.R., P.A. Newman, J.E. Rosenfield, and M.R. Schoeberl, An objective determination of the polar vortex using Ertel's potential vorticity, *J. Geophys. Res.*, 101, 9471-9478, 1996
- Newell, R. E. and S. Gould-Stewart, A stratospheric fountain? *J. Atmos. Sci.*, 51, 38,2789-2796, 1981.

- Newman, P., L. Lait, M. Schoeberl, M. Seabloom, M. Proffitt, M. Loewenstein, J. R. Podolske, J. W. Elkins, C. R. Webster, R. D. May, D. W. Fahey, G. S. Dutton, K. R. Chan, Measurements of Polar Vortex Air in Midlatitudes, *J. Geophys. Res.*, 101, 12879-12891, 1996.
- Newman, P., et al., An overview of the SOLVE/THESEO 2000 campaign, *J. Geophys. Res.*, (in press), 2002
- Nielsen, J. E. and A. R. Douglass, Simulation of bromoform's contribution to stratospheric bromine, *J. Geophys. Res.*, 106, 8089-8100, 2001.
- Olague, E. P., H. Yang, and K. K. Tung, A Reexamination of the radiative balance in the stratosphere, *J. Atmos. Sci.*, 49, 1242-1263, 1992.
- Olsen, M. A., and J. L. Stanford, Evidence of stratosphere-to-troposphere transport within a mesoscale model and Total Ozone Mapping Spectrometer total ozone, *J. Geophys. Res.*, 106, 27323-27334, 2001.
- Olsen, M. A., A. R. Douglass, and M. R. Schoeberl, Estimating downward cross-tropopause ozone flux using column ozone and potential vorticity, *J. Geophys. Res.*, in press/2001JD002041, 2002a.
- Olsen, M. A., A. R. Douglass, and M. R. Schoeberl, A Comparison of Northern and Southern Hemisphere Cross-tropopause Ozone Flux, *submitted to Geophys. Res. Lett.*, 2002b.
- Oltmans, S. J., and D. J. Hofmann, Increase in lower-stratospheric water vapour at a mid-latitude northern hemisphere site from 1981 to 1994, *Nature*, 374, 146-149, 1995.
- Oort, A. and H. Liu, Upper-air temperature trends over the globe, *J. Clim.*, 6, 292-307, 1993.
- Pawson, S., K. Labitzke, and S. Leder, Stepwise changes in stratospheric temperature, *Geophys. Res. Lett.*, 25, 2137-2160, 1998.
- Pawson, S., et al. The GCM-Reality Intercomparison Project for SPARC: Scientific Issues and Initial Results, *Bull. Am. Meteorol. Soc.*, submitted 1999.
- Penner et al., *Aviation and the Global Atmosphere*, IPCC Working Groups I and III, Cambridge Univ. Press, 370 pp., 1999
- Pierson, J. M., et al., An investigation of performance and simulation of polar ozone recovery in the 1997 Southern Hemisphere winter, in preparation, 1999.
- Pitari, G., and V. Rizi, An estimate of the chemical and radiative perturbation of stratospheric ozone following the eruption of Mt. Pinatubo, *J. Atmos. Sci.*, 19, 3260 - 3276, 1993.
- Plumb, R. A., Stratospheric transport, *J. Met. Soc. Japan*, 80, 739-809, 2002.
- Plumb, R. A., and J. Eluszkiewicz, The Brewer-Dobson circulation: Dynamics of the tropical upwelling, *J. Atmos. Sci.*, 56, 868-890, 1999.
- Plumb, R. A., A "Tropical Pipe" model of stratospheric transport, *J. Geophys. Res.*, 101, 3957-3972, 1996.

Postel, G. A. and M. Hitchmann, A climatology of rossby wave breaking along the subtropical tropopause, *J. Atmos. Sci.*, 56,359-373, 1999

Price, J. D., Stratospheric-tropospheric exchange in cut-off-low systems, Ph.D. thesis, Univ. Coll. of Wales, Aberystwyth, 1990.

Price, J., and G. Vaughan, The potential for stratosphere-troposphere exchange in cut-off-low systems, *Q. J. R. Meteorol. Soc.*, 119, 343-365, 1993.

Randel, W. J., and P. A. Newman, The stratosphere in the southern hemisphere, *Meteorological Monographs*, Vol. 27, 243-282, 1998.'

Randel, W. J., F. Wu, J. M. Russell III, J. W. Waters, and L. Froidevaux, Ozone and temperature changes in the stratosphere following the eruption of Mount Pinatubo, *J. Geophys. Res.*, 100, 16,753 - 16,764, 1995.

Rex, M. et al., On the unexplained stratospheric ozone losses during cold Arctic Januaries, *J. Geophys. Res.*, (in press), 2002b.

Rex, M., et al., Chemical depletion of Arctic ozone in winter 1999/2000, *J. Geophys. Res.*, 107 (D20), 8276, doi: 10.1029/2001JD000533, 2002a.

Rex, M., et al., Prolonged stratospheric ozone loss in the 1995 – 96 Arctic winter, *Nature*, 389, 835–838, 1999.

Rex, M., et al., Chemical ozone loss in the Arctic winter 1994/95 as determined by the MATCH technique, *J. Atmos. Chem.*, 32, 35–39, 1998a.

Rex, M., et al., In situ measurements of stratospheric ozone depletion rates in the Arctic winter 1991/1992: A Lagrangian approach, *J. Geophys. Res.*, 103, 5843–5853, 1998b.

Ray, E., et al., Transport into the northern hemisphere lowermost stratosphere revealed by in situ tracer measurements, *J. Geophys. Res.*, 104, 25623-25645, 1999.

Riishojgaard, L. P., I. Stajner and G.-P. Lou, The GEOS Ozone Data Assimilation System, *Adv. Space Res.*, 25, 1063-1072, 2000.

Rind, D., J. Lerner, K., Shah, and R. Suozzo, Use of on-line tracers as a diagnostic tool in general circulation model development 2. Transport between the troposphere and stratosphere, *J. Geophys. Res.*, 104, 9151-9167, 1999.

Robock, A. Enhancement of surface cooling due to forest fire smoke, *Science*, 242, 911-913, 1988.

Rodgers, H, W. Norton, A. Lambert, and R. Grainger, Transport of Mt. Pinatubo aerosol, *J. Geophys. Res.*, 104, 4051-4063, 1999.

Rodgers, H, W. Norton, A. Lambert, and R. Grainger, Isentropic, diabatic, and sedimentary transport of transport of Mt. Pinatubo aerosol by tropospheric synoptic-scale and stratospheric planetary-scale waves, *Q. J. Roy. Met. Soc.*, 124, 193-209, 1998.

Rood, R. B., A. R. Douglass, M. C. Cerniglia, W. G. Read, Synoptic-scale mass exchange from the troposphere to the stratosphere, *J. Geophys. Res.*, 102, 23467-23485, 1997.

Rood, R. B., A. R. Douglass, and C. J. Weaver, Tracer exchange between tropics and middle latitudes, *Geophys. Res. Lett.*, 19, 805-808, 1992.

- Rosenfield, J.E., A.R. Douglass, and D.B. Considine, The impact of increasing carbon dioxide on ozone recovery, *J. Geophys. Res.*, 107, 10.1029/2001JD000824, 2002.
- Rosenfield, J.E. and A.R. Douglass, Doubled CO₂ effects on NO_y in a coupled 2D model, *Geophys. Res. Lett.*, 25, 4381-4384, 1998.
- Rosenfield, J.E., P.A. Newman, and M.R. Schoeberl, Computations of diabatic descent in the stratospheric polar vortex, *J. Geophys. Res.*, 99, 16,677-16,689, 1994.
- Rosenfield, J.E. and A.R. Douglass, Doubled CO₂ effects on NO_y in a coupled 2D model, *Geophys. Res. Lett.*, 25, 4381-4384, 1998.
- Rosenfield, J.E., D. Considine, M. R. Schoeberl and E. Browell, The impact of subvisible cirrus clouds near the tropical tropopause on stratospheric water vapor, *Geophys. Res. Lett.*, 25, 1883-1886, 1998.
- Rosenfield, J.E., D.B. Considine, P.E. Meade, J.T. Bacmeister, C.H. Jackman, and M.R. Schoeberl, Stratospheric effects of the Mt. Pinatubo aerosol studied with a coupled two-dimensional model, *J. Geophys. Res.*, 102, 3649-3670, 1997.
- Rosenlof, K.H., et al., Stratospheric water vapor increases over the past half-century, *Geophys. Res. Lett.*, 28, 1195-1198, 2001.
- Russell, J. M., L. L. Gordley, J. H. Park, S. R. Drayson, W. D. Hesketh, R. J. Cicerone, A. F. Tuck, J. E. Frederick, J. E. Harries, P. J. Crutzen, The Halogen Occultation Experiment, *J. Geophys. Res.*, 98, 10777-10797, 1993.
- Schoeberl, M. R., A. R. Douglass, Z. Zhu, and S. Pawson, The Age-Spectrum as a Diagnostic of Stratospheric Trace Gas Transport, *J. Geophys. Res.*, in press, 2002a
- Schoeberl, M. R. et al., "An Assessment of the Ozone Loss During the 1999-2000 SOLVE/ THESEO 2000 Arctic Campaign," *J. Geophys. Res.* (in press), 2002b
- Schoeberl, M. and G. Morris, A Lagrangian Simulation of Subsonic and Supersonic Aircraft Exhaust Emissions, *JGR*, 103, 10817-10825, 1998a.
- Schoeberl, M. R., C. Jackman, and J. Rosenfield, A Lagrangian Estimate of aircraft effluent lifetime, *J. Geophys. Res.*, 103, 10817-10825, 1998b.
- Schoeberl, M. R. et al., An estimation of the dynamical isolation of the tropical lower stratosphere using UARS wind and trace gas observations of the quasi-biennial oscillation, *Geophys. Res. Lett.*, 24, 53-56, 1997.
- Schoeberl, M.R. et al., 1996: The development of the Antarctic ozone hole *J. Geophys. Res.*, 101, 20909-20924, 1996.
- Schoeberl, M. R. and L. Sparling, Trajectory Modeling, in *Diagnostic Tools in Atmospheric Physics*, G. Fiocco and G. Visconti eds., Proceedings of the International School of Physics "Enrico Fermi", Vol. 124, 289-306, 1995
- Schoeberl, M., M. Luo, J. M. Russell, J. E. Rosenfield, An Analysis of the Antarctic HALOE Trace Gas Observations, *J. Geophys. Res.* 100, 5159-5172, 1995.

Schoeberl, M. R. and L. Lait, Conservative Coordinate Transformations for Atmospheric Measurements, in *The Use of EOS for the Study of Atmospheric Physics*, Proceedings of the International School of Physics, "Enrico Fermi" Course CXV, G. Visconti and J. Gille, eds., North Holland, NY, 419-430, NATO Summer School, 1992.

Schoeberl, M. R., P. K. Bhartia, and J. R. Herman, Tropical Ozone Loss Following the Eruption of Mt. Pinatubo, *Geophys. Res. Lett.*, **20**, 29-32, 1992.

Schoeberl, M.R., and L. R. Lait, Conservative-coordinate transformations for atmospheric measurements, The use of EOS for studies of atmospheric physics, Proceedings of the International School of Physics "Enrico Fermi", *Italian Phys. Soc.*, 419-431, 1993.

Seo, K.-H., and K. P. Bowman, A climatology of isentropic cross-tropopause exchange, *J. Geophys. Res.*, **106**, 28,159–28,172, 2001.

Shapiro, M. A., Turbulent mixing within tropopause folds as a mechanism for the exchange of chemical constituents between the stratosphere and the troposphere, *J. Atmos. Sci.*, **37**, 994-1004, 1980.

Sherwood, S.C., and A.E. Dessler, On the control of stratospheric humidity, *Geophysical Research Letters*, **27** (16), 2513-2516, 2000.

Sherwood, S.C., A stratospheric "drain" over the maritime continent, *Geophysical Research Letters*, **27** (5), 677-680, 2000.

Shepherd, T., Issues in stratosphere-troposphere coupling, *J. Met. Soc. Japan*, **80**, 769-792, 2002.

Shindell, D. T., D. Rind and P. Lonergan, Increased polar stratospheric ozone loss and delayed eventual recovery owing to increasing greenhouse gas concentrations, *Nature*, **392**, 589-592, 1998.

Shine, K.P. et al., Radiative forcing due to changes in ozone: a comparison of different codes, in *Atmospheric Ozone as a Climate Gas*, W-C. Wang and I.S.A. Isaksen, Eds., Springer, Berlin, 1995.

Shine, K. Sources and sinks of zonal momentum in the middle atmosphere diagnosed using the diabatic circulation, *Q. J. R. Meteorol. Soc.*, **115**, 265-292, 1989.

Sparling, L. C. and J. T. Bacmeister, Scale dependence of the tracer microstructure: PDF's intermittency and the dissipation scale, *Geophys. Res. Lett.*, **28**, 2823-2826, 2001.

SPARC, Assessment of water vapor in the upper troposphere and lower stratosphere, WMO/TD-1043, World Meteorological Organization, Paris, 2000.

Sparling, L. C., Statistical perspectives on stratospheric transport, *Revs. of Geophys.*, **38**, 417-436, 2000.

Sparling, L. C., J. A. Kettleborough, P. H. Haynes, M. E. McIntyre, J. E. Rosenfield, M. R. Schoeberl, and P. A. Newman, Diabatic cross-isentropic dispersion in the lower stratosphere, *J. Geophys. Res.*, **102**, 16491-16505, 1997.

- Spencer, R., and J. Christy, Precision lower stratospheric temperature monitoring with the MSU: Technique, validation and results 1979-1991, *J. Clim.*, 6, 1194-1204, 1993.
- Staehelin, J. et al., Trends in surface ozone concentrations at Arosa (Switzerland). *Atmos. Env.*, 28, 75-87, 1994.
- Stajner, I., L. P. Riishojgaard, and R. B. Rood, The GEOS ozone data assimilation system: specification of error statistics, in preparation, 1999.
- Stolarski, R. S., et al., 1995 Scientific assessment of the atmospheric effects of stratospheric aircraft, NASA reference publication 1381, 1995.
- Swinbank, R. and A. O'Neill, A stratosphere-troposphere data assimilation system, *Mon. Weather Rev.*, 122, 686-702, 1994.
- Tabazadeh, A., K. Drdla K., M. Schoeberl, P. Hamill, O. B. Toon, Arctic "ozone hole" in a cold volcanic stratosphere, *Proc. of the Natl. Acad.*, 99, 2609-2612, 2002.
- Tabazadeh et al., Nitric acid scavenging by mineral and biomass burning aerosols, *Geophys. Res. Lett.*, 25, 4183-4188, 1998.
- Tanre, D. et al., Global observation of anthropogenic aerosols from satellite, *Geophys. Res. Lett.*, 28, 4555-4558, 2001
- Thakur et al., Distribution of reactive nitrogen species in the remote free troposphere: Data and model comparisons, *Atmos. Env.*, 33, 1403-1422, 1999.
- Thompson, A.M., J.C. Witte, R.D. McPeters, S.J. Oltmans, F.J. Schmidlin, J.A. Logan, M. Fujiwara, V.W.J.H. Kirchhoff, F. Posny, G. J.R. Coetzee, B. Hoegger, S. Kawakami, T. Ogawa, B.J. Johnson, H. Vömel and G. Labow, The 1998-2000 SHADOZ (Southern Hemisphere Additional Ozonesondes) Tropical Ozone Climatology. 1. Comparisons with TOMS and Ground-based Measurements, *J. Geophys. Res.*, in press, 2002.
- Thompson, A. M. et al., Tropical tropospheric ozone and biomass burning, *Science*, 291, 2128-2132, 2001.
- Thompson, A. M. et al., A tropical Atlantic paradox: Shipboard and satellite views of a tropospheric ozone maximum and wave-one in January-February 1999, *GRL*, 27, 3317-3320, 2000.
- Thompson, A. M. and R. D. Hudson, Tropical Tropospheric Ozone(TTO) maps from Nimbus-7 and Earth-Probe TOMS by the modified-residual method: Evaluation with sondes, ENSO signals and trends from Atlantic regional time series, *J. Geophys. Res.*, in press, 1999.
- Thuburn, J. and G. Craig, GCM tests for theories of the height of the tropopause, *J. Atmos. Sci.*, 54, 869-882, 1997.
- Tie, X. X., G. P. Brasseur, B. Briegleb, and C. Granier, Two-dimensional simulation of Pinatubo aerosol and its effect on stratospheric ozone, *J. Geophys. Res.*, 99, 20,545 - 20,562, 1994.
- Timmreck, C. H. Graf, and J. Feichter, Simulation of Mt. Pinatubo volcanic aerosol with the Hamburg climate model ECHAM4, *Theor. and App. Climat.*, 62, 85-108, 1999.

- Toon, O. B., and R. C. Miake-Lye, Subsonic Aircraft: Contrail and Cloud Effects Special Study (SUCCESS), *Geophys. Res. Lett.*, 25, 1109, 1998.
- Toon, O. B., J. Kasten, R.P. Turco, M.S. Liu, The sulfur cycle in the marine atmosphere, *J. Geophys. Res.*, 92, 943-963, 1987.
- Toon, O.B., R.P. Turco, J. Jordan, J Goodman, G. Ferry, Physical processes in polar stratospheric ice clouds, *J. Geophys. Res.*, 94, 11359-11380, 1989.
- Toon, O.B., R.P. Turco, D. Westphal, R. Malone, and M.S. Liu, A multi-dimensional model for aerosols: Description of computational analogs, *J. Atmos. Sci.*, 45, 2123-2143, 1988.
- Torres, O., P.K. Bhartia, J.R. Herman, Z. Ahmad and J. Gleason, Derivation of aerosol properties from satellite measurements of backscattered ultraviolet radiation, Theoretical Basis, *J. Geophys. Res.*, 103, 17099-17110, 1998
- Trepte C. R., R. E. Veiga, and M. P. McCormick, The poleward dispersal of Mount Pinatubo volcanic aerosol, *J. Geophys. Res.*, 98, 18,563 - 18,573, 1993.
- Turco, R. and M. Jacobson, SMVGear - A sparse-matrix, vectorized gear code for atmospheric models, *Atmos. Env.*, 28: 273-284, 1994
- Young, R. E., H. Houben, and O. B. Toon, Radiatively forced dispersion of the Mt. Pinatubo volcanic cloud and induced temperature perturbations in the stratosphere during the first few months following the eruption, *Geophys. Res. Lett.*, 21, 369 - 372, 1994.
- Vaughan, G., and J. Price, Ozone transport into the troposphere in a cut-off low event, Ozone in the Atmosphere, R. D. Bojkov and P. Fabian [eds.], pp.415-418, A. Deepak, Hampton, Va., 1989.
- Volk C. M. et al. Quantifying transport between the tropical and mid-latitude stratosphere, *Science*, 272, 1763-1768, 1996.
- Weaver, C. J., A. R. Douglass and R. B. Rood, Lamination frequencies as a diagnostic for horizontal mixing in a 3D transport model, *J. Atmos. Sci.*, (in press) 1999.
- Wernli, H., and M. Bourqui, A Lagrangian “1-year climatology” of (deep) cross-tropopause exchange in the extratropical Northern Hemisphere, *J. Geophys. Res.*, 107, 4041, doi:10.1029/2001JD000812.
- Westphal, D., O. B. Toon, The short-term temperature response to smoke from oil fires, *Geophys. Res. Lett.*, 18, 1873-1876, 1991a.
- Westphal, D., O. B. Toon, Simulations of microphysical, radiative, and dynamical processes in a continental-scale forest fire smoke plume, *J. Geophys. Res.*, 96, 22379-22400, 1991b.
- Wong, J. and Z. Li, Retrieval of optical depth for heavy smoke aerosol plumes: Uncertainties and sensitivities to the optical properties, *J. Atmos. Sci.*, 59, 250-261, 2002.
- WMO, Atmospheric Ozone, 1985, WMO, 16, Geneva, Switzerland, 1986
- Yang, H. and K. K. Tung, Cross-isentropic stratospheric-troposphere exchange of mass and water vapor, *J. Geophys. Res.*, 101, 9413-9423, 1996.

Zhao, X., R. Turco, and M. Shen, A new family Jacobian solver for global three-dimensional modeling of atmospheric chemistry, J. Geophys. Res., 104, 1767-1799, 1999.

Zhao, J., R. P. Turco, and O. B. Toon, A model simulation of volcanic aerosol evolution in the stratosphere, J Geophys. Res 100, 7315-7328, 1995.

Ziemke, J.R., S. Chandra, and P.K. Bhartia, "Two new methods for deriving tropospheric column ozone from TOMS measurements: Assimilated UARS MLS/HALOE and convective-cloud differential techniques" J. Geophys. Res. 103, 22115-22127, 1998

Tables

Table 1 Data Sets Archived in the Science System

| Data Type | Mission |
|---------------------|--|
| Satellite | UARS (HALOE, CLAES, MLS, HRDI, ISAMS), POAM, SAGE, SBUV, TOMS, ADEOS, CRISTA |
| Aircraft | STEP, AAOE, AASE I, AASE II, SPADE, STRAT, TOTE/VOTE, POLARIS, SUCCESS, SONEX, WAM, ACCENT, CRYSTAL-FACE |
| Ground, Balloon | NDSC, Rawinsondes, POLARIS ozonesondes, OMS balloon |
| Meteorological Data | NCEP Analysis (1979-), NMC Re Analysis (1955-), UKMO (1991-), DAO (various versions) (1991-) |
| Model Calculations | Diabatic heating rates for the Meteorological analysis, CTM runs (1995-1996, 1997-1998) |

Table 2. New data sets to be used under this proposal

| EOS Data Set Available within the next 3 years | Usage under this proposal |
|--|---|
| AIRS | More precise measurements of the temperature of the lower stratosphere and upper troposphere to estimate the cross tropopause mass flux, also upper tropospheric and lower stratospheric ozone |
| MOPITT | CO Measurements as tracers of upper tropospheric circulation and as indicators (along with TOMS aerosols) of biogenic aerosols |
| MISR | Aerosol information to be used in conjunction with TOMS |
| TOMS Aura OMI | Tropospheric aerosols, column ozone (and column SO ₂ . The SO ₂ will be used in volcanic aerosol studies. The column ozone will be used in computing the tropospheric residual. NO ₂ (OMI) column will be used as precursor for ozone. |
| SAGE III | Stratospheric ozone and aerosol profiles. The ozone data is to be used with TOMS data to compute the ozone residual |
| GLAS | Tropospheric aerosol, SVC and cloud height distribution |
| DAO FVDAS | Drives transport models and trajectory models |
| Aura HIRDLS | UTLS HNO ₃ , O ₃ , Aerosols |
| Aura TES | Tropospheric Ozone, CO, UTLS NO ₂ , HNO ₃ , ClONO ₂ , CH ₄ , N ₂ O |
| Aura MLS | Stratospheric and UTLS Ozone, HCl, N ₂ O, T |

Table 3. SCIAMACHY data products.

| | NADIR | | | Limb/Occultation | | |
|----------------|---|--|---------------------|--|--|-----------|
| Type | UV/Vis | IR | UV/Vis IR | UV/Vis | IR | UV/Vis/IR |
| NRT | O ₃ , NO ₂ , SO ₂ *, OCIO*, H ₂ CO* | H ₂ O, CO, N ₂ O, CH ₄ | Clouds, Aerosols | | | |
| OFFLINE | O ₃ , NO ₂ , BRO*, SO ₂ *, OCIO*, H ₂ CO* | H ₂ O, CO, CO ₂ , N ₂ O, CH ₄ , P, T | Clouds, Aerosols | O ₃ , NO ₂ , BrO | H ₂ O, CO, CO ₂ , N ₂ O, CH ₄ , P, T | Aerosols |

| | | | | | | |
|---|--|--|--|--|--|--|
| | | | | | | |
| (*) These molecules can only be detected under special conditions | | | | | | |